Dorsal activity of maternal squint is mediated by a non-coding function of the RNA

Lim, Shi Min

2013

Lim, S. M. (2013). Dorsal activity of maternal squint is mediated by a non-coding function of the RNA. Doctoral thesis, Nanyang Technological University, Singapore.

https://hdl.handle.net/10356/58582

https://doi.org/10.32657/10356/58582

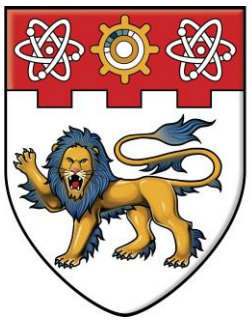

NANYANG
TECHNOLOGICAL
UNIVERSITY

Dorsal activity of maternal *squint* is mediated by a non-coding function of the RNA

LIM SHI MIN
SCHOOL OF BIOLOGICAL SCIENCES
2013

Dorsal activity of maternal *squint* is mediated by a non-coding function of the RNA

LIM SHI MIN

SCHOOL OF BIOLOGICAL SCIENCES

A thesis submitted to the Nanyang Technological University in partial fulfillment of the requirement for the degree of Doctor of Philosophy
2013

Acknowledgements

Work in this thesis was performed in the laboratory of Dr. Karuna Sampath at Temasek Lifesciences Laboratory (TLL). I thank Karuna for taking me in as an undergraduate intern, exposing me to the beautiful world of developmental biology, and giving me a chance to train under her as a graduate student. I am especially grateful for her excellent supervision, earnest encouragement and unrelentless efforts at making sure I was getting the best training possible. To Karuna: Thank you very much. I think I have grown up a lot, under your wings.

I wish to thank my Thesis Advisory Committee members, Dr. Stephen Cohen and Prof. Mark Featherstone, for allowing me an opportunity to pursue and complete my graduate studies. Their critics and constructive suggestions helped greatly in moulding this work. I thank Singapore Millenium Foundation for the pre-doctoral scholarship. And I thank the TLL confocal, fish and sequencing facilities for their technical support.

My heartfelt thanks also go to all past and present members of the Sampath laboratory: Aniket, Tian Jing, Srinivas, Albert, Li Sun, Ruan Hua, Adita, Patrick, Arvind, Shi Jie, Pavle, Helen, Pooja, Long, Wang Yin and Cherish, for their technical assistance, meaningful discussions and friendship. I really like how everyone just feels like family.

I thank my parents for giving me the freedom to choose which path to take and for their unwavering emotional support over the years. Last but not least, I thank my husband Ziyan for his immense patience and understanding during the course of my study, and my beautiful first-born Ying Jia for coming into our lives.

Table of Contents

List of Figures

Introduction

Results

Discussion

List of Tables

Results

Abbreviations

AP	Antero-posterior
AV	Animal-vegetal
DIG	Digoxigenin
DV	Dorso-ventral
ich	*ichabod*
LR	Left-right
lncRNA	long non-coding RNA
mRNA	messenger RNA
miRNA	micro RNA
MZ	Maternal-Zygotic
ndr1	*nodal-related 1*
oep	*one-eyed pinhead*
PCR	Polymerase Chain Reaction
RT-qPCR	Reverse Transcriptase-quantitative Polymerase Chain Reaction
SDS-PAGE	Sodium Dodecyl Sulfate Polyacrylamide Gel Electrophoresis
sqt	*squint*
TALEN	Transcription activator-like effector nucleases
TGFβ	Transforming Growth Factor β
TILLING	Targeting Induced Local Lesions in Genomes
UTR	Un-translated region
WISH	Whole-mount in situ hybridization
wnt	*wingless/int-1*
WT	Wild-type
ZFN	Zinc Finger Nucleases

Abstract

The earliest steps of axis formation in zebrafish are thought to be regulated by maternal factors, for instance, that activate Wnt/β-Catenin signaling to specify the dorsal axis. It was previously shown that asymmetric localization of maternal transcripts of the conserved zebrafish TGF-β factor, Squint (Sqt/Nodal-related 1, Ndr1), in 4-cell stage embryos predicts the position of the future embryonic dorsal, preceding dorsal nuclear accumulation of β-Catenin (Gore et al., 2005). The *nodal* genes are classically involved in mesoderm and endoderm formation, left-right axial patterning, neural patterning and stem cell maintenance. However, cell ablations and antisense oligonucleotides that deplete Sqt lead to dorsal deficiencies, suggesting that localized maternal *sqt* RNA functions in dorsal specification. Due to discrepancies between the genetic *nodal* mutants and the ablations/antisense knock-down results, the function and mechanism of maternal *sqt* was debated (Bennett et al., 2007; Gore et al., 2007). In this study, I show that *sqt* RNA has activity independent of *Sqt* protein in dorsal specification. Surprisingly, over-expression of mutant/non-coding *sqt* RNA and particularly, the *sqt* 3'UTR, leads to increased number of β-Catenin-positive nuclei and expands dorsal gene expression. Dorsal activity of *sqt* RNA requires Wnt/β-Catenin but not co-receptor Oep-dependent Nodal signaling, explaining the discrepancy between the *nodal* signaling mutants and the morpholino phenotypes. Also, depletion of maternal *sqt* RNA abolishes nuclear β-Catenin, providing the mechanism for the loss of dorsal in the morphants, and places activity of maternal *sqt* RNA upstream of β-Catenin. Remarkably, this loss of early dorsal gene expression can be rescued by the *sqt* 3'UTR sequences. My findings identify new non-coding functions for the *nodal* genes, and support a model wherein *sqt* RNA acts as a scaffold to bind and deliver/sequester maternal factors to future embryonic dorsal.

CHAPTER I:
INTRODUCTION

1.1 Symmetry breaking and pattern formation

Symmetry breaking and pattern formation are fundamental properties of biological systems. Be it a single cell or an architecturally complex multicellular organism, generation of polarity paves the route to achieving subsequent functional complexity. In the biological context, polarity is crudely defined as "the persistent asymmetrical and ordered distribution of structures along an axis" (Cove et al. 1999). Apart from generating asymmetric axes in an adult organism, cell polarity also plays a role in both individual and collective cell movements during embryonic development such as epiboly, invagination and apical constriction.

At different developmental time points, each cell of an embryo can either be specified or determined. The former scenario is reversible, whereas the latter situation is irreversible. The phenomenon of specification can be further classified into two main types, autonomous and conditional. An autonomously specified cell will assume a fate dictated by the cytoplasmic determinants it contains, regardless of the surrounding environment it is in. The first demonstration of autonomous specification was done in 1887 by Laurent Chabry, who made use of tunicate embryos which have a small number of cells and relatively few cell types. He observed that embryos with certain cells ablated lose only structures that were normally formed from those destroyed cells. Also, when he separated cells and grew them in isolation, those isolated cells still gave rise to their specified structures.

On the contrary, a cell undergoing conditional specification develops according to positional cues provided by neighbouring cells or morphogen gradients. In other words, the commitment of such a cell to a certain fate requires interaction with its environment. In 1892, Hans Driesch separated sea urchin blastomeres from each other at the 2-cell stage and surprisingly found that each of the blastomere was capable of generating a complete larva by itself. He then extended his analysis to 4-cell and 8-cell stage sea urchin embryos, and found that some of the separated blastomeres regulated their development into an entire larva, although each larva is not identical to one another.

Although simple as it seems, the making of a multicellular organism from a spherical egg involves more complex intertwining of the two themes of autonomous and conditional

specification. During specification, some of the prevalent mechanisms include RNA localization, unequal cell divisions, extrinsic morphogen cues etc.

1.2 Mechanisms of axes specification in invertebrates and vertebrates

1.2.1 *Caenorhabditis elegans*

The free-living non-parasitic soil nematode, *Caenorhabditis elegans*, is a popular experimental model with researchers, given its short embryogenesis period (about 16 hours), transparent cuticle and ease of housing (Kenyon 1988; Wood 1988; Donald 1997). Having exactly 959 somatic cells, *C. elegans*' entire cell lineage has been mapped, with little variance across individuals (Sulston et al. 1983).

The unfertilized *C. elegans* egg begins as a single cell with no obvious asymmetries. Upon sperm entry, cytoskeletal growth nucleated by its centrioles gives rise to cytoplasmic movements that re-position P granules to the posterior end of the embryo (Hird and White 1993; Goldstein and Hird 1996; Kemphues and Strome 1997). In genetic screens conducted to identify regulators of cytoplasmic partitioning in *C. elegans* embryo, a group of genes called *par* (*partitioning defective*) genes were discovered from mutants displaying early defects in asymmetry (Kemphues et al. 1988; Kirby et al. 1990; Morton et al. 1992; Cheng et al. 1995; Guo and Kemphues 1996; Kemphues and Strome 1997). PAR-1 to -6 encode six different proteins that function cooperatively to compartmentalize maternal regulatory factors (Bowerman and Shelton 1999; Wallenfang and Seydoux 2000). For example, translational regulators contained in P granules eventually segregate into germ cells, following their localization to posterior cytoplasm immediately after fertilization (Strome and Wood 1983; Hird et al. 1996; Amiri et al. 2001; Smith et al. 2002; Wang et al. 2002). This process requires an intact microfilament cytoskeleton because Cytochalasin D treatment resulted in aberrant phenotypes such as "reverse polarity", "dual anteriors" or "dual posteriors" (Hill and Strome 1990).

Following the establishment of the anterior-posterior (AP) axis, two distinct cells, AB and P granules-containing P1 arise from the first asymmetric cell division. The AB cell divides symmetrically in a direction perpendicular to the AP axis, giving rise to two equipotent cells, ABa and ABp (Figure 1.2.1). This positioning is also mediated by

asymmetrically distributed PAR proteins, which influence the placement of mitotic cleavage spindles (Cheng et al. 1995; Etemad-Moghadam et al. 1995; Tsou et al. 2003). In contrast, polarity of PAR proteins is re-established in P1 (Basham and Rose 1999; Pichler et al. 2000; Munro et al. 2004), causing P1 to divide asymmetrically into two daughter cells, EMS and P2. By the 4-cell stage, ancestral cells leading to different lineages become precisely positioned, as a result of a combination of factors involving mitotic spindle positioning, as well as, spatial constraints exerted by the chorion. ABa cell forms the anterior pharyngeal tissue, whereas the dorsally-located ABp cell forms the hypodermis and neurons. At the posterior, P2 blastomere gives rise to pre-dominantly germ-line tissues. Its mitotic sibling, EMS cell, defines the future ventral region of the embryo, forming muscle and gut cells. The intricate positioning of those cells allow for subsequent fortification of the dorso-ventral (DV) axis because GLP-1 receptor is only selectively expressed in AB cells (Evans et al. 1994), while P2 blastomere expresses the corresponding APX-1 ligand (Mickey et al. 1996). This results in asymmetric activation of GLP-1 in ABp cell which physically contacts P2 cell, thereby inducing dorsal fates in ABp cell's progeny (Mango et al. 1994; Mello et al. 1994; Moskowitz et al. 1994).

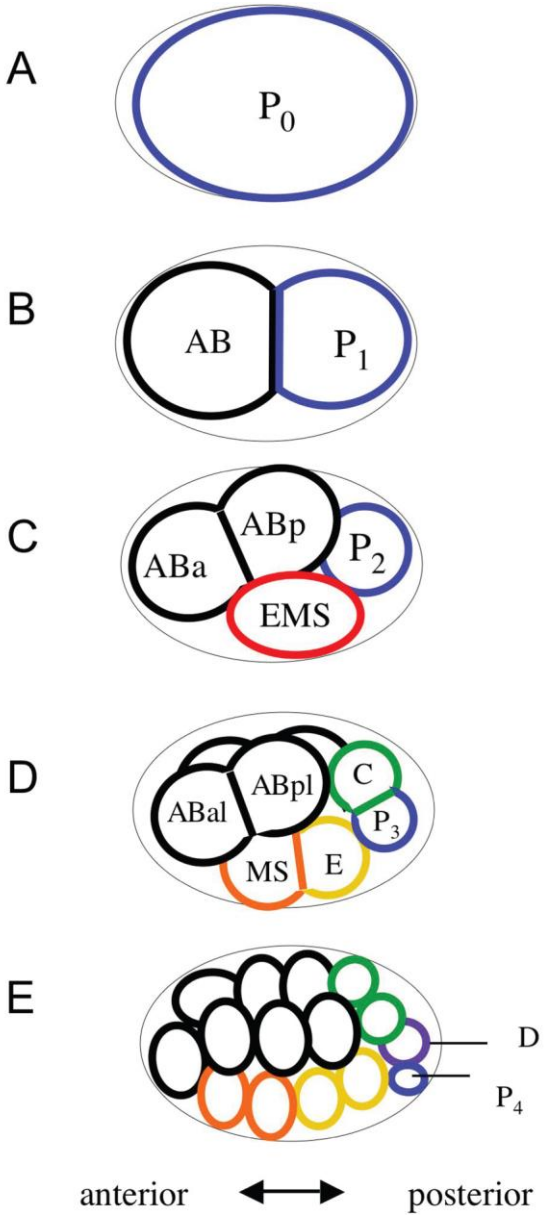

Figure 1.2.1 Generation of founder cells in the early *Caenorhabditis elegans* embryo. Anterior is to the left, posterior to the right, dorsal is up and ventral down in this and all subsequent figures. The germ-line precursors (P cells) are shown outlined with blue. Each of the founder cells generated by asymmetric division are indicated with a different color. The founder cells each display a characteristic cell cycle rate and lineage: The AB lineage produces hypodermis, neurons, anterior pharynx and other cell types; MS produces the somatic gonad, muscle, the majority of the pharynx, neurons and gland cells; E produces all intestine; C produces muscle, hypodermis and neurons; D produces muscle; P4 is the germ-line precursor. The 16-cell embryo shown in (E) is simplified and does not show the daughters of the 4th AB cell division, which occurs at approximately the same time as the P3 division. (adapted from Worm Book)

1.2.2 *Drosophila*

The next example of an invertebrate model system, *Drosophila*, has traditionally been used to teach Mendelian genetics and study inheritance of traits. The ease of breeding, rapid embryonic growth and external development makes it very amenable to experimentations. *Drosophila* is one of the few organisms whose entire genome is deciphered early (Adams et al. 2000) and many genes have been identified. In addition, mutants are readily available using both forward and reverse genetics approaches (Bourbon et al. 2002; St Johnston 2002; Bellen et al. 2004). In fact, the 1995 Nobel Prize-winning screen performed by Christian Nusslein-Volhard and Eric Wieschaus in 1980 (Nusslein-Volhard and Wieschaus 1980) led to the identification of many genes involved in segmentation and polarity, which also have conserved pivotal functions in higher vertebrates such as mammals.

Prior to the knowledge of *Drosophila* genetics, observations from Sander's laboratory hinted at the presence of morphogenetic gradients in a *Drosophila* oocyte. Using classic embryological techniques, Klaus Sander discovered that halving the oocyte transversely very early-on in oogenesis gave rise to strictly anterior and posterior pieces of the embryo, with no middle body segments. The longer the egg was allowed to develop, the two separated halves of the embryo increasingly retain the capacity to pattern middle body segments. This simple set of observations suggests that positional information provided by two ends of the Drosophila egg organize embryonic AP patterning. The nature of the positional information was soon uncovered to be mRNAs, as ultraviolet and RNAse treatment of the anterior pole resulted in embryos lacking head and thoracic segments (Kandler-Singer and Kalthoff 1976).

Through recessive female sterile screens conducted in (Orr et al. 1989; Schupbach and Wieschaus 1989; Schupbach and Wieschaus 1991), the identities of several maternal-effects genes involved in different spatial and temporal aspects of oogenesis were revealed. Subsequent research indeed supports mRNA localization as a prevalent theme for pattern formation during *Drosophila* oogenesis. In *Drosophila*, its AP axis is entirely patterned by maternal products, namely Bicoid, Hunchback, Nanos and Caudal, whose mRNAs are deposited by nurse cells (Riechmann and Ephrussi 2001). The anterior localization of *bicoid* mRNA is an active process that is dependent on its 3'UTR which has binding sites for Exuperentia and Swallow proteins. The *bicoid* mRNA-containing ribonucleoprotein complex (RNP) is tethered to the minus ends of the microtubule cytoskeleton via Dynein (Cha et al.

2001). Upon fertilization, translated Bicoid protein diffuses from the anterior pole, forming a gradient along the longitudinal axis. High levels of Bicoid at the anterior pole translationally repress uniformly distributed *caudal* mRNA, such that posteriorizing Caudal protein is restricted to the opposite end (Chan and Struhl 1997; Wu and Lengyel 1998; Niessing et al. 2000). Bicoid further fortifies anterior fates by enhancing the transcription of *hunchback* at the anterior (Driever and Nusslein-Volhard 1989; Struhl et al. 1989).

Similar to *bicoid* RNA, *nanos* RNA is actively sequestered and translated at the posterior end of the Drosophila oocyte in a process that involves several other proteins such as Oskar, Staufen, Vasa etc. (Lehmann and Nusslein-Volhard 1986; Schupbach and Wieschaus 1986; Ferrandon et al. 1994; Brendza et al. 2000). Nanos protein forms a diffusion gradient emanating from the posterior pole, and cooperates with Pumilio to inhibit translation of uniformly distributed hunchback RNA by a deadenylation mechanism (Tautz 1988; Barker et al. 1992; Wreden et al. 1997). On the other hand, Pumilio-bound hunchback transcripts are translated normally at the anterior end. Taken together, AP axis in Drosophila is initiated in the syncytial egg by asymmetrically localized *bicoid* and *nanos* transcripts, whose protein products form diffusion gradients that further regionalize the embryo in a concentration-dependent manner (Figure 1.2.2).

Next, the establishment of DV polarity is mediated by a gradient of Dorsal protein, a transcription factor. As *Drosophila* genes are named based on their mutant phenotypes, the wild-type function of Dorsal protein is to specify ventral fates (Roth et al. 1989; Rushlow et al. 1989; Steward 1989). Unlike Bicoid, Dorsal is initially uniformly distributed throughout the embryo, and differentially translocated into nuclei of ventral cells upon receiving asymmetric cues. It was discovered that these cues result from cell-cell signalling events initiated by Gurken protein, whose transcripts are restricted in an antero-dorsal fashion (Schupbach 1987; Forlani et al. 1993; Neuman-Silberberg and Schupbach 1993).

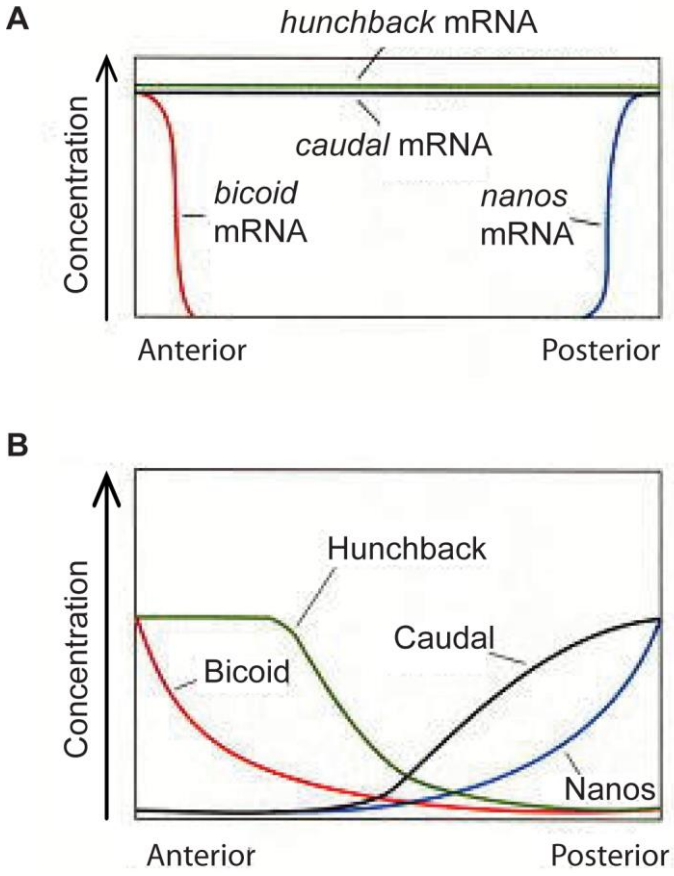

Figure 1.2.2 A model of anterior-posterior pattern generation by the *Drosophila* maternal effect genes. (A) The *bicoid*, *nanos*, *hunchback* and *caudal* mRNAs are placed in the oocyte by the ovarian nurse cells. The *bicoid* message is sequestered anteriorly; the nanos message is sent to the posterior pole. (B) Upon translation, the Bicoid protein gradient extends from anterior to posterior, while the Nanos protein gradient extends from posterior to anterior. Nanos inhibits the translation of the *hunchback* message (in the posterior), while Bicoid prevents the translation of the *caudal* message (in the anterior). This inhibition results in opposing Caudal and Hunchback gradients. (adapted from Developmental Biology, 10th edition, Scott F. Gilbert)

1.2.3 Tunicates

Tunicates are members of the Tunicata, a subphylum of the phylum Chordata. They have a simple sac-like body structure and are evolutionarily related to vertebrates. The phenomenon of autonomous specification was first observed in tunicates where isolated blastomeres gave rise to cell types determined by their cellular content, independent of the physical environment they are in. Both the DV and AP axes of tunicates are established at the onset of embryogenesis by a common mechanism called "ooplasmic segregation" which refers to the dramatic rearrangement of egg cytoplasm to achiever the aim of regionalization. This process is triggered by growth of the sperm's astral microtubules, accompanied by calcium ion waves that result in the contraction of cytoplasm at the animal pole (Sawada and Schatten 1989; Speksnijder et al. 1990b; Speksnijder et al. 1990a; Roegiers et al. 1995). It is possible to visualize movements of the ooplasm using regular light microscopy because most tunicate eggs have distinctly colored ooplasm, namely clear ectoplasm containing vesicles and fine particles, grey-colored endoderm containing yolk platelets, and yellow-colored myoplasm containing pigment granules, mitochondria, lipids and endoplasmic reticulum (Zalokar and Sardet 1984; Kawamura and Fujiwara 1994).

Prior to the first mitotic cleavage, the DV axis is already evident from the presence of a yellow "cytoplasm cap" at the vegetal pole. Surgical removal of the cap at the beginning of embryogenesis produces embryos that neither possess a DV axis nor enter gastrulation. Hence, the location of the cap dermacates the region fated to be dorsal and is also the site of gastrulation initiation (Bates and Jeffery 1987). Following the formation of the DV axis, the ooplasm undergoes a second rearrangement which further confines the yellow-pigmented myoplasm to a sub-equatorial zone (observed morphogically as a "yellow crescent"), marking the future posterior of the embryo (Nishida 1994). Removal of this posterior-vegetal cytoplasm (PVC) inhibits formation of the AP axis, whereas transplantation of this cytoplasm into an embryo devoid of the yellow crescent was sufficient to induce AP patterning. These observations made from surgical manipulations in the tunicate embryos suggest that maternal determinants,with inductive capabilities, are apportioned to different regions before the first mitosis (Nishida 1994; Nishida 1996).

Since mRNA localization is commonly used in other systems to create polarity, tunicates researchers attempted to identify possible asymmetrically localized maternal

mRNAs that may be responsible for axis induction. Using microarray, a large number of maternal mRNAs (postplasmic/PEM RNAs) localized to the "yellow crescent" was identified (Yoshida et al. 1996; Sasakura et al. 1998b; Sasakura et al. 1998a; Makabe et al. 2001; Nakamura et al. 2003). The function of these PEM RNAs in AP axis formation was further studied using overexpression and knockdown experiments. It was also demonstrated that the 3'UTRs of those RNAs have regulatory roles in their localization and translation (Prodon et al. 2007).

1.2.4 *Xenopus*

Xenopus is an excellent model organism for studying biology because of its ease of breeding and maintenance in the lab (Dawid and Sargent 1988). In the 1930s, *Xenopus* was mainly used for physiological studies. Lancelot Hogben established *Xenopus* as one of the world's first pregnancy test-kit because he discovered that the human chorionic gonadotropin (hCG)-containing urine of pregnant women can cause *Xenopus* females to ovulate. Subsequently, *Xenopus* rose in status as a good model organism for developmental and molecular biology because it lays many large (~1 mm) eggs, and is amenable to microsurgical and microinjection techniques. In fact, most of what is known about vertebrate development is derived from studies using *Xenopus*.

At the point of egg laying, the mature *Xenopus* oocyte has a pre-determined pigmented animal pole and clear vegetal pole. It is radially symmetrical around its animal-vegetal (AV) axis. The animal pole contains the nucleus and maternally deposited RNAs and proteins, whereas the vegetal pole consists of mainly yolk granules and nutrition for early embryogenesis. Owing to the pigmented cytoplasm that separates the two hemispheres, a process known as "cortical rotation" which gives rise to the inductive "gray crescent" is readily observable (Vincent et al. 1986; Vincent and Gerhart 1987). Upon sperm entry, the sperm centrioles nucleate the formation of astral microtubules within the egg's cortical cytoplasm, causing microtubule motors to move along parallel microtubule arrays, resulting in a 30^{o} shift of the cortical cytoplasm relative to the inner cytoplasm, towards the sperm entry point (Vincent and Gerhart 1987; Elinson and Rowning 1988; Houliston and Elinson 1991a; Houliston and Elinson 1991b; Weaver et al. 2003). The "gray crescent" formed marks the future dorsal side of the embryo and it has been shown that blocking cortical rotation by methods such as UV irradiation, nocodazole treatment etc. prevents its formation, and thus

disrupts DV axis specification (Gerhart et al. 1989). It was then hypothesized that the process of microtubule-dependent cortical rotation possibly translocated dorsal determinants.

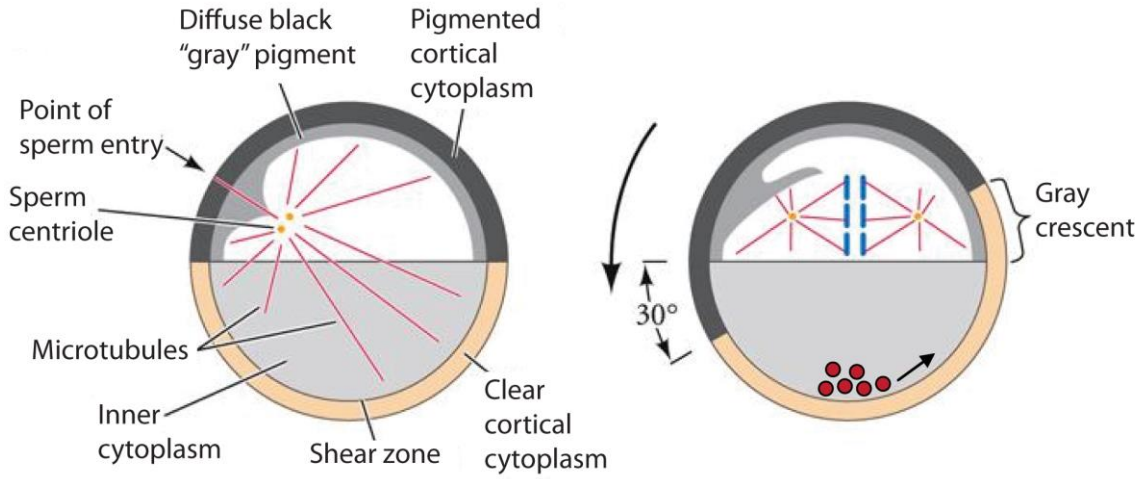

Figure 1.2.4 The phenomenon of cortical rotation in a newly fertilized Xenopus egg. Schematic of the cross-section of an egg midway through the first cleavage cycle. The egg has radial symmetry about its animal-vegetal axis. The sperm has entered at one side, and the sperm nucleus is migrating inward. The cortex represented is like that of *Rana*, with an unpigmented vegetal hemisphere. After fertilization, about 80% of the way into the first cleavage, the cortical cytoplasm rotates 30^{o} relative to the internal cytoplasm, displacing maternal determinants (red dots). Gastrulation will begin in the gray crescent, the region opposite the point of sperm entry where the greatest displacement of cytoplasm occurs. (modified from Developmental Biology, 10th edition, Scott F. Gilbert)

β-catenin was amongst the earliest candidates for the determinants. Upon injection of anti-sense oligonucleotides (morpholinos, MO) targeting maternal β-catenin RNA, frog embryos develop without the dorsal mesoderm (Heasman et al. 1994). This ventralized phenotype could be readily rescued by providing capped β-catenin mRNA. It has also been shown that the overexpression of β-catenin can lead to the establishment of a secondary DV axis in frogs (Funayama et al. 1995). Schneider et al., 1996 reported the asymmetric nuclear translocation of β-catenin in dorsal marginal blastomeres, suggesting activation of canonical Wnt signalling there (Schneider et al. 1996). Subsequently, Rowning et al. 1997 observed the translocation of endogenous membrane-bound organelles towards dorsal in a microtubule-dependent manner and β-catenin co-localized with the parallel microtubule arrays at the future dorsal side of the embryo (Rowning et al. 1997). The dorsal stabilization of β-catenin was discovered to be attributed to the dorsal accumulation of Dishevelled (Dsh) and GSK3 binding protein (GBP) (Miller et al. 1999; Weaver and Kimelman 2004). GBP can bind Dsh directly (Li et al. 1999; Salic et al. 2000; Lee et al. 2001; Hino et al. 2003), and they act synergistically to stabilize β-catenin, which is otherwise constantly targeted for degradation by the combinatorial action of GSK3, Axin and APC (Yost et al. 1996; Farr et al. 2000). Although the presence of downstream components of the canonical Wnt/β-catenin pathway has been described, it was only in 2005 when the signalling dorsal determinant was identified to be Wnt11 (Tao et al. 2005). Whole-mount RNA in situ hybridization showed that maternal *Xwnt11* mRNA localizes to two dorsal-vegetal blastomeres of an 8-cell frog embryo. *Xwnt11* overexpression and knock-down experiments confirmed its involvement in embryonic DV patterning.

1.3 Axis specification in zebrafish

1.3.1 Zebrafish as a model organism

The zebrafish, Danio rerio, is a tropical freshwater fish that belongs to the family Cyprinidae. It originated from the streams in south-eastern Himalayas (Mayden et al. 2007) and is also found in streams, rivers and rice fields of India and Burma. The zebrafish acquired its colloquial name due to its striped appearance, reminiscent of a zebra's stripes. On its body, five alternating blue-black stripes contain two types of pigment cells, melanophores and iridiophores, and silvery-yellow stripes contain xanthophores and iridophores (Schilling 2002). In the wild, an adult zebrafish can grow up to 6.4 cm in length, however it rarely

measures larger than 5 cm in captivity (DeTolla et al. 1995). And in a typical laboratory setting, zebrafish have a maximal recorded life-span of 5.5 yrs, with an average of 3.5 yrs (Gerhard et al. 2002).

In the late 1970s, zebrafish was first introduced as a model organism for studying vertebrate genetics and development by George Streisinger. It is favoured by researchers due to its simple husbandry requirements, relative ease of use and developmental similarities to humans. Female zebrafish typically lay ~100-200 eggs per clutch. Upon fertilization, the embryo develops rapidly *ex utero* and major organ precursors appear within 36 hours post fertilization (hpf), much faster in comparison to similar events in human foetal development. The early embryo is optically transparent, thereby extremely amenable to *in vivo* fluorescent techniques to track single molecules or cells through development.

Notably, the zebrafish genome is fully sequenced and large number of mutations that disrupt embryonic development have been isolated via both forward and reverse genetic screens/techniques, making it an ideal proxy for studying the development and diseases of higher vertebrates using a genetic approach (Mullins et al. 1994; Mullins et al. 1996; Dosch et al. 2004; Pelegri and Mullins 2004; Wagner et al. 2004). In addition, transgenesis methods are well established in zebrafish, allowing for the fluorescent-tagging, trapping and/or knockout of genes (Stuart et al. 1988; Stuart et al. 1990; Bayer and Campos-Ortega 1992; Higashijima et al. 1997; Long et al. 1997; Kawakami et al. 2004; Suster et al. 2009). Gene function can also be analysed using anti-sense synthetic oligonucleotides called morpholinos that function to reduce gene expression by binding to specific transcripts (Nasevicius and Ekker 2000). And more recently, the successful implementation of the engineered nuclease technology in zebrafish further enhanced the toolkit for studying genes and regulatory elements (Doyon et al. 2008; Meng et al. 2008; Sander et al. 2011b; Hwang et al. 2013; Zu et al. 2013).

1.3.2 Early embryonic development of zebrafish

A zebrafish embryo develops rapidly. In fact, by 24 hours post fertilization, the basic body plan is already laid down, and the embryo has a clearly defined anterior-posterior and dorsal-ventral axis. The early developmental events can be broadly chronicled into seven

periods: zygote, cleavage, gastrula, segmentation, pharyngula and hatching (Kimmel et al. 1995)).

The zygote period (0-0.75hpf): Chorion of the newly fertilized egg swells after the sperm enters through the micropyle. Within the embryo, cytoplasmic streaming begins with non-yolky cytoplasm moving towards the animal pole, separating the animal yolk-free cytoplasm (blastodisc) and the vegetal yolk granule-rich cytoplasm. The blastodisc is the region where discoidal meroblastic cleavage occurs to form the body of the embryo, while the yolk supplies maternal factors and nutrition to support embryonic development.

The cleavage period (0.75-2.25hpf): During this time, rapid synchronous cell divisions occur in a highly reproducible manner at 15 min intervals. As these cleavages are incomplete, the cells maintain some connections with each other and some of them also remain connected to the underlying yolk, allowing for small molecules to transit between them.

The blastula period (2.25-5.25hpf): Staging of the embryo during this period can be done by observing the cell size and shape of the blastoderm. Important events such as zygotic transcription during mid-blastula transition (MBT), yolk syncytial layer (YSL) formation and the emergence of coordinated cell movements (epiboly) occur. MBT begins during the tenth cell cycle (512-cell stage) where the zygotic genome switches on while maternal products get degraded. Also at this stage, the marginal layer of blastomeres collapse into the underlying yolk forming a syncytium with the yolk cytoplasm, termed the YSL. The second tier of cells next to the previous marginal cells now assume the marginal postion, forming the enveloping layer (EVL) cells with no cytoplasmic connections with the yolk. During the later part of the blastula period, the first cell movement termed epiboly begins in the embryo. Briefly, the superficial cells thin and spread downwards over the yolk cell while deep cells move outwards to radially intercalate with the more superficial cells, though the mixing is incomplete, and the EVL remains as a compartmentalized monolayer. These cell movements rely on cytoskeletal restructuring too.

The gastrula period (5.25-10.33hpf): Epiboly continues during this stage, accompanied by more varied morphogenetic cell movements such as involution, convergence and extension. Collectively, these processes position the three important primary germ layers, ectoderm, mesoderm and endorderm. Involution begins at about 50% epiboly at the future dorsal side of

the embryo, where superficial cells move underneath the margin and towards the animal pole. By 60% epiboly, a localized thickening called the embryonic shield appears as a consequence of rapid convergence movements. This structure is functionally equivalent to Xenopus's dorsal lip. The first cells to involute and move anteriorwards correspond to precursors of the prechordal plate. Eventually, gastrulation is deemed completed once the spreading cells completely engulf the entire yolk cell. At the end of gastrulation, a thickened structure called the tailbud forms at the posterior dorsal end of the embryo.

The segmentation period (10.33-24hpf): This period is characterized by somite development, body axis elongation and precursor formation of primary organs. At the end of this period, the first body movements of the embryo can also be visualized. Somitogenesis proceeds in a highly predictable orderly manner of three somites per hour, followed by two somites per hour after the formation of the 6^{th} somite, in an anterior-posterior manner. Simulataneously, the Kupffer's vesicle organizer is generated at the tailbud region, relaying left-right (LR) asymmetry information to the lateral plate mesoderm, placing organ primordial in their respective postions along the LR axis.

The pharyngula period (24-48hpf): During this period, the pharyngeal arches of the embryo develop rapidly such that individual arches become distinguishable. In the pericardial region, a group of highly refractile cells called the hatching gland cells is also very prominent. The embryo continues to lengthen along its AP axis, however, with a reduced rate. In addition, fins start developing, circulatory system start functioning, and pigment cells start differentiating. Also, the embryo will exhibit a marked behavioural change due to increase in tactile sentivity.

The hatching period (48-72hpf): This refers to the period of time when the larvae start hatching out of the chorion. As the time of hatching varies between individuals within and amongst clutches, it is typically not useful as a staging index. By this time, organ morphogenesis is mostly completed with the exception of the digestive system. Over the next few days, the gut and its associated structures will mature once the larva start to feed.

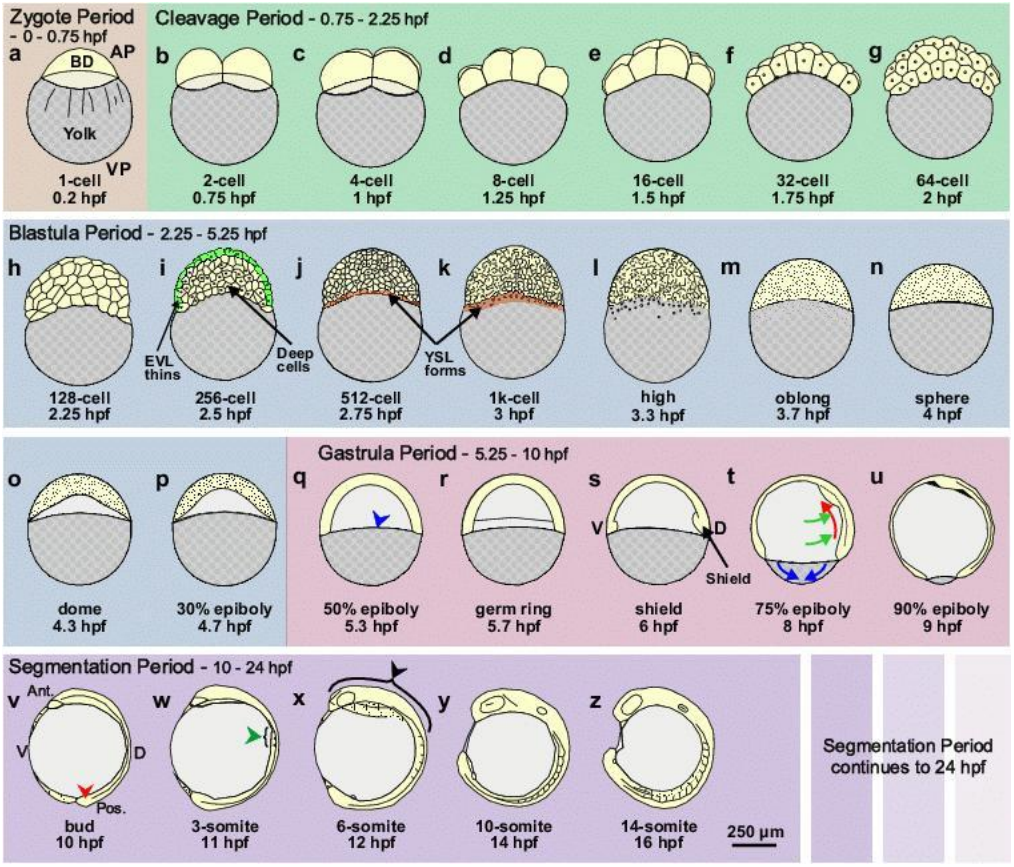

Figure 1.3.2 Schematic representation of zebrafish development from the Zygote Period to the mid-Segmentation Period. (A) Zygote period (0-0.75 hpf). (B-G) Cleavage period (0.75-2.25 hpf). (H-P) Blastula period (2.25-5.25 hpf). (Q-U) Gastrula period (5.25-10 hpf). (V-Z) Segmentation period (10-24 hpf). (modified from Kimmel et al., 1995)

1.3.3 Maternal factors and events in early embryonic polarity

One of the crucial steps in embryogenesis is the early determination of the various body axes, upon which the body plan can be laid on. However, prior to that, an important process termed oogenesis is indispensable. During oogenesis, maternal products build up and gets stored in the maturing oocyte (Selman et al. 1993). During the primary growth phase (Stage IA and IB), chromosomes decondense and DNA becomes highly extended with characteristic loops protruding laterally. This morphology is characteristic of active transcription and in fact, maternal RNAs begin to be synthesized rapidly during this time, leading to a gradual increase in oocyte volume (Baumeister 1973). Subsequently, the oocyte contacts its surrounding follicle cells, forming cell-cell junctions that permit the uptake of small molecules by the oocyte (Kessel et al. 1985). To fulfil the growing oocyte's energy requirements, mitochondria start to accumulate, and together with other structures such as the Golgi, endoplasmic reticulum, they form an electron-dense "nuage", which is implicated in germline determination (Kessel et al. 1984). The next stages (Stage II and III) involve the massive accumulation of protein and lipids necessary for egg activation and embryogenesis. In particular, the major yolk protein, vitellogenin, gets deposited in the yolk, where it will be assimilated by the growing embryo before it can feed independently. Finally, oocyte growth, which encompasses production and uptake of maternal factors, terminates during the final step of oocyte maturation (Stage IV). Morphologically, the step is characterized by the translocation of the germinal vesicle towards the pre-determined animal pole and the arrest of meiosis II metaphase stage.

A mature zebrafish oocyte is radially symmetrical around its animal-vegtal (AV) axis. Its DV axis only becomes morphologically evident at 6 hpf with the appearance of the embryonic shield. However, the molecular events that lead to that happen much earlier during the early cleavage stages. Several classical surgical experiments, performed in different teleosts, that remove the vegetal-most portion of the yolk produce radially symmetrical embryos that do not have axial structures (Oppenheimer 1936; Mizuno et al. 1999; Ober and Schulte-Merker 1999). It was observed that performing the same manipulation at later stages, progressively lead to weaker DV defects in the embryo, thus suggesting that the vegetal region of the yolk contains maternal factors that function in DV axis specification. Reinforcing this idea is another set of experiments from Jesuthasan and Strahle, which shows blocking of microtubule polymerization using nocodazole in a newly fertilized embryo gives

rise to severe ventralization, whereas the same treatment 15-20 mins post fertilization did not lead to loss of dorsal axial structures (Jesuthasan and Stahle 1997).

The initial vegetal localization followed by subsequent translocation of the dorsal determinant in teleosts seem reminiscent of the dorsal axis specification process in *Xenopus*. It is known that the sperm entry point in *Xenopus* determines the future dorsal region of the embryo via the process of cortical rotation (Vincent et al. 1986; Gerhart et al. 1989). However in zebrafish, the sperm enters through a micropyle, whose position is fixed on the chorion at the animal pole (Hart and Donovan 1983). And it is only recently that processes similar to cortical rotation is discovered through the displacement of parallel microtubule arrays (Tran et al. 2012) and proteins e.g. Syntabulin (Nojima et al. 2010). These events culminate in the local activation of the canonical Wnt/β-catenin pathway, exemplified by the appearance of nuclear-localized β-catenin, a transcription factor that positively regulates the expression of dorsal-specific transcripts such as *dharma/bozozok* (Fekany et al. 1999).

1.4 Research objectives

In zebrafish, nuclear β-catenin accumulation in cells destined to become dorsal begin as early as the 128-cell stage (Schneider et al. 1996; Dougan et al. 2003). However, unlike the situation in Xenopus (Tao et al. 2005), the mechanism by which β-catenin gets stabilized and enter the nucleus to activate dorsal gene expression is still unclear in zebrafish.

A large number of maternal RNAs become differentially distributed after fertilization (Figure 1.4) (Howley and Ho 2000). Some RNAs do not show specific localization in the blastomeres e.g. *cyclinB* (Howley and Ho 2000), whereas others like *vasa* and *nanos* localize to the cleavage furrows (Olsen et al. 1997; Yoon et al. 1997; Knaut et al. 2000; Koprunner et al. 2001). In 2005, our lab reported the asymmetric localization of a maternal *squint* RNA, a member of the Transforming Growth Factor β superfamily (Gore et al. 2005). The protein form of members of this family have been shown to be essential in a plethora of processes such as dorsal organizer formation, mesendoderm induction, nervous system patterning, anterior-posterior and left-right asymmetry specification etc. (Levin et al. 1995; Collignon et al. 1996; Lowe et al. 1996; Sampath et al. 1997; Sampath et al. 1998; Schier and Shen 2000; Thisse et al. 2000; Schier and Talbot 2001). Depending on their innate properties e.g. stability,

these secreted morphogens can act locally or at a distance (Jones et al. 1995; Chen and Schier 2001; Williams et al. 2004; Le Good et al. 2005; Tian et al. 2008) upon binding to Activin receptors and co-receptors (Gritsman et al. 1999; Gritsman et al. 2000), transmitting activation signals through Smads and other transcription factors e.g. FoxH1 (Shen and Schier 2000; Yeo and Whitman 2001), activating downstream target genes.

Through whole-mount RNA in situ staining, endogenous *sqt* RNA shows punctate localization in one or two cells of a four-cell stage embryo (Gore et al. 2005). Using fluorescently-labelled synthetic *sqt* RNA, Gore et al was able to visualize and reconstitute the transport of *sqt* RNA from the yolk to the blastoderm and its final localized position. Upon morpholino-based knockdown of maternal *sqt* RNA or ablating *sqt* RNA-containing cells, embryos develop with a loss of dorsal axial structures, similar to the ventralized phenotypes observed in Wnt/β-catenin signalling-deficient *ichabod* (*ich*) mutants (Kelly et al. 2000). This makes localized maternal *sqt* RNA an even earlier marker of embryonic dorsal than nuclear β-catenin.

However, as maternal-zygotic genetic mutants of *sqt* (MZ*sqt*) that are presumably protein nulls (Feldman et al. 1998) do not display the severe dorsal deficiencies manifested by the morphants, maternal *sqt*'s requirement and function in dorsal specification was contentious (Bennett et al. 2007; Gore et al. 2007). In this thesis, I aim to 1) address the requirement of localized maternal *squint* RNA and 2) analyze the mechanism of maternal *sqt* in early DV specification.

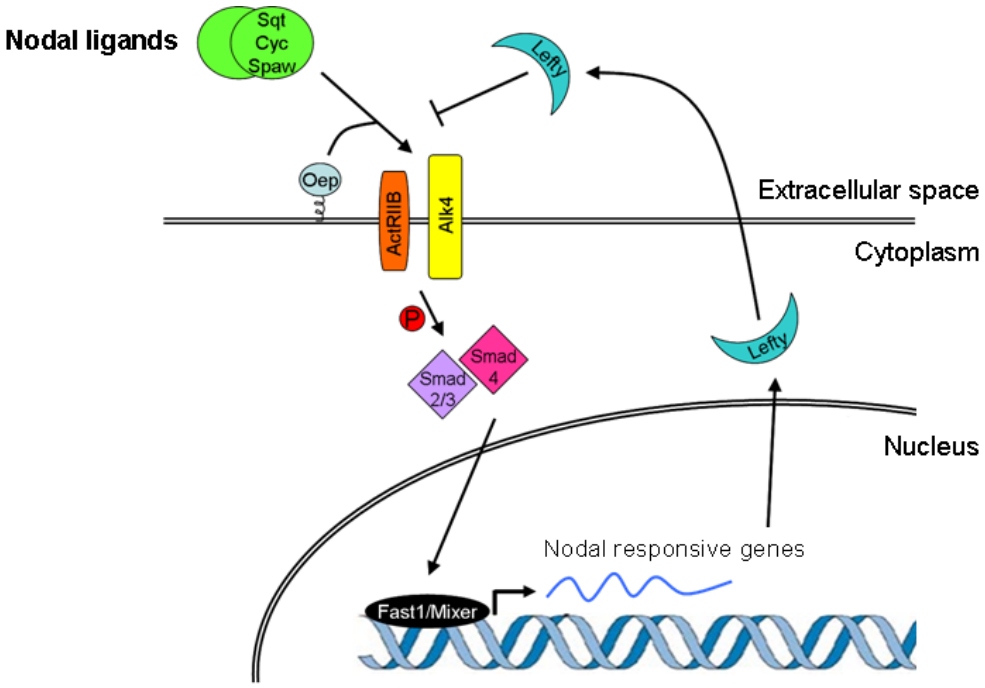

Figure 1.4 Schematic representation of Nodal pathway. Nodal signalling is activated when Nodal ligands interact with the Activin receptors and EGF-CFC co-receptors, and inhibited by Leftys. Nodal signalling is transmitted intracellularly via the phosphorylation of Smad2/3, which then associates with Smad4 and transcription factors Fast1 and Mixer, to activate downstream target gene expression.

CHAPTER II:
MATERIALS AND METHODS

2.1 Zebrafish embryo and larval cultures

All experimental procedures involving adult zebrafish and embryos were carried out in accordance with the guidelines slated by the Institutional Animal Care Use Committee (IACUC) at Temasek Lifesciences Laboratory.

2.1.1 Zebrafish maintenance and strains

AB wild-type (Johnson et al. 1994) and MZ*sqt*^{cz35}, MZ*sqt*^{hi975}, MZ*dicer*^{hu715}, MZ*oep*^{tz57} and homozygous *ich*^{p1} mutant fish were maintained at 26.5^{o}C in the fish facility (Westerfield 2007). To prepare fish for mating, pairwise crosses were set up in 2L crossing tanks fitted with separators the evening before. Next morning, the separators were removed to allow natural mating. Embryos were collected within 10 minutes of egg-laying using a sieve, and transferred into E3 medium in a 85 mm petri dish. If no injection or drug treatment was required, embryos were immediately incubated at 28.5^{o}C and staged according to hours post fertilization (hpf) as described in Kimmel et al, 1995.

2.1.2 Genotyping

The mutants MZ*sqt*^{cz35},MZ*sqt*^{hi975} and MZ*oep*^{tz57} were available in lab stocks. Their genotypes were determined by polymerase chain reaction (PCR), using primers described in (Feldman et al. 1998; Zhang et al. 1998; Golling et al. 2002) respectively. To generate fish with germ-line homozygous for *dicer*^{hu715} mutation, the germ-line replacement technique was used (Ciruna et al. 2002) (to be detailed in Section 2.1.7). Adult female zebrafish that has undergone the transplant were out-crossed to WT AB zebrafish. The embryos obtained were visually screened at 24hpf for *dicer* phenotype and then individually lysed to confirm genotype by PCR. The *dicer*^{hu715} mutation can be detected by PCR and sequencing as described in the Zebrafish Mutation Resource (http://www.sanger.ac.uk/cgi-bin/Projects/D_rerio/mutres/mutation.pl?project_id=1177&mutation_id=320). Homozygous *ich*^{p1} mutant females were identified by out-crossing with WT AB zebrafish (Kelly et al. 2000; Bellipanni et al. 2006). The mutant females used in this study yielded 100% radialized embryos lacking a head, notochord and with little trunk development (Kelly et al. 2000; Bellipanni et al. 2006).

2.1.3 Microinjection into mature oocytes and embryos

Microinjection was performed using needles with fine tips pulled from borosilicate glass micro-capillaries using a P-97 Flaming/Brown Micropipette puller (Sutter Instruments). The micro-capillaries used have an outer diameter (O.D.) of 1.0 mm and inner diameter (I.D.) of 0.58 mm with filament (Sutter Instruments). After filling the needle from the rear using a fine pipette tip, it was fitted to a microinjection setup that comprises of a micromanipulator (Narishige) attached to a pressure injection system (Harvard Apparatus). Next, the tip of the needle is clipped with a pair of forceps, and the injection drop size measured using a 1 mm stage graticule slide. Before injection, oocytes or embryos were lined on ramps moulded in 2% agarose/E3 medium in a 85 mm petri-dish. Typically, 1-2 nl of solution was injected into each oocyte or embryo. To obtain mature oocytes, adult female WT zebrafish were anaesthetized in 1X Tricaine/E3 medium (Sigma Cat.#A5040), rinsed briefly in clean E3 medium and dabbed dry using 'C'-fold paper towel. Next, the female was placed on a clean, dry 85 mm petri dish, and gentle pressure was applied on the belly in an anterior-to-posterior direction to expel mature oocytes from the body. Mature oocytes were kept inactivated during injection with 1X HanksPlus.

2.1.4 *In vitro* fertilization

Injected oocytes were fertilized by *in vitro* means. Adult male WT zebrafish were anaesthetized in 1X Tricaine/E3 medium, rinsed briefly in clean E3 medium and dabbed dry using 'C'-fold paper towel. Next, the male was slotted head-first, ventral-up into a slit cut into a soft sponge. Using a micro-capillary to tease apart the anal fins, gentle pressure was applied just under the anal fins in an anterior-to-posterior direction to collect the sperm. The collected sperm was transferred immediately into 50 µl of fetal bovine serum (FBS, Sigma Cat.# F0926) and stored on ice. To begin *in vitro* fertilization, the sperm/FBS suspension was added to the oocytes, followed by 100 µl of I-buffer and mixed well. After 30 seconds, sperms were activated by the addition of 250 µl of fructose egg water. The mixture was incubated at ambient temperature for another 2 minute 30 seconds. After fertilization, embryos were incubated at 28.5^{o}C in E3 medium.

2.1.5 Adult fish dissection

To obtain whole ovaries for total RNA extraction, adult female zebrafish were sacrificed. After anaesthetizing the fish with 1X Tricaine, it was rinsed in clean E3 medium and dabbed dry using 'C'-fold paper towel. The head was amputated with a sterile scalpel and the belly was sniped open in an anterior to posterior direction. Using a pair of fine forceps (Dumont No. 5), the skin of the belly was peeled apart to reveal the abdominal cavity. The ovary is a whitish mass located next to the swim bladder, a balloon-like structure.

2.1.6 Cycloheximide treatment to block translation

After injection, embryos were manually dechorionated using a pair of fine forceps (Dumont No. 5) in 30% Danieau's solution and kept in 1% agarose-coated 35 mm petri-dishes. Cycloheximide (CHX, Sigma Cat. #C4859) was added to the medium at the 16-cell stage to a final concentration of 10 µg/ml. The embryos were incubated at 28.5^{o}C with CHX till the 128-cell stage, when nuclear β-catenin accumulates in dorsal cells in wild-type embryos (Schneider et al. 1996; Dougan et al. 2003). To wash out the drug, the embryos were transferred to fresh 85 mm petri dishes, and rinsed with five changes of 30% Danieau's solution at 1-min intervals. Following this, the embryos were transferred into fresh 85 mm petri-dishes, incubated at 28.5^{o}C, and fixed at oblong stages in 4% paraformaldehyde/PBS for whole mount RNA *in situ* hybridization analysis. As a control for the drug treatment, dimethyl sulfoxide (DMSO, Sigma Cat. #D8418) was used in place of CHX.

2.1.7 Germline transplant to generate maternal-zygotic (MZ) mutants

For germline transplant to generate MZ mutants which are otherwise embryonic lethal, wild-type host embryos were used. To create a germline homozygous for *dicer*^{hu715} mutation in the host, host embryos were injected with 2-3 ng of *deadend* morpholino (*dnd* MO) at 1-cell stage to eliminate its own primordial germ cells (PGCs). On the other hand, donor embryos were obtained by crossing heterozygous *dicer*^{hu715}/*dicer*$^{+}$. In order to trace the transplanted cells, donor embryos were injected at 1-cell stage with 1 nl of 0.1% fluorescein 10,000 MW dextran and 80 pg of *gfp:nos*3'UTR capped RNA. As *nanos* 3'UTR (*nos* 3'UTR) was selectively stabilized in PGCs, GFP expression at 24 hpf marked the PGCs (Koprunner et al. 2001; Saito et al. 2006). The injected dextran marked all cells in the embryo uniformly.

After injection, both host and donor embryos were manually dechorionated in 30% Danieau's solution, and incubated at 28.5^{o}C till 512 cell stage. Before transplant, the transplant ramp was moistened with 30% Danieau's solution (penicillin and streptomycin added), and donor embryos were lined in a column, followed by 2-3 host embryos in each row corresponding to each donor. Using a transplant needle, approximately 100 cells were removed along the margin from a donor embryo and ~30 cells were deposited at the same position in each host. Therefore, cells from one donor can be transplanted into 2-3 embryos. After the transplant, host embryos are maintained individually in 24-well tissue culture dish (1% agarose-coated), whereas their respective donor embryos were lysed individually to obtain genomic DNA for genotyping. Host embryos that were transplanted with homozygous *dicer*^{hu715} PGCs were raised till adulthood.

2.2 Molecular biology techniques

2.2.1 Cloning

For each cloning, plasmid vectors were digested with respective restriction enzymes and compatible inserts were ligated to it using the Rapid DNA ligation kit (Roche Cat.#11635379001). Inserts were either generated by polymerase chain reaction (PCR) or by restriction enzyme digest. Ligation products were transformed into competent *Escherichia coli* strain XL1-Blue by heat-shocking at 42^{o}C for 1 min 30 seconds. Following a 1h recovery at 37^{o}C in 2x Yeast Extract Typtone (2xYT) media, transformed culture was plated on 2xYT media agar containing the relevant selection antibiotic, and kept in the 37^{o}C incubator overnight. Colonies were individually inoculated with shaking in selection media for 5h at 37^{o}C, and plasmids were extracted from the bacterial cells using an alkaline-lysis-based QIAprep spin miniprep kit (Qiagen Cat. #27106). To identify the right clone, restriction digest was performed on the extracted plasmid DNAs. The clones were subsequently sequenced and confirmed.

Plasmids encoding *sqt* ZFN1 and sqt ZFN2 nuclease pairs were obtained from ToolGen, Inc. (South Korea). The *sqt* TALENs target sites were designed using an online tool (TAL Effector-Nucleotide Targeter, TALE-NT; https://tale-nt.cac.cornell.edu/). To check for unique targeting sites, BLAST and UCSC BLAT search was performed with the zebrafish genome assembly (Zv9) using the target site sequences. The TAL effector repeats were

constructed from 4 TAL effector single unit vectors (pA, pT, pG^{NN} and pC) using the "unit assembly" method (Huang et al. 2011).

2.2.2 DNA Sequencing

In this study, sequencing on both PCR products and plasmid DNA were performed using the BigDye® Terminator Cycle Sequecing Kit (Applied Biosystems). Firstly, PCR was carried out using relevant primers on a thermocycler, and the resultant products were scanned on an automated sequence scanning machine 3730xl DNA Analyzer 34 (Applied Biosystems). DNA sequences were analyzed using softwares e.g. EditSeq, Chromas and Sequencher and compared with sequences on Ensembl Zv9 database.

2.2.3 *In vitro* capped mRNA synthesis

Plasmid templates for capped mRNA synthesis were digested with *Not*I (New England Biolabs) and electrophoresed on 0.8% agarose/1XTBE (Tris/Borate/EDTA) gel. The linearized form was excised from gel and extracted using QIAquick Gel Extraction kit (Cat.#28706). Next, the *in vitro* transcription reaction was assembled at room temperature using components from the mMessenger mMachine® SP6 Kit (Ambion®).

Linearized template	~1µg
2X NTP/CAP	10.0µl
10X Reaction Buffer	2.0µl
SP6 enzyme mix	2.0µl

Top up to 20µl using sterile water.

The transcription reaction was allowed to proceed at 37^{o}C for 2 h, followed by DNase I (1.0 µl added per reaction) digest at 37^{o}C for 40 mins. The reaction was stopped by adding one-fifth volume worth of ammonium acetate. Newly synthesized capped mRNA was purified via phenol:chloroform extraction, followed by chloroform extraction. The purified RNA was precipitated using 100% isopropanol overnight at -20^{o}C. Precipitated RNA was pelleted by cold centrifugation at 12,000 g and the RNA pellet was washed in chilled 80% ethanol. After removing the 80% ethanol, the RNA pellet was air-dried and dissolved in 20µl autoclaved, DEPC-treated (diethyl pyrocarbonate) sterile water. To examine its integrity and

concentration, 1.0µl of the mRNA sample was electrophoresed at 65 V in a 1.2% agarose/phosphate-buffer pH 6.5 gel, alongside a 0.5-10 kb RNA ladder (Invitrogen^{TM}).

Capped TALEN mRNAs were similarly transcribed *in vitro* from 1.0 µg of the respective *Not*I linearized TALEN expression vectors, using the SP6 mMESSAGE mMACHINE kit (Ambion). To synthesize capped ZFN mRNAs, *sqt*-specific ZFN plasmids were linearized with *Xho*I and transcribed using T7 RNA polymerase (Promega). RNA was was post-treated with DNase I, purified and resuspended as above,

2.2.4 Anti-sense DIG/Fluorescein labeled probe synthesis

Plasmid templates for antisense RNA probe synthesis were digested with their respective enzymes and purified as detailed earlier. The formula for the *in vitro* transcription reaction is as follows.

Linearized template	~1µg
5X Transcription Buffer (Promega)	10.0µl
100mM Dithiothreitol (DTT, Promega)	5.0µl
RNasin® Ribonuclease Inhibitor (Promega)	1.0µl
10X DIG/Fluorescein RNA labelling mix (Roche)	5.0µl
T7 RNA polymerase (Promega)	1.0µl
Top up to 50µl using sterile water.	

After incubating the above transcription reaction for 2 h at 37^{o}C, the DNA template was removed by DNase I digest at 37^{o}C for 40 mins. The reaction was stopped by addition of 1 µl of 0.5 M EDTA and the newly synthesized RNA probe was precipitated overnight at -20^{o}C using 1 µl of 4 M $LiCl_2$, 1 µl of glycogen and 100 µl of chilled 100% ethanol. The precipitated RNA was pelleted, resuspended and checked for quality and quantity as described above.

2.2.5 Tail fin-clipping

To obtain genomic DNA from adult fish for genotyping, the ‘fin-clip’ procedure was performed. Firstly, adult fish was anaesthetized in 1X Tricaine, followed by rinsing with

fresh E3 medium before drying it with 'C'-fold paper towel. Using a sterile surgical blade, 0.5mm of the tail fin was cut before returning the fish into the recovery tank that contains 2X E3 medium with 1 drop of methylene blue added to prevent fungus growth. Each clipped fish had been maintained individually until its genotype was confirmed.

2.2.6 Genomic DNA extraction

Embryos and clipped tail fins were lysed in 1X genomic DNA extraction buffer (Proteinase K added to 100 µg/ml) at 55^{o}C for 5 h. After the incubation, proteinase K was inactivated at 65^{o}C for 30 mins. To remove debris and proteins, the genomic DNA suspension was purified through phenol/chloroform and chloroform extraction and precipitated using 100% isopropanol. Next, purified genomic DNA was pelleted by centrifuging at 8,000 g and the pellet was washed in chilled 80% ethanol. After removing the 80% ethanol, the DNA pellet was air-dried and dissolved in 50-100 µl of 1X TE pH 8.0. Both quality and quantity of the genomic DNA was assayed on the Nanodrop machine.

2.2.7 Total RNA isolation

TRIzol reagent (Invitrogen) was used to extract total RNA from zebrafish whole ovaries, mature oocytes and fertilized embryos at various stages of development. Samples were homogenized in TRIzol (+ glycogen) by pumping through an 18½ G needle fitted to a 1 ml syringe. For whole ovary, this step was preceded by grinding of the tissue with a micropestle. Next, the homogenized samples were incubated at room temperature for 5 mins to completely dissociate nucleoprotein complexes. One-fifth volume of chilled chloroform was added to the sample and the mixture was shook vigorously by hand for 15 secs. Following a 2-3 mins incubation at room temperature, the mixture was centrifuged at 12,000 g for 15 mins at 4^{o}C to separate the upper aqueous, interphase and lower organic phases, which contain RNA, protein and DNA respectively. The RNA-containing aqueous phase was pipetted out into a clean tube, and precipitated for 10mins at room temperature using chilled 100% isopropanol. After incubation, RNA was pelleted by centrifuging at 12,000 g for 10 mins at 4^{o}C. Upon removing the supernatant, the RNA pellet was washed with chilled 80% ethanol, and pelleted again by centrifuging at 7,500 g for 5 mins at 4^{o}C. Finally, the RNA pellet was allowed to air-dry briefly before dissolving it in an appropriate volume of RNase-free sterile water. To remove residual genomic DNA in the total RNA prep, the total RNA

was further treated with DNaseI. After DNaseI treatment, total RNA was purified again through phenol/chloroform and chloroform extraction. Good quality total RNA runs as three distinct bands (28S, 18S and tRNA) on gel and measures around 1.9 for the A_{260}/A_{280} ratio.

2.2.8 *In vitro* reverse transcription

Complementary DNA (cDNA) was synthesized from total RNA using the Superscript II Reverse Transcriptase (Invitrogen Cat # 18064-022). cDNA synthesis was primed with either random hexamer ($p(dN)_6$, Roche Cat # 1034731) or oligo-dT ($p(dT)_{15}$, Roche #10814270001). 500-1000 ng of total RNA was denatured with 200 ng of primer in a total volume of 12.0 µl, at 70^{o}C for 10 mins and quenched on ice for 1 min. Following brief centrifugation, the following reagents were added to the denatured RNA and primer mixture on ice.

5X First Strand Synthesis Buffer (Invitrogen)	6.0µl
100 mM Dithiothreitol (DTT, Invitrogen)	2.0µl
10 mM dNTPs (Promega)	2.0µl
RNasin® Ribonuclease Inhibitor (Promega)	0.5µl
Sterile water	6.5µl

The reaction mixture was either incubated at 42^{o}C (for oligo-dT) for 2 mins or 25^{o}C (for $p(dN)_6$) for 5 mins before adding 1.0µl of Superscript II Reverse Transcriptase to each reaction. Then, the final reaction mixture (30.0 µl, termed RT+) was incubated at 42^{o}C for 1h 30mins. As a control for genomic DNA contamination, an RT- reaction (no reverse transcriptase added) was performed for every total RNA sample.

2.2.9 Polymerase Chain Reaction

Polymerase chain reactions (PCRs) were carried out with a thermocycler (Thermo Scientific and BioRad), using polymerases such as GoTaq® (Promega), HotStarTaq (Qiagen), PhusionTaq (New England Biolabs) and Taq (made in-house), according to manufacturer's instructions. Taq was used in combination with self-made CES buffer. In general, every new pair of primers was tested for specificity under different PCR conditions (1.5 mM to 2.5 mM of $MgCl_2$, different annealing temperatures).

2.2.10 Reverse Transcriptase-Quantitative Polymerase Chain Reaction

Total RNA was extracted from embryos using TRIzol reagent (Invitrogen). For cDNA synthesis, 250 ng of total RNA from WT, MZ*sqt*^{hi975} and MZ*sqt*^{cz35} embryos and 250 ng of total RNA from lacZ:glo or lacZ:sqt RNA-injected embryos were used. In every 10 µl PCR reactions, 1 µl first-strand cDNA was used. To check for genomic DNA contamination, PCR was performed to detect *actb2* (*act*), *sqt, dharma* (*dha*; *bozozok*), *vox* and *vent*. Following that, RT-PCR was performed on an ABI 7900HT Fast Real-Time PCR System (Applied Biosystems) using the comparative C_T method. In addition, control experiments to measure changes in C_T with template dilutions were performed to test whether amplification efficiencies of target (*sqt, dha, vox* and *vent*) and control (*act*) primers were similar. All results were normalized to *act.*

2.2.11 Semi-quantitative Reverse Transcriptase-Polymerase Chain Reaction

Using TRIzol reagent (Invitrogen), both genomic DNA and total RNA were extracted from single 30% epiboly stage and 2 dpf. (for *htr1ab* expression) embryos obtained from heterozygous *sqt*$^{sg27/+}$ and *sqt*$^{sg32/+}$ crosses. For genotyping, 50 ng of genomic DNA was used as template in 20 µl PCR reactions. For first-strand cDNA synthesis, 250 ng of total RNA was used in a pdN6-primed reaction using SuperScript® II Reverse Transcriptase (Life Technologies). 1 µl of first-strand cDNA was used in 20 µl PCR reactions to detect expression of *sqt*, *ring finger protein* (*rnf180), 5-hydroxytryptamine (serotonin) receptor 1A b (htr1ab), eukaryotic translation initiation factor 4E binding protein 1(eif4ebp1)* and control *actin (act).*

2.2.12 *In vitro* translation

The TNT® SP6 Coupled Rabbit Reticulocyte Lysate System (Promega) was used to transcribe and translate from the following plasmid templates: pCS2+, pCS2+sqtFL:sqt, pCS2+sqt^{STOP}, pCS2+sqt^{cz35}, pCS2+FLAGsqtFL, pCS2+FLAGsqt^{STOP}, pCS2+T-sqt and pCS2+sqtFL:glo. Using 1.0 µg of circular plasmid as template, the following reaction mixture was assembled on ice, and subsequently incubated at 30^{o}C for 1h 30mins.

Circular plasmid template	1.0µg
Rabbit Reticulocyte Lysate	25.0µl
TNT Reaction Buffer	2.0µl
Sp6 RNA polymerase	1.0µl
Amino acid mix, - Leucine	0.5µl
Amino acid mix, - Methionine	0.5µl
RNasin® Ribonuclease Inhibitor	1.0µl
Biotin-Lysyl tRNA	2.0µl

Top up to 50µl using nuclease-free sterile water.

The resultant translation products contained biotin-labeled lysine residues, facilitating subsequent detection via immuno-blotting using appropriate antibodies.

2.2.13 Identification of new *sqt* founders (F_0)

To detect *sqt* mutations in founder (F_0) embryos, at least 10 TALEN- and ZFN-injected embryos were individually lysed at 24 hpf in 20.0 µl of DNA extraction buffer for 5 h at 55^{o}C, followed by heat inactivation of proteinase K at 65^{o}C for 10 min. Genomic DNA was diluted 5-fold using 1X TE Buffer (pH 8.0), and 2 µl aliquots were used in 20 µl PCR reactions. For single nuclease pair experiments, fragments containing 100-150 base pairs upstream and downstream of the expected target sites were amplified with GoTaq polymerase (Promega). For double TALEN or TALEN+ZFN experiments, primers annealing to regions 100-150 base pairs upstream of 5' TALEN and downstream of the 3'TALEN or ZFN target sites were used in PCR from genomic DNA template using Phusion polymerase (New England Biolabs) following the manufacturer's instructions. Five µl of products from 10 single embryo PCRs were pooled, gel purified to remove primer dimers and cloned into either Promega pGEM-T easy TA cloning vector or Fermantas pJET1.2 blunt end cloning vector, and transformed using XL1-blue heat-shock competent bacterial cells. At least 48 bacterial colonies were picked for screening by PCR. PCR products were diluted 3-fold, and 1 µl was used directly for sequencing using the same primer pairs. Sequences were analyzed by comparison to the Zv9 Zebrafish Genome Assembly.

To assess the germ cell transmission rate, injected F_0 fish were raised to adulthood, and mated either with siblings or wild-type fish to obtain F_1 progeny. To screen for germ-line

transmission events at the endogenous *sqt* locus, progeny obtained from pairwise mating of potential founders were analyzed. Single embryos from 6 founder fish (3 pairs) were screened per 96-well plate. At least 30 embryos (24hpf) from each mating were collected, lysed and analyzed by PCR using the same primer pairs as used above for the transient assays. This number allowed efficient detection of germ-line transmission events (whose frequency ranged from 3-10%), and recovery of the mutation. Bands of aberrant sizes were either sequenced directly or after cloning into the pGEM®-T easy vector system. F_1 progeny of positive F_0s were raised to adulthood, and heterozygous carriers for the deletions were identified by fin-clipping and routine genotyping PCRs.

2.3 Biochemistry

2.3.1 Extraction of total protein from embryos

Embryos were manually dechorionated using a pair of fine forceps in 30% Danieau's solution. Then, they were transferred into a 1.5 ml eppendorf tube using a fire-polished glass pipette. The 30% Danieau's solution was removed and replaced with 100 µl of ionic lysis buffer (with protease inhibitor, 1 tablet /10 ml of ionic lysis buffer) (per 50 embryos). Embryos were homogenized using a 1 ml syringe fitted with a 26 1/2G needle. Then, the contents were briefly spun at 200 g, 4^{o}C for 10 secs to pellet the debris. The supernatant was collected into a fresh tube and stored at -20^{o}C.

2.3.1 SDS-PAGE separation of proteins

Denatured proteins were separated on 10-12% sodium dodecyl sulphate-polyacrylamide gels (SDS-PAGE) [10-12% (v/v) acrylamide/bis-acrylamide (29:1, Bio-Rad), 375 mM Tris-HCl pH 8.8 (for separating gel) or pH 6.8 (for stacking gel), 0.1% (v/v) SDS, 0.1% (w/v) ammonium persulphate (APS), 0.4% (v/v) N, N, N', N'-Tetramethylethylenediamine (TEMED)] using a Bio-Rad mini-gel electrophoresis system at 25 mA till the samples pass through the stacking gel and at 25-50 mA till the dye front reaches the end. Using the pre-stained Spectra Multicolor Broad Range Protein Ladder (10 – 230 kDa), the extent of protein migration was estimated. After SDS-PAGE, the separated proteins were transferred by electrophoretic blotting onto Hybond-C Extra membranes (GE Healthcare) in 1X transfer buffer at 100 V for 100 min.

2.3.2 Immuno-blotting

For detecting *in vitro* translated products, immunoblotting was performed using avidin and biotinylated HRP (1:200 dilution) (Ultra-sensitive ABC peroxidase Rabbit IgG Staining kit; Pierce). Proteins were detected by Kodak Biomax MS film using the SuperSignal West Femto Maximum Sensitivity Substrate (Pierce). FLAG epitope-tagged peptides were detected with anti-FLAG M2 mouse monoclonal primary antibody (1:2500 dilution; Sigma) and HRP-conjugated antimouse IgG secondary antibody (1:5000 dilution; DAKO).

2.4 Staining and imaging techniques

2.4.1 Whole-mount RNA in situ hybridization (WISH)

For detecting endogenously expressed genes, whole embryos were subjected to RNA *in situ* hybridization. Embryos were fixed using either 4% paraformaldehyde/1X PBS or 4% paraformaldehyde;4% sucrose/1X PBS, overnight at 4^{o}C. Next day, they were washed 3 times 10 mins each with 1X PBST (1X PBS + 0.1% Tween20), dechorionated and dehydrated using ascending grades of methanol. Embryos were stored in 100% methanol at –20^{o}C for at least a day.

On the first day of WISH, embryos were rehydrated using descending grades of methanol and washed 2 times for 10 mins with 1X PBST. Embryos were then treated with 2.5 µg/ml of Proteinase K briefly (duration of treatment depends on embryo stage) to render cells more permeable to the probe. This was followed by fixation to inactivate Proteinase K and embryos were subsequently washed thoroughly using 1X PBST. Prior to probe hybridization, embryos were equilibrated in pre-hybridization buffer at 65^{o}C for 4 hours, followed by the antisense probe-containing hybridization solution overnight at 65^{o}C. After hybridization, the embryos were washed multiple times with high stringency 2X SSC and 0.2X SSC containing buffers at 65^{o}C and 1X maleic acid buffer (MAB) at room temperature. Then, embryos were blocked in 0.5% Blocking Reagent (Roche) in 1X MAB for 1 h, before the addition of 1:2000 dilution of anti-DIG antibody conjugated with alkaline phosphatase (Roche) in blocking buffer. The antibody was pre-adsorbed with fish powder to reduce non-specific binding. Typically, the embryos were allowed to incubate with the antibody overnight at 4^{o}C.

After antibody incubation, embryos were washed repeatedly using 1X MAB. Then, they were washed 3 times 10 mins with freshly prepared 1X NTMT buffer. Staining was developed in the dark using a precipitating substrate BM Purple (Roche). For *sqt* in situs, staining was performed using diluted BM Purple/1X NTMT (1:1) over a span of 2-3 days, mostly at 4^{o}C, but with 4-5 h at room temperature each day. Upon completion of staining, embryos were washed in 1X PBST 3 times 10 minutes each and fixed using 4% PFA to terminate alkaline phosphatase activity. After that, embryos were washed with PBST and cleared in PBST: Glycerol (1:1). For imaging, embryos were mounted in 100% glycerol.

2.4.2 Anti-β-catenin antibody staining

To detect nuclear β-Catenin, embryos at the 512-cell stage were fixed in 4% paraformaldehyde/PBS at room temperature for 4.5 h, washed, dechorionated and dehydrated in ascending grades of methanol. The embryos were incubated in 100% methanol for 30 mins at room temperature, rehydrated and blocked in 1% BSA/1% DMSO/1X PBST for 2 h and incubated with a rabbit polyclonal anti-β-Catenin antibody (1:200 dilution; Sigma C2206), followed by detection using Alexa488-conjugated goat anti-rabbit secondary antibody (1:1000 dilution; Molecular Probes).

2.4.3 Nuclei/DNA staining

After the antibody staining, embryos were incubated at 1:10000 dilution of 4',6-diamidino-2-phenylindole (DAPI; Sigma) for 30 mins at room temperature and subsequently washed thrice 10 mins each with 1X PBST.

2.4.4 Imaging

Live embryos injected with fluorescent RNAs or expressing Sqt-GFP fusion protein were manually dechorionated, mounted in 2.5% methylcellulose (Sigma) and visualized using a Zeiss Axioplan2 microscope with a CoolSNAP HQ camera (Photometrics). MetaMorph (Universal Imaging Corporation) and ImageJ (NIH) software packages were used to acquire and process images. Stained embryos from in situ hybridization and immunohistochemistry experiments were mounted in 100% glycerol and imaged using a

Zeiss Axioplan2 microscope equipped with a Nikon DXM1200 color camera. Images were acquired using ACT-1 software (Nikon) and cropped using Adobe Photoshop. For β-catenin- and DAPI-stained embryos, images were acquired using a Zeiss LSM 5 Exciter upright confocal microscope. To quantify β-catenin positive nuclei, 15-25 optical sections at 1.76 µm intervals starting from the yolk syncytial layer nuclei were examined per embryo. We detected β-catenin-positive nuclei in many sections. However, owing to intense membrane and cytoplasmic β-catenin staining that obscured nuclear staining upon z-projection of all sections obtained, three serial confocal sections for each embryo were selected, z-projected using LSM Image Browser software, and cropped using Adobe Photoshop.

2.4.5 Measurement of expression domains

Animal pole view images of embryos stained for *gsc* were used. In ImageJ, I drew a best-fit circle for the circumference of the embryo using the Circle tool. Using the xy coordinates, the diameter of the circle along the x- and y-axes and its center were determined. The Radial Grid tool in ImageJ and the center coordinates were used to mark the center, and using the Angle and Measure tools the angle of *gsc* expression was determined.

2.5 Recipes

E3 medium

5 mM	NaCl
0.17 mM	KCl
0.33 mM	$CaCl_2$
0.33 mM	$MgSO_4$

25X Tricaine (3-amino benzoic acidethylester)
400 mg Tricaine powder
97.9 ml double distilled water
Approximately 2.1 ml 1M Tris pH 9.0
Adjust pH to 7.0

I-buffer

116 mM	NaCl
23 mM	KCl
6 mM	$CaCl_2$
2 mM	$MgSO_4$
29 mM	$NaHCO_3$
0.5%	Fructose

Adjust pH to 8.0

HanksPlus (Hank's with BSA)

0.137 M	NaCl
5.4 mM	KCl
0.25 mM	Na_2HPO_4
0.44 mM	KH_2PO_4
1.3 mM	$CaCl_2$
1.0 mM	$MgSO_4$
4.2 mM	$NaHCO_3$

Danieau's Solution (30X)

1740 mM	NaCl
21 mM	KCl
12 mM	$MgSO_4 \cdot 7H_2O$
18 mM	$Ca(NO_3)_2$
150 mM	HEPES buffer

Add water to 1 L and stir until dissolved. Store at 4°C. The pH is 7.6.
For working solution, dilute 100X.

DNA extraction buffer

10 mM	Tris pH 8.2
10 mM	EDTA
200 mM	NaCl
0.5 %	SDS
100 µg/ml	Proteinase K

Ionic lysis buffer

50 mM	Tris pH8.0
150 mM	NaCl
0.5%	NP-40
0.5%	Deoxycholic acid
0.05%	SDS

10X TGS (Western blot running buffer)

30.3g	Tris-base
144.1g	Glycine
1%	SDS

Top up to 1 litre with sterile water
Store at 4 ^oC

1X Transfer buffer

1X	TGS
20%	Methanol

Store at 4^oC

TBST

20ml	1M Tris (pH7.5)
30ml	5M NaCl
5ml	Tween 20

Top up to 1 litre with sterile water

PBSTw

1X	PBS pH7.4 (DEPC-treated)
0.1%	Tween 20

4%PFA (paraformaldehyde)

2 g	PFA
50 ml	1X PBS pH7.4

Dissolve at 65.0^{o}C for ~2hours. Invert tube every 20mins.
Filter with 0.45µm.
Store at 4^{o}C.
Use within a week.

Fish Fix

2 g	PFA
2 g	sucrose
50 ml	1X PBS pH7.4

Dissolve at 65.0 ^{o}C for ~2hours. Invert tube every 20mins.

6 ul	1M $CaCl_2$

Filter with 0.45µm.
Store at 4^{o}C.
Use within a week.

Hybridization solution

50%-65%	Formamide
5X	SSC
1mg/ml	Torula RNA
100ug/ml	Heparin
1X	Denhardt's solution
0.1%	CHAPS
10mM	EDTA
0.1%	Tween 20
9mM	Citric acid (to adjust pH to 6.5)

FSTw

50-65%	Formamide
5X	SSC
0.1%	CHAPS
0.1%	Tween 20
9mM	Citric acid (to adjust pH to 6.5)

MABTw

0.1M	Maleic acid
0.15M	NaCl

Adjust pH to 7.2-7.5 using 5M NaOH

NTMT

0.1 M	Tris-HCl pH 9.5
50 mM	$MgCl_2$
0.1 M	NaCl
1 mM	levamisole

0.1%	Tween 20

CES Buffer

375 mM	Tris-HCl (pH 8.8 at 25°C),
100 mM	$(NH_4)_2SO_4$,
0.5 %	Tween 20
2.7 M	Betaine
6.7 mM	DTT
6.7 %	DMSO
55 ug/ml	BSA

CHAPTER III:
RESULTS

3.1 Is there a maternal requirement for squint?

In 2005, our lab reported that asymmetrically localized maternal *sqt* transcripts mark the future dorsal region of zebrafish embryos (Gore et al. 2005). Further experimentation such as morpholino-based *sqt* knock-down and using cell-ablation to remove *sqt* RNA-containing blastomeres produce a range of severely ventralized phenotypes, suggesting a function for maternally-deposited *sqt* transcripts in early dorso-ventral patterning. However, these observations were not supported by the mild dorsal deficiencies manifested by MZ*sqt*^{cz35} and MZ*sqt*^{hi975} embryos, many of which survive to adulthood (Erter et al. 1998; Feldman et al. 1998; Feldman and Stemple 2001; Aoki et al. 2002; Amsterdam et al. 2004; Bennett et al. 2007; Pei et al. 2007). Hence, the role of maternal *sqt* was a matter of debate (Bennett et al. 2007; Gore et al. 2007).

3.1.1Morpholino-based knockdown of *sqt*

In order to examine the immediate effect of *sqt* morpholinos (*sqt* MOs) on dorso-ventral (DV) patterning, I looked at expression of early dorsal markers in injected embryos. To target maternal *sqt* RNA, *sqt* MOs were injected into unactivated eggs, which were subsequently fertilized using wild-type sperm. Injected embryos were fixed at high and oblong stages, and subjected to whole mount RNA in situ hybridization for detecting *goosecoid* (*gsc*), an early dorsal marker. I observed the loss of *gsc* expression in *sqt* MO-injected embryos (Figure 3.1.1), consistent with the loss of dorsal structures observed in *sqt* morphants reported previously (Gore et al. 2005). Control MO-injected embryos show robust *gsc* expression at comparable stages, similar to uninjected wild-type embryos (Figure 3.1.1). Thus, maternal *sqt* is required for the initiation of early dorsal gene expression.

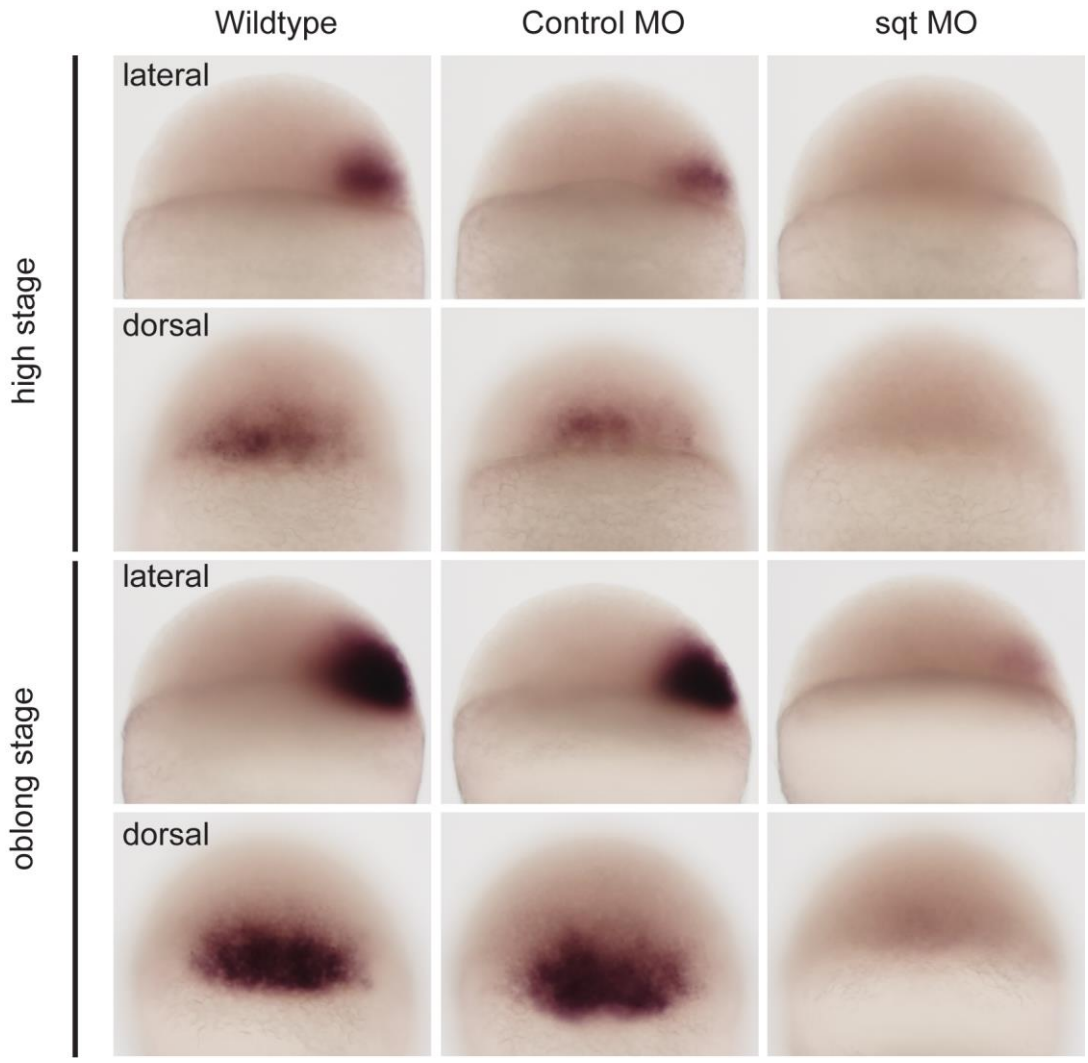

Figure 3.1.1 Early loss of dorsal in *sqt* morphants. Lateral and dorsal views of wild-type and control MO-injected embryos show early expression of *gsc* at high and oblong stages. At comparable stages, *sqt* MO-injected embryos show either reduced or total loss of *gsc* expression.

3.1.2 MZ*sqt* genetic mutants

Both sqt^{cz35} and sqt^{hi975} are molecular lesions located at the genomic *sqt* locus on zebrafish's chromosome 21. The sqt^{cz35} allele was generated by a spontaneous insertion of an approximately 1.9 kb fragment in exon 1 of *sqt*, whereas the sqt^{hi975} allele arose from a retroviral-based insertion of a 6.0 kb sequence into exon 2 of *sqt*. As both *cz35* and *hi975* insertion sequences have multiple translation stop signals, both alleles were regarded as genetic nulls.

Loss of *sqt* results in embryos exhibiting varying degrees of cyclopia and reduction in forebrain structures and prechordal plate. Studies from several labs have suggested that the incomplete penetrance of the *sqt* phenotype is due to partial redundancy with *cyclops (cyc)*, a second nodal-related gene in zebrafish, in mesoderm development, as well as environmental and genetic factors. For example, raising embryos at a higher temperature can significantly increase the phenotypic penetrance of *sqt*, whereas the same temperature shift does not affect wild-type embryos. Pei et al., 2007 further demonstrated that the sensitivity of *sqt* phenotypic penetrance towards alterations in temperature is likely due to compromised Heat-shock protein 90 (HSP90)'s function in the genetic background of *sqt* mutants.

It is noteworthy that the notion of no maternal requirement for *sqt* was based entirely on the analysis of sqt^{cz35} and sqt^{hi975} genetic mutants, on the assumption that they are nulls. But are they really complete RNA and protein nulls? Expression of gsc in wild-type embryos dermacates early dorsal (Figure 3.1.2A). Loss of early *gsc* expression is observed via MO-mediated knockdown of maternal *sqt* (Figure 3.1.1 and 3.1.2B). In contrast, the initiation of early *gsc* expression is unaffected in MZ*sqt*, MZ*oep* and *sqt;cyc* double mutant embryos at comparable stages (Figure 3.1.2C,D,). Taken together, these observations suggest that maternal *sqt* RNA but not functional Nodal signalling is required for the early initiation of dorsal *gsc* expression.

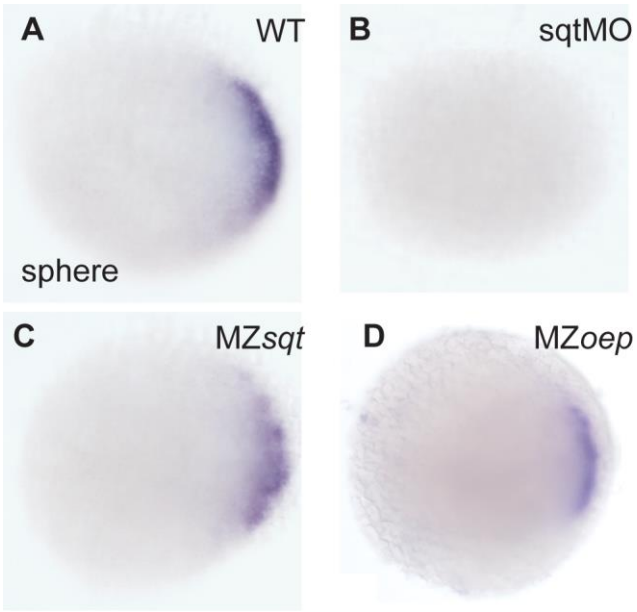

Figure 3.1.2 Presence of dorsal in *sqt* signaling mutants. At sphere stage, *sqt* MO-injected embryos exhibit loss of gsc expression (B). In contrast, gsc expression is observed in MZ*sqt* (C) and MZ*oep* (D) mutant embryos, similar to that observed in wild-type (A). Animal pole views.

3.1.3 Detection of maternal *sqt* mutant (*sqt*^{mut}) transcripts in MZ*sqt*

As maternal *sqt* is present as transcripts in wild-type ovaries, oocytes and early cleavage stage embryos (Gore and Sampath 2002), I first examined the presence of *sqt* transcripts in embryos obtained from MZ*sqt*^{cz35} and MZ*sqt*^{hi975} via semi-quantitative RT-PCR. I observed that similar to wild-type, *sqt*^{cz35} and *sqt*^{hi975} transcripts (*sqt*^{mut} transcripts) are detected at 4-cell stage (Figure 3.1.3A panel I and II), indicating that maternal *sqt* RNA is still made and deposited in the eggs by MZ*sqt* females. Using *sqt* intron II-spanning primers on p(dN)$_6$-primed cDNA, I detected two different PCR products (615 bp and 696 bp, Figure 3.1.3A panel I). Upon sequencing, the 615 bp product corresponds to *sqt* with intron II spliced, whereas the 696 bp product still retains the 81 bp intron II. On the other hand, using the same PCR primers on oligo-dT-primed cDNA, I only detected the 615 bp spliced product in wild-type and MZ*sqt* 4-cell embryos (Figure 3.1.3A panel II). Taken together, the data suggests that both maternal wild-type and *sqt*^{mut} transcripts exist as non-polyadenylated un-spliced forms, as well as, polyadenylated spliced forms.

The presence of *sqt* transcripts in MZ*sqt* embryos was further confirmed and quantitated using reverse transcriptase-quantitative PCR (RT-qPCR). At 1-cell and 4-cell stages, the level of expression of maternal *sqt* transcripts do not show a significant difference between wild-type and MZ*sqt* samples. However later during gastrulation, when zygotic *sqt* expression is expected to peak, MZ*sqt* samples recorded a decrease in *sqt* levels (Figure 3.1.3B). This observation is consistent with the inability of maternal *sqt*^{mut} RNA to encode functional wild-type Sqt protein (discussed later in Section 3.1.5 and (Feldman et al. 1998)), which is required to induce zygotic expression of *sqt* (Meno et al. 1999; Pogoda et al. 2000; Shimizu et al. 2000; Sirotkin et al. 2000).

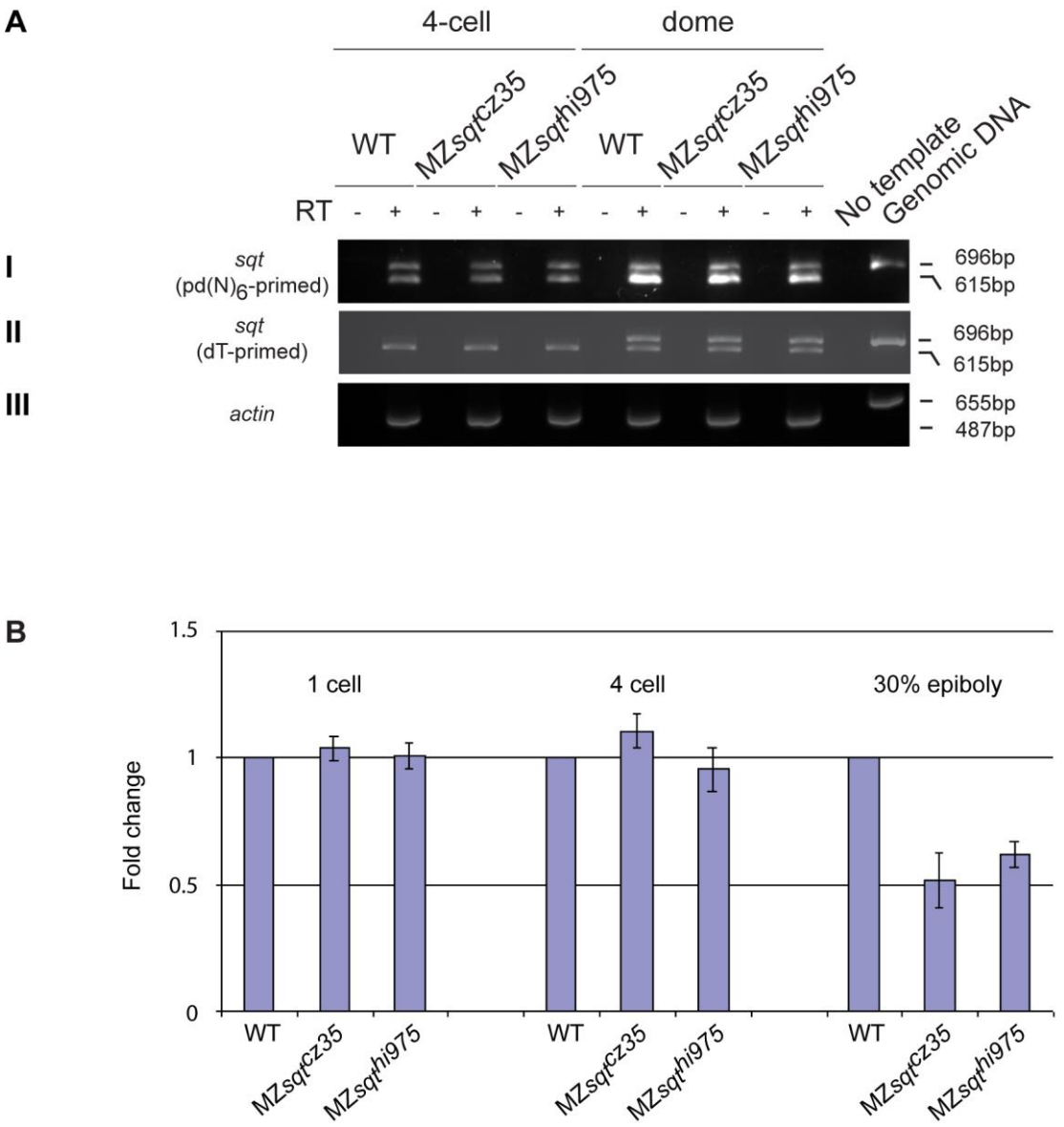

Figure 3.1.3 Presence of un-spliced and spliced maternal *sqt* RNA in MZ*sqt* mutant embryos. (A) Semi-quantitative RT-PCR using pd(N)6-primed cDNAs (panel I) or oligo-dT-primed cDNA (panel II) to detect *sqt* RNA in 4-cell and dome stage wild-type, MZ*sqt*^{cz35} and MZ*sqt*^{hi975} embryos. PCR using pd(N)6-primed cDNA shows un-spliced (696 bp) and spliced *sqt* (615 bp) RNA. Spliced *sqt* product is detected in oligo-dT-primed cDNA at early stages, and no PCR product is detected in RT- and no template controls. *actin* RT-PCR (panel III) and genomic DNA PCR were used as positive controls. (B) Reverse transcriptase-quantitative PCR to detect *sqt* RNA show that maternal *sqt* transcript levels in MZ*sqt* mutants are similar to that of wild-type embryos at the 1-cell and 4-cell stage, and reduced *sqt* transcript levels are observed at gastrula stages.

3.1.4 Architecture of *sqt*^{cz35} full-length transcript

From total RNA extracted from whole ovary of a MZ*sqt*^{cz35} female, I generated first-strand cDNA using oligo-dT primers. Using two sets of primers (F1+R1, F2+R2, Figure 3.1.4A) and MZ*sqt*^{cz35} ovary cDNA as PCR template, I amplified two overlapping fragments of ~2.2 kb and ~1.4 kb respectively. In the second round of PCR, using primer pair F1+R2 and the two overlapping PCR fragments as template, I cloned the full-length ~ 3.2 kb *sqt*^{cz35} transcript. After sequencing, full-length *sqt*^{cz35} transcript was found to have both 5' and 3' un-translated regions (UTRs) like wild-type *sqt* RNA. Except for its exon 1 which is interrupted at position 136 by an ~ 1.9 kb *cz35* sequence, both exon 2 and 3 of *sqt*^{cz35} transcript are intact (Figure 3.1.4B). This indicates that non-truncated *sqt*^{cz35} transcript is made in MZ*sqt*^{cz35} females.

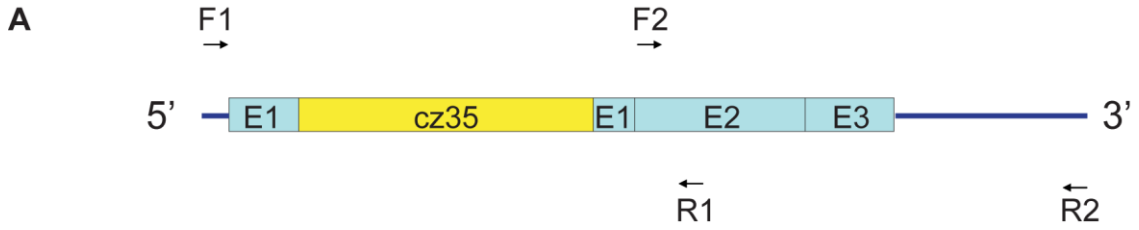

B

```
WT          ACGAGCTTTATTTCAATAACTGCGTGTGGATTATTACCTTGATTTGACATGTTTTCCTGC 60
cz35        ACGAGCTTTATTTCAATAACTGCGTGTGGATTATTACCTTGATTTGACATGTTTTCCTGC 60
            ************************************************************

WT          GGGCTCCTGAGCGTAGTTTTGGCCCTCGCGGTCGGCCTGGTGAGCTGCACGGGAAACCTT 120
cz35        GGGCTCCTGAGCGTAGTTTTGGCCCTCGCGGTCGGCCTGGTGAGCTGCACGGGAAACCTT 120
            ************************************************************

WT          GCTGGATTTCAAGAG---------------------------------------------- 135
cz35        GCTGGATTTCAAGAGACTAGAGATGCGCGGTTGGCGGTTATAGCCGCGGACTCCGCGGAT 180
            ***************

WT          ------------------------------------------------------------
cz35        AAACCGCGGATCGGGCGGATGACGTTACGAAAAAATAATATTTTAATTAAATTCGGGCGG 240

WT          ------------------------------------------------------------
cz35        GTGGCGGGCGGTTGTACTGATTTTATATTCATAGCTGGCGCACCAACGAAAAAGCCTAGG 300

WT          ------------------------------------------------------------
cz35        ACTGACTTCACAGAATGGGAGGAGGAATCGGATACATTAATTCTGGATGAAGTGTACAGA 360

WT          ------------------------------------------------------------
cz35        AGTATTCCTCTACAAACTTCCGTATAGACGGATCAGCAGAGGAAAATCTACTTTCCCTTT 420

WT          ------------------------------------------------------------
cz35        GGGAGAAATAAGACCAGGCATTCCCATGACTACAGCACCTTTCCAAGAGAATTCTATGCA 480

WT          ------------------------------------------------------------
cz35        TTTCAGCAACAAGTGCTGCGAGCGAGCGCTCCTTCAGTGCAGCAGGGCGCATTATAGTGG 540

WT          ------------------------------------------------------------
cz35        CTATGCAGGCGCTCCCGTCTGAATCCTGACACTGTAGATGCTATTTTATTCCTGCATTGT 600

WT          ------------------------------------------------------------
cz35        GCCAAGAAAAAATCAAACTAGACCTAAGGTCAGGCATATTAAACCAATTAGCCTATGTTA 660
```

Figure 3.1.4 Architecture of full-length *sqt*^{cz35} mutant transcript. (A) Schematic of *sqt*^{cz35} mutant transcript and position of cloning primers (F1, F2, R1 and R2). Dark blue bars indicate the UTRs. E1, E2 and E3 represent *sqt* exons. *cz35* insertion is represented by a yellow bar. (B) Sequence alignment of full length wild-type *sqt* and mutant *sqt*^{cz35} transcripts.

```
WT              ------------------------------------------------------------
cz35            TTTAGGCTACACATATGTTCAATATAAACTTTTGAGTTCGGTCAGCTGATAATTTTACGT 720

WT              ------------------------------------------------------------
cz35            TCATATTGGTTTAGCCTATTCTATTCTAGACATGTTGGCCTCGCTTTTACGTTCCGAGGC 780

WT              ------------------------------------------------------------
cz35            TATTTTGCCAGAATTTCTTTGTCGCAAATTTAATGGCGTATTATTTCGTTATGCTTCAAG 840

WT              ------------------------------------------------------------
cz35            TTTGAGGGGAATGGGGATGATCCTAAGTCCATGGGTTATTGGGGCACTTGTCATACATGC 900

WT              ------------------------------------------------------------
cz35            ACTTTAGCCTGGTCAGGTTCGCTCAAAGAGGGATGGCATATCTATTTTTCTAATTTAATT 960

WT              ------------------------------------------------------------
cz35            TCTAATTGTGGGGGTGACTGATCCTACACAAGTTTGAGGGGAATGGGGATGATCCTAAGT 1020

WT              ------------------------------------------------------------
cz35            CCATGGGTTATTGGGGCACTTGTCATACATGCACTTTAGCCTGGTCAGGTTCGCTCAAAG 1080

WT              ------------------------------------------------------------
cz35            AGGGATGGCATATCTATTTTTCTAATTTAATTTCTAATTGTGGGGGTGACTGATCCTACA 1140

WT              ------------------------------------------------------------
cz35            AAAAAATAGTCGNAAAACTGTGCCCATTAATTAGATGTGCAAGGCAAGCAGGTATACGTT 1200

WT              ------------------------------------------------------------
cz35            TTTGGGGTTGCTATGGACAACTACAAATGTAAACATTAATGTAAATGACTTATTCTATCT 1260

WT              ------------------------------------------------------------
cz35            ATTTACTAAAAATTAAGTGAAATAGGCATTTAGTAGTAGGCTAAATAGCAGCATGTTGAA 1320

WT              ------------------------------------------------------------
cz35            ATGATGTGTCAATGCGTTTTCTATTAGGCTACAATAAAAAAAGTTGTATAGTACAGTGCG 1380

WT              ------------------------------------------------------------
cz35            TTTAATTTAGGCTATTTATTTATTTTTGTCCCTGTGCGCCGATTGGAGACGGAGTTCACT 1440
```

```
WT              ------------------------------------------------------------
cz35            GCTGATATTCTGAGAGCTCGGGCGCTTCTCATTTCTTATTTGTGCATCCTCGTTTCCTTT 1500

WT              ------------------------------------------------------------
cz35            CCTTGCTTTCTTTCCTCGTGTTTCCACCCCACCGGGATACGAGGGAAGGACGCAAGGAAA 1560

WT              ------------------------------------------------------------
cz35            AGACTGAAGGACCGAGGAATCGAATCAAGTGAAAAGACACGTCCTCGTATCTTTAGCGTC 1620

WT              ------------------------------------------------------------
cz35            ACTTCAAAGCGTCGTCAATTAATGACTTACACGTTTGGATTAACTGCATGTCTACATTAA 1680

WT              ------------------------------------------------------------
cz35            AGTCATTCTCTATTATATAATGATCAATAAAGAAACATTCATTTAATAAAAAAAAGGAAT 1740

WT              ------------------------------------------------------------
cz35            AAGCCATTCAAATAAAGAGCCCAATCAGCAGATGGCGGGCGGGTGCGGTTTTAAAAATTG 1800

WT              ------------------------------------------------------------
cz35            GTCTAAAATGTTAGTGCGGATGGATGGCGGACGGATGATTAATTTTGTCATGCGGTTGCG 1860

WT              -----------------------------------ACCCTCAGGAATAAAATGCGAGC 158
cz35            GATGAAATAATAGCCCATCCGCGCATCTCTACAAGAGACCCTCAGGAATAAAATGCGAGC 1920
                                                    **********************

WT              AGCTGGCAGAAACGGCGGAGGTCGGGCAGGTCACGGCCGACATCTGACCAGATATCCGCT 218
cz35            AGCTGGCAGAAACGGCGGAGGTCGGGCAGGTCACGGCCGACATCTGACCAGATATCCGCT 1980
                ************************************************************

WT              GTATATGATGCACCTCTACCGGACACTTCTGACTGGAGACGAAAAACACTTCAGCCATGA 278
cz35            GTATATGATGCACCTCTACCGGACACTTCTGACTGGAGACGAAAAACACTTCAGCCATGA 2040
                ************************************************************

WT              GAATCCAACTCTTTACGAGTCTGACTCCGTCTTGAGCCTCGTCGCTAAAAGTTGTCATCA 338
cz35            GAATCCAACTCTTTACGAGTCTGACTCCGTCTTGAGCCTCGTCGCTAAAAGTTGTCATCA 2100
                ************************************************************

WT              GGTTGGTGACAAATTCGCAGTGACATTTGACATGTCCTCCATATCAGCAAGCGATGACGT 398
cz35            GGTTGGTGACAAATTCGCAGTGACATTTGACATGTCCTCCATATCAGCAAGCGATGACGT 2160
                ************************************************************

WT              CCAGCGAGCTGAACTTCGCATTCGGCTTCCGCATCTCAGGTCTGAGTTGGAGGTGGATAT 458
cz35            CCAGCGAGCTGAACTTCGCATTCGGCTTCCGCATCTCAGGTCTGAGTTGGAGGTGGATAT 2220
                ************************************************************
```

```
WT              TTATCACGCATCTACACCGGAGTGTGAGAGAAGCCCCTGCGAAGAAGTCCGGGTCCACCT 518
cz35            TTATCACGCATCTACACCGGAGTGTGAGAGAAGCCCCTGCGAAGAAGTCCGGGTCCACCT 2280
                ************************************************************

WT              GGGAACCTTGAACGCCAACCCGATTAACTCAACCTTCCGCTCCTCTTGGAGGATCTTCAA 578
cz35            GGGAACCTTGAACGCCAACCCGATTAACTCAACCTTCCGCTCCTCTTGGAGGATCTTCAA 2340
                ************************************************************

WT              CATCACTGCGCTCCTCAAGTACTGGTTGCACCAGAGTGAGCGTGTGCCGTTTGAGGAACC 638
cz35            CATCACTGCGCTCCTCAAGTACTGGTTGCACCAGAGTGAGCGTGTGCCGTTTGAGGAACC 2400
                ************************************************************

WT              CACACAGATGCCGCCAATGGCTGAGGGACACAAGAGCGTTCATCATCCTACAGCGAACCG 698
cz35            CACACAGATGCCGCCAATGGCTGAGGGACACAAGAGCGTTCATCATCCTACAGCGAACCG 2460
                ************************************************************

WT              AGTGATGATGGTGGTTTACTCCAAGCAGAACCGGGCAAAGACGTCCACTCTCATCCGGAC 758
cz35            AGTGATGATGGTGGTTTACTCCAAGCAGAACCGGGCAAAGACGTCCACTCTCATCCGGAC 2520
                ************************************************************

WT              TGCCGAGCACTCCAAGTATGTAGCTCTGGATCGGGCTGGTGGTGGAAGTGAACCTGTGCC 818
cz35            TGCCGAGCACTCCAAGTATGTAGCTCTGGATCGGGCTGGTGGTGGAAGTGAACCTGTGCC 2580
                ************************************************************

WT              TCGGCGCCACAGAAGGAACCACAGAACTGATGATAGGGTCCGCGATGCAGCAGCAGGGAT 878
cz35            TCGGCGCCACAGAAGGAACCACAGAACTGATGATAGGGTCCGCGATGCAGCAGCAGGGAT 2640
                ************************************************************

WT              GATTCCTGGTGTTTCCCATGAAGGTGGAGAGAAGAAACCTCTCTGCAAGAAGGTGGATAT 938
cz35            GATTCCTGGTGTTTCCCATGAAGGTGGAGAGAAGAAACCTCTCTGCAAGAAGGTGGATAT 2700
                ************************************************************

WT              GTGGGTGGACTTTGATCAGATTGGTTGGAGCGACTGGATTGTTTATCCAAAGCGTTACAA 998
cz35            GTGGGTGGACTTTGATCAGATTGGTTGGAGCGACTGGATTGTTTATCCAAAGCGTTACAA 2760
                ************************************************************

WT              CGCTTATCGGTGTGAAGGCAGTTGTCCCACACCAGTAGATGAAACCTTCACTCCAACAAA 1058
cz35            CGCTTATCGGTGTGAAGGCAGTTGTCCCACACCAGTAGATGAAACCTTCACTCCAACAAA 2820
                ************************************************************

WT              CCATGCATACATGCAGAGTCTTTTGAAGCTGCACCACCCAGATCGCGTCCCATGCTTGTC 1118
cz35            CCATGCATACATGCAGAGTCTTTTGAAGCTGCACCACCCAGATCGCGTCCCATGCTTGTC 2880
                ************************************************************

WT              CTGCGTACCCACCCGTCTGGCTCCACTCTCCATGCTCTACTATGAGAATGGCAAGATGGT 1178
cz35            CTGCGTACCCACCCGTCTGGCTCCACTCTCCATGCTCTACTATGAGAATGGCAAGATGGT 2940
                ************************************************************

WT              CATGAGACACCATGAAGGCATGGTTGTTGCAGAATGCGGCTGCCACTGATTCTTCAAACC 1238
cz35            CATGAGACACCATGAAGGCATGGTTGTTGCAGAATGCGGCTGCCACTGATTCTTCAAACC 3000
                ************************************************************
```

```
WT              CCAAAGGAACTCAACTCTAGCACTTTGGATATGCTCCTTGACCCCAAAAATATGTATTTA 1298
cz35            CCAAAGGAACTCAACTCTAGCACTTTGGATATGCTCCTTGACCCCAAAAATATGTATTTA 3060
                ************************************************************

WT              AGAAAAACTGCTGTCAATTATTCCCACTTGAAATTATTATGGTTTCCTGCACTGAGGCAC 1358
cz35            AGAAAAACTGCTGTCAATTATTCCCACTTGAAATTATTATGGTTTCCTGCACTGAGGCAC 3120
                ************************************************************

WT              CTGGATAACTTGATGCTATTATTGAAAGCTTTGCGTGTTTGCCTTATCTGTAAATAGTAG 1418
cz35            CTGGATAACTTGATGCTATTATTGAAAGCTTTGCGTGTTTGCCTTATCTGTAAATAGTAG 3180
                ************************************************************

WT              AGTATGTAAATTACCAAATGTAATAAAATGTTTTCATAATGTTTAAAAAAAAAAAAAAAA 1478
cz35            AGTATGTAAATTACCAAATGTAATAAAATGTTTTCATAATGTTTAAAAAAAAAAAAAAAA 3240
                ************************************************************

WT              AA 1480
cz35            AA 3242
                **
```

3.1.5 Detection of wild-type Sqt protein from sqt^{mut} transcripts

It has been reported by several labs that *sqt*^{cz35} and *sqt*^{hi975} insertional alleles are likely to be genetic nulls, due to the numerous in-frame translational stop signals present within the inserted sequences (Feldman et al. 1998; Bennett et al. 2007). Feldman et al, 1998 also suggested that even if a protein product is made in *sqt*^{cz35} embryos, it is likely to be a 17 kDa C-terminally-truncated peptide that does not encode a functional Sqt ligand.

Using an in vitro rabbit reticulocyte lysate-based transcription and translation coupled system, I expressed both wild-type full-length *sqt* and *sqt*^{cz35} which were cloned in pCS2+ expression vectors. A 44 kDa protein is detected from wild-type full-length *sqt*, which corresponds to the size of un-processed immature Sqt, having its leader (signal sequence), pro and mature domains (Figure 3.1.5 and (Erter et al. 1998; Tian et al. 2008)). No mature form of Sqt is detected probably because the rabbit reticulocyte lysate lacks Subtilisin-like proprotein convertases (SPC) e.g. Furin (Spc1) and PACE4 (Spc4), which are responsible for cleaving Nodal precursors to form the mature Nodal ligands (Beck et al. 2002). In contrast, I only detected an approximately 17 kDa translation product from *sqt*^{cz35}, consistent with the Feldman et al., 1998 prediction (Figure 3.1.5). This truncated product is likely to arise from the utilization of a premature in-frame translation stop signal present in *cz35* sequence (Figure 3.1.4B). Nevertheless, this data shows that *sqt*^{cz35} is incapable of supporting wild-type Sqt protein synthesis.

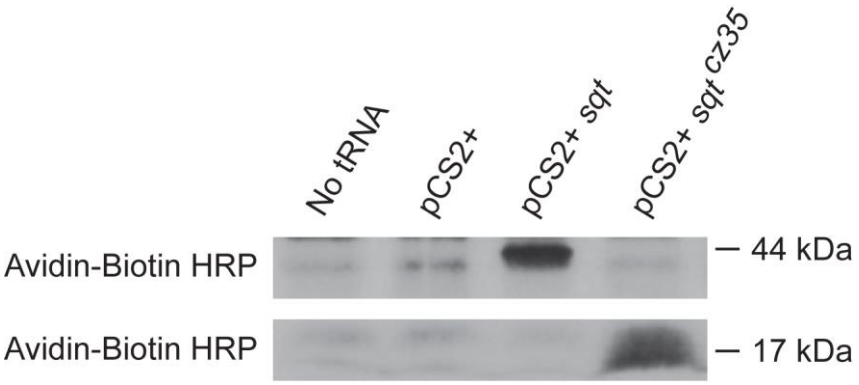

Figure 3.1.5 *sqt*^{cz35} produces a truncated protein. In vitro rabbit reticulocyte lysate transcription-translation coupled assay shows that wild-type *sqt* encodes a full-length 44 kDa Sqt precursor, whereas mutant *sqt*^{cz35} produces a truncated ~17 kDa polypeptide. "No tRNA" and "pCS2+" served as negative controls.

3.1.6 Localization pattern of maternal sqt^{mut} transcripts in MZ*sqt*

Since *sqt*^{mut} transcripts are deposited maternally in embryos derived from MZ*sqt* females, I next examined their localization pattern in early cleavage stage embryos by whole-mount RNA in situ hybridization. In wild-type embryos, maternal *sqt* transcripts become restricted to one or two cells by the 4- and 8-cell stage ((Gore et al. 2005) and Figure 3.1.6A). Similarly, I observed localized expression of maternal *sqt*^{cz35} transcripts in two cells of 8-cell stage MZ*sqt*^{cz35} embryos (Figure 3.1.6B). The genotypes of the stained embryos were confirmed by PCR using primer pair 1 and 3, which amplifies a 163 bp wild-type product, and primer pair 1 and 2 which amplifies a 266 bp product in the presence of the *cz35* insertion (Figure 3.1.6B,C).

The observed similarity in the early asymmetric localization of maternal wild-type and *sqt*^{cz35} transcripts in wild-type and MZ*sqt*^{cz35} embryos respectively was not surprising. This is because *sqt*^{cz35} transcript has an intact 3'UTR (Figure 3.1.4B), which has been shown previously in Gore et al., 2005, to be both necessary and sufficient for localizing heterologous sequences fused to it.

Collectively, the above data suggests that *sqt*^{cz35} and *sqt*^{hi975} insertion alleles are not maternal transcript nulls and in fact, *sqt* transcripts are localized in MZ*sqt* embryos similar to wild-type *sqt* RNA. Since I have shown that *sqt*^{cz35} transcripts are incapable of generating wild-type Sqt protein, the data seems to hint at a possible functional non-coding role for maternal *sqt* transcripts in early zebrafish development.

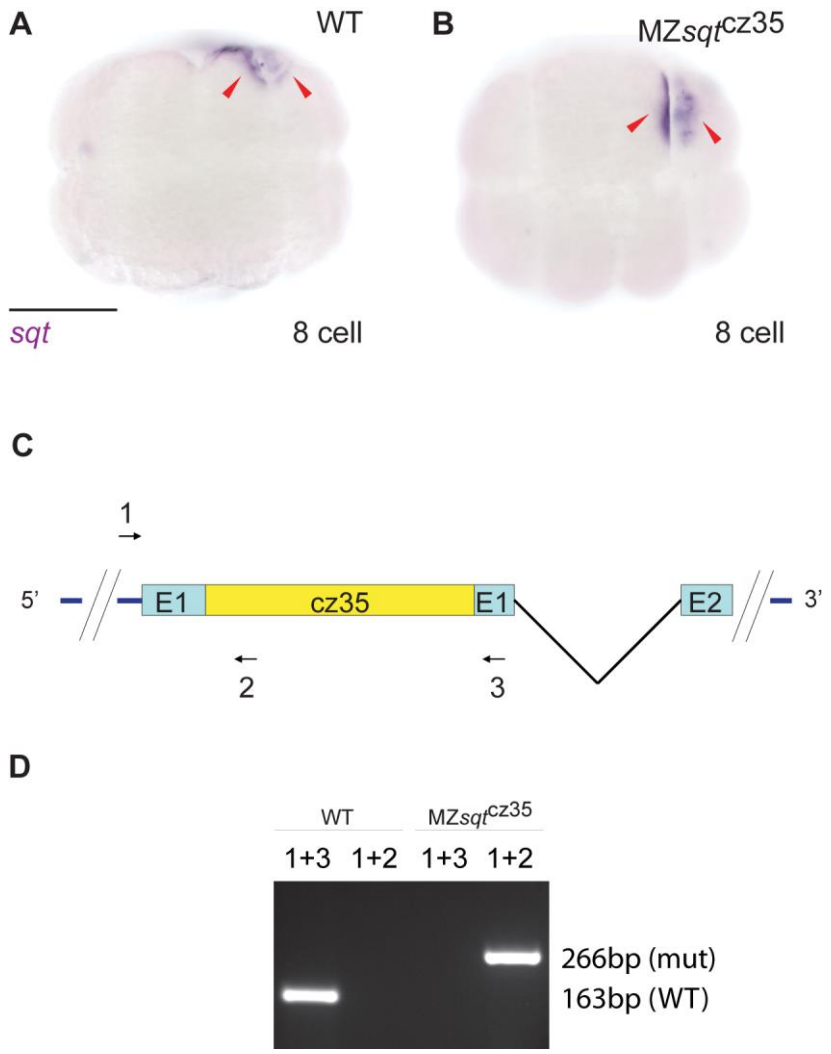

Figure 3.1.6 Maternal sqt^{mut} transcripts localize asymmetrically in MZ*sqt* embryos. Whole mount *in situ* hybridization to detect localization of maternal *sqt* RNA (red arrowheads) in 8-cell stage wild-type (A) and MZ*sqt*^{cz35} mutant embryos (B). (C) Schematic representation of genomic *sqt* locus showing the *cz35* insertion (yellow bar) and positions of genotyping primers (black arrows 1, 2 and 3). Genotype of wild-type (A) and mutant MZ*sqt* (B) embryos was confirmed by PCR to detect either wild type (primer pair 1+3) or mutant *sqt* (primer pair 1+2) alleles (D).

3.2 Characterization of activity of sqt^{mut} transcripts

To explore the possibility that maternal *sqt* transcripts might be functional in its RNA form, I first generated a series of mutant *sqt* (sqt^{mut}) constructs that bear mutations targeted at disrupting wild-type Sqt protein synthesis.

3.2.1 Constructs and protein synthesis test

Firstly, to rule out the possibility that the *cz35* insertion sequence itself has any form of functional role, and to minimize disruption to the wild-type RNA sequence, I engineered a single nucleotide change of T to A in *sqt* exon 1, which in turn resulted in an amino acid substitution of Leucine11 (TTG) with a premature STOP (TAG) (Figure 3.2.1A). This construct is named sqt^{STOP}:sqt.

Next, I generated a 5' truncated mutant *sqt* construct (T-sqt:sqt, Figure 3.2.1A) (Bennett et al. 2007) that has its coding region for the leader domain (signal sequence) of Sqt removed. As Sqt is a secreted morphogen (Chen and Schier 2001), T-Sqt, without its signal sequence, will not be able to exit the cell and act on cell surface receptors to activate intra-cellular signalling cascades.

Before I use these sqt^{mut} constructs to examine the non-coding function of *sqt* RNA, I checked if they were really incapable of synthesizing wild-type Sqt protein using the rabbit reticulocyte lysate expression system. Indeed, wild-type *sqt* sequence led to the translation of a 44 kDa full-length immature Sqt protein (Figure 3.2.1B, Lane 3), whereas *sqt^{cz35}:sqt* sequence resulted in a 17 kDa C-terminally-truncated peptide (Figure 3.2.1B, Lane 4). Both sqt^{STOP}:sqt and T-sqt:sqt sequences led to the translation of an approximately 39 kDa polypeptide (Figure 3.2.1B, Lanes 5,6), presumably due to the utilization of an internal ATG (downstream of engineered TAG in sqt^{STOP}:sqt) that encodes Met35. Indeed this was the case, as the anti-FLAG antibody did not pick up the 39 kDa product when FLAG epitope tagged-sqt^{STOP}:sqt (FLAG tag is before engineered STOP) was used as reaction template (Figure 3.2.1A,B, Lanes 7,8).

Taken together, the data shows that none of the sqt^{mut} constructs can generate wild-type Sqt protein. Hence, they can be used as tools to further decipher the non-coding role of *sqt* RNA.

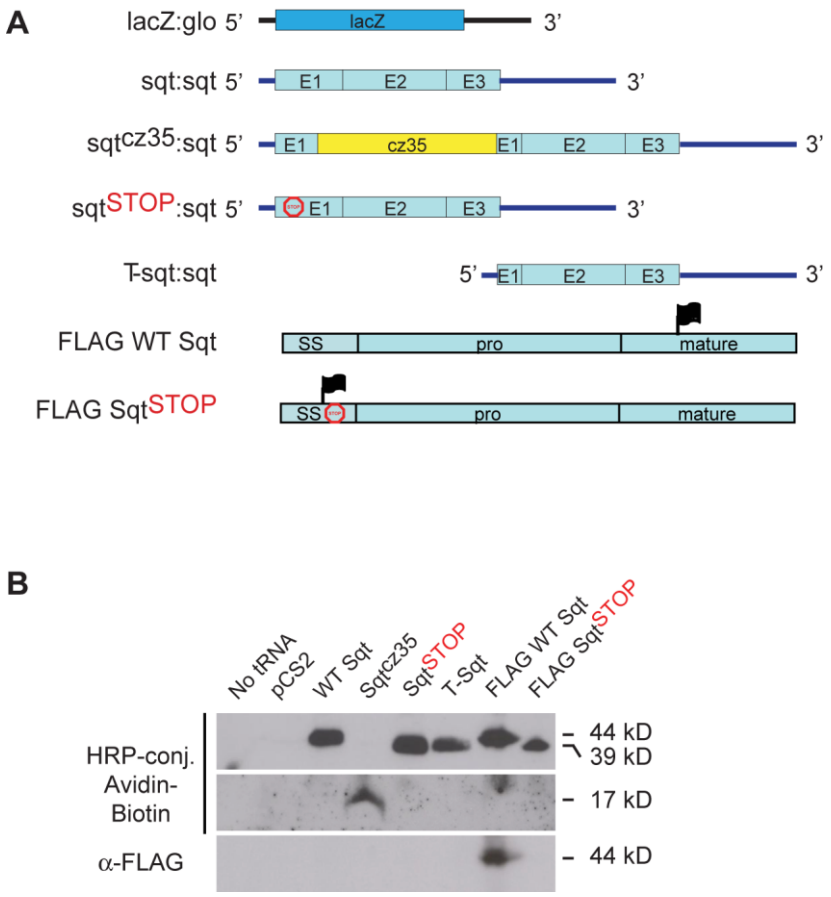

Figure 3.2.1 Mutant *sqt* constructs and *in vitro* translation test. (A) Schematic of constructs to express lacZ, wild-type *sqt* (WT Sqt), *sqt*^{cz35} (Sqt^{cz35}), *sqt* with a terminator codon in exon 1 (Sqt^{STOP}), 5'truncation of *sqt* (T-Sqt), and FLAG epitope-tagged wild-type *sqt* (FLAG WT Sqt) and sqt^{STOP} (FLAG Sqt^{STOP}), in rabbit reticulocyte lysates. LacZ sequences are shown in turquoise, *sqt* coding sequences are in cyan, and the *sqt*^{cz35} insertion is shown in yellow. Black line indicates *Xenopus globin* UTR sequences, and blue line indicates the *sqt* UTR. Red octagons indicate position of the terminator codon in sqt^{STOP} and FLAG sqt^{STOP}, *sqt* exons are indicated as E1-3, and black flags marks the position of the FLAG epitope tags. *In vitro* translation to express Sqt proteins (B) from the constructs in (A) show the expected 44 kDa wild-type Sqt protein, a C-terminus truncated 17 kDa Sqt^{cz35} peptide, and both sqt^{STOP} and T-sqt produce the predicted 39kDa protein from Met35.

3.2.2 Analysis of early DV markers in sqt^{mut}-overexpressed embryos

To test if sqt^{mut} transcripts have any form of activity, I synthesized capped full-length *sqt*^{cz35}, sqt^{STOP} and T-sqt RNA, injected it into early one-cell stage wild-type embryos, and examined those embryos for nuclear accumulation of β-catenin and dorsal expression of *goosecoid* (*gsc*) and *chordin* (*chd*) at early blastula and gastrula stages.

In the injected embryos, I observed that the sqt^{mut}:sqt RNA-injected embryos (Figure 3.2.2.1E-H) reached developmental milestones at the same time as control-injected embryos (Figure 3.2.2.1A-D), suggesting the absence of any morphogenetic delay. However, to rule out the involvement of varying developmental timings in the subsequent different observations, every injected embryo was carefully stage-matched before fixing for antibody staining or whole mount RNA in situ hybridization.

At early cleavage stages, apart from asymmetrically localized maternal *sqt* RNA, nuclear accumulation of β-catenin in 1-2 cells starting from the 128-cell stage definitively marks embryonic dorsal (refs). At the 512-cell stage, embryos injected with mutant *sqt* RNAs (sqt^{mut}:sqt) showed expansion of nuclear β-catenin expression, with ~16 β-catenin-positive nuclei (n=18 embryos, Figure 3.2.2.2C,D), as compared with control lacZ:glo RNA-injected embryos that showed about five positive nuclei (n=10 embryos; Figure 3.2.2.2A,B). In more than 50% of sqt^{mut}:sqt RNA-injected embryos, I observed at least 15 β-catenin-positive nuclei and in fact, three embryos showed more than 25 β-catenin-positive nuclei (n=18; Figure 3.2.2.2E). Consistent with yolk syncytial layer (YSL) formation at the 10th mitosis (512-cell to 1000-cell stage), the lower borders of the first tier blastoderm cells are not visible (Figure 3.2.2.2A,C) (Kimmel and Law 1985). I observed increased numbers of β-catenin-positive nuclei in both the blastoderm (red arrows, Figure 3.2.2.2C,D) and dorsal YSL of sqt^{mut}:sqt-injected embryos (yellow arrows, Figure 3.2.2.2C,D), whereas in wild-type and control-injected embryos, YSL expression of β-catenin is not detected until the 1000-cell stage (Figure 3.2.2.2A,B) (Dougan et al. 2003). Thus, injected mutant *sqt* RNA can significantly increase the dorsal nuclear accumulation of β-catenin in the YSL and blastoderm.

At early gastrula stages of 30%, the sqt^{mut}:sqt-injected embryos show expanded *gsc* expression (Figure 3.2.2.3F). I observed that the expansion of *gsc* expression is only along

the margin and does not extend animally. In contrast, control embryos injected with lacZ:glo RNA did not manifest *gsc* expansion at comparable stages (Figure 3.2.2.3A). Although striking, dorsal expansion by sqt^{mut}:sqt RNAs was transient, and by 60% epiboly *gsc* expression was indistinguishable from that of control lacZ:glo RNA-injected embryos (Figure 3.2.2.3E,J). To quantify dorsal expansion, I measured the angle of *gsc* expression around the gastrula margin in injected embryos (Figure 3.2.2.3K). In wild-type embryos and control lacZ:glo-injected embryos, the *gsc* angle is ~70°, whereas in embryos injected with sqt^{mut}:sqt RNA, the arc of *gsc* expression is much broader, resulting in angles ranging between 70° and 150°, with a mean exceeding 95° (Figure 3.2.2.3L). Similarly, *chd* expression at 40% epiboly also expanded substantially in sqt^{mut}:sqt-injected but not control-injected embryos (Figure 3.2.2.3B,G). In addition to *gsc* and *chd,* I also observed expansion of a pan-mesodermal gene *no tail* (*ntl*) around the entire margin in response to over-expression of sqt^{mut}:sqt RNA (Figure 3.2.2.3C,H). Consistent with the expansion of dorsal fates, I detected a loss in ventral fates exemplified by the reduction in expression of a ventral mesodermal marker *GATA-binding protein 2a* (*gata2a*) (Figure 3.2.2.3D,I).

Collectively, these data suggest that sqt^{mut}:sqt RNA, that is incompetent of translating into wild-type Sqt protein or generating the classical Sqt ligand, still possess an activity that expands dorsal and reduces ventral gene expression.

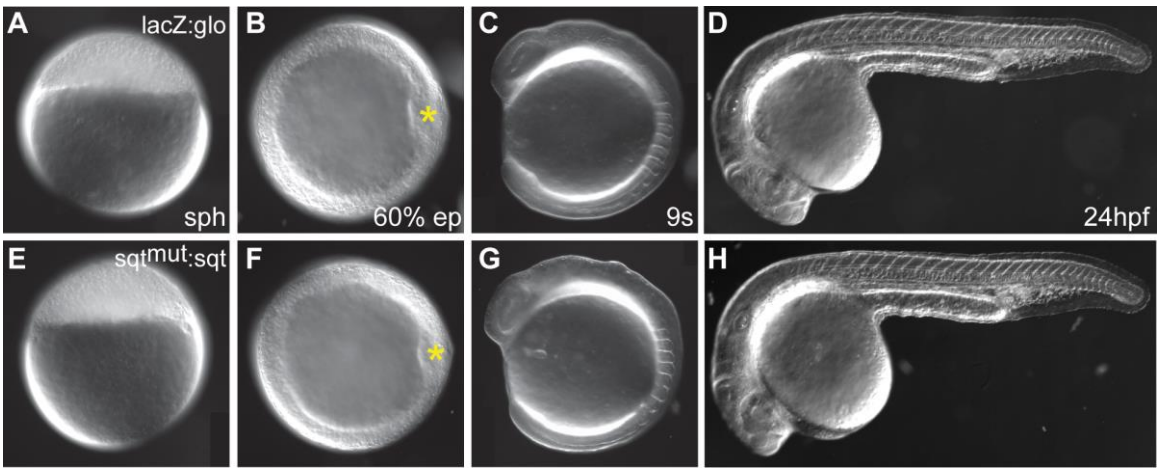

Figure 3.2.2.1 No obvious morphogenetic delay detected in sqt^{mut}:sqt overexpressed embryos. sqt^{mut}:sqt-injected embryos (E-H) reach developmental landmarks at the same time as control lacZ:glo-injected embryos (A-D). DIC images were captured at sphere (A,E), 60% epiboly (B,F), 9 somites (C,G) and 24 hpf (D,H) stages. (A,C,D,E,G,H) Lateral views. (B,F) Animal pole views, dorsal to the right. (C,G) Dorsal to the right. (D-H) Anterior to the left. Yellow asterisk marks the shield.

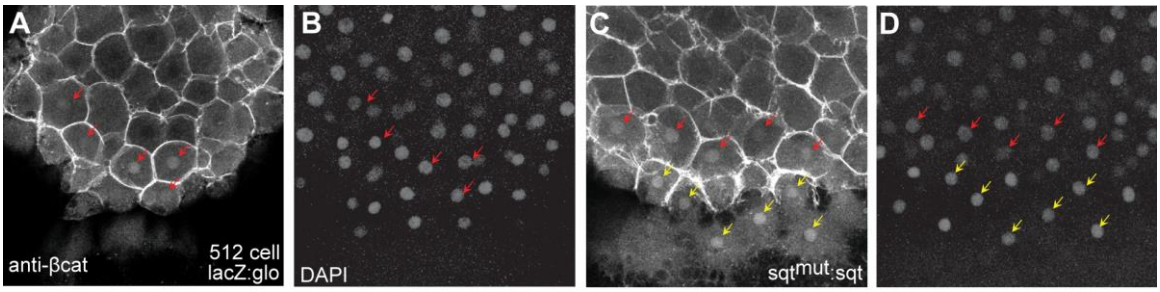

E

	% embryos					
	Number of β-catenin positive nuclei					
	0-2	**3-5**	**6-9**	**10-15**	**>15**	**Total N**
lacZ:glo	0	100%	0	0	0	10
sqt^{mut}:sqt	0	0	16.7%	33.3%	50%	18

Figure 3.2.2.2 Mutant *sqt* RNAs expand dorsal in late blastula stage embryos. Embryos injected with capped lacZ:glo mRNA show β-catenin in nuclei of ~5 cells at the 512-cell stage (A,B), in comparison to mutant *sqt* RNA injected embryos which show ~11 β-catenin positive nuclei (C,D). Red arrows indicate β-catenin-positive nuclei in the blastoderm, whereas yellow arrows show β-catenin positive nuclei in the YSL. DAPI staining (B,D) shows all nuclei in blastoderm and YSL. (E) Table shows percentage of embryos exhibiting varying extents of nuclear accumulation of β-catenin.

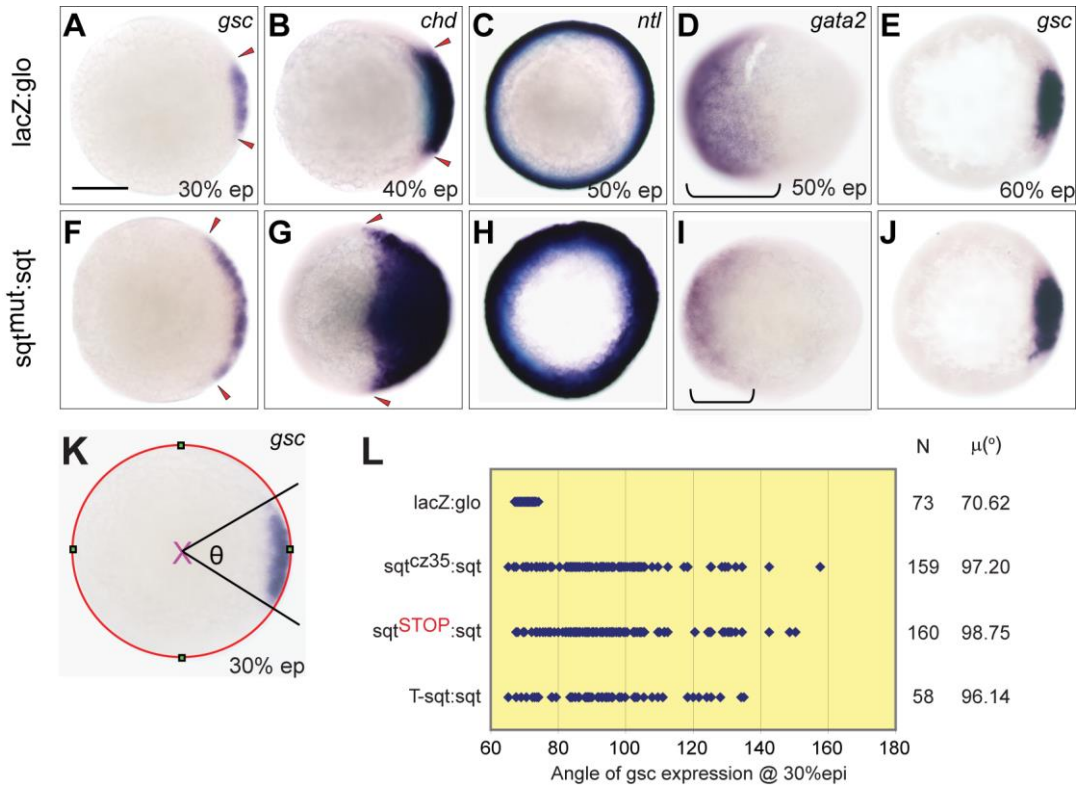

Figure 3.2.2.3 Mutant *sqt* RNAs expand dorsal and reduce ventral in early gastrula stage embryos. Normal expression of *gsc* (A), *chd* (B), and *ntl* (C) in lacZ:glo embryos, at 30% epiboly, 40% epiboly, and 50% epiboly respectively, in comparison to expanded *gsc* (F), *chd* (G), and *ntl* (H) in embryos injected with mutant sqt:sqt UTR (sqt^{mut}:sqt) RNA. Expression domain of the ventral marker *gata2* (brackets in D,I) is reduced in sqt^{mut}:sqt RNA injected embryos (I), in comparison to controls (D). At 60% epiboly, *gsc* expression is similar in lacZ:glo (E) and mutant sqt:sqt (J) injected embryos. (K) Schematic showing measurement of *gsc* angle (θ). Red circle denotes drawn best-fit circle, green squares mark X and Y coordinates, magenta 'X' marks the origin. Graph in L shows angle of *gsc* expression in mutant *sqt* RNA or control lacZ-injected embryos at 30% epiboly. Each blue dot represents a single embryo. N's indicate number of injected embryos for each RNA, and μ(°) is the mean angle of *gsc*. (A-K) Animal pole views. (A,B,D,E,F,G,I,J,K) Animal pole views, dorsal to the right. Red arrowheads in A, B, F and G mark the extent of *gsc* and *chd* expression. Scale bar in A is 25 μm.

3.3 Dorsal-inducing activity requires *sqt* UTR

Thus far, the data implies that it is the RNA form of maternal *sqt* that has the functionality of initiating dorsal expansion. From previous published work, it has been established that the 3'UTR of *sqt* is both necessary and sufficient for dorsal localization (Gore et al. 2005). In addition, sequence and structural information found within the first 50 bases of the 3'UTR is pivotal in localizing *sqt* RNA to dorsal progenitor cells (Gilligan et al. 2011). Hence, I investigated if dorsal expansion by overexpression of *sqt* RNA also requires the 3'UTR.

3.3.1 Constructs and analysis of early DV markers in *glo* UTR vs *sqt* UTR-overexpressed embryos

To test the above hypothesis, I engineered a new construct, replacing the 5' and 3' UTRs of sqt^{STOP}:sqt with Xenopus globin UTRs (Figure 3.3.1A). Together with sqt^{STOP}:sqt, sqt^{STOP}:glo was used to assess the requirement of *sqt* UTRs in expansion of dorsal gene expression. As shown in Gore et al. 2005, *sqt* 3'UTR was found to be sufficient to confer localization of heterologous *lacZ* sequences to future dorsal cells. Hence, to test if the UTR is required in the context of dorsal expansion, I will compare the overexpression outcomes of *venus:glo* and *venus:sqt* capped RNA (Figure 3.3.1A).

Whereas sqt^{STOP}:sqt RNA injection expanded gsc expression at 30% epiboly (Figure 3.3.1C), injection of sqt^{STOP}:glo had no discernible effect (Figure 3.3.1B). When measured at 30% epiboly, sqt^{STOP}:sqt RNA injections resulted in *gsc* expansion angles with a mean of 98.75^{o} compared to 71.84^{o} observed mean angle for sqt^{STOP}:glo RNA injections (Figure 3.3.1J). As with previous observations, I noted that the expansion of dorsal gene expression was transient as *gsc* expression at 60% epiboly was indistinguishable in both sqt^{STOP}:sqt- and sqt^{STOP}:glo-injected embryos (Figure 3.3.1F,G). I then examined whether the *sqt* 3'UTR was sufficient for dorsal expansion. Embryos were injected with RNA encoding the fluorescent protein Venus fused with either *sqt* 3'UTR or *globin* 3'UTR (Figure 3.3.1A). The embryos injected with venus:sqt RNA showed transient *gsc* expansion ranging up to 160^{o}, with a mean of 96^{o} (Figure 3.3.1J). Control venus:glo-injected embryos showed a mean *gsc* angle of 72^{o} (Figure 3.3.1J). These data suggest that *sqt* UTR is both necessary and sufficient for expansion of dorsal gene expression.

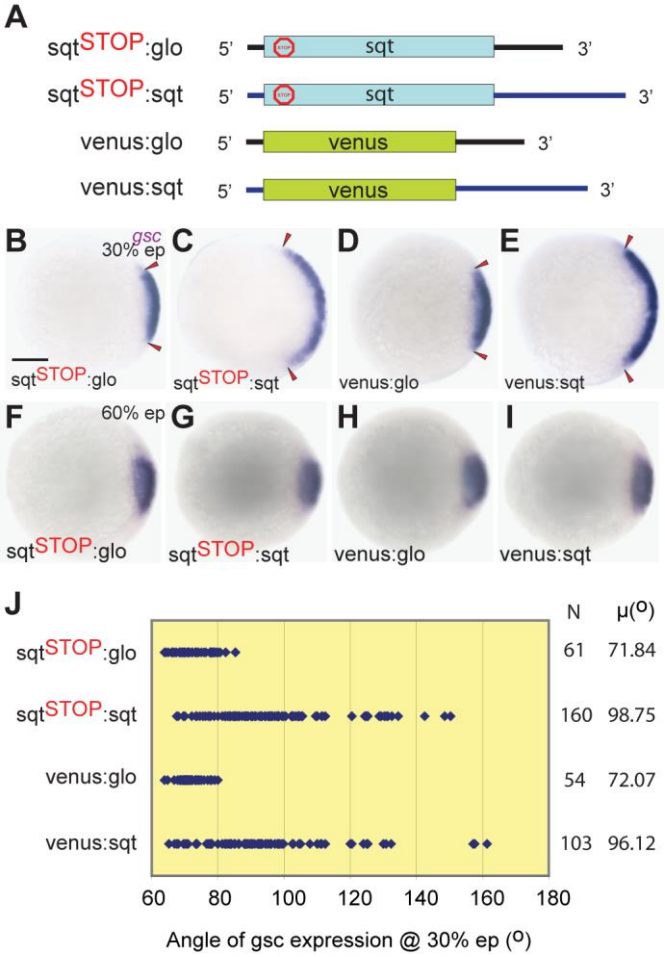

Figure 3.3.1 The *sqt* 3'UTR is necessary and sufficient for dorsal activity of *sqt* RNA. (A) Schematic of constructs used to express mutant *sqt* fused with *globin* 3'UTR (black; sqt^{STOP}: glo), *sqt* 3'UTR (blue; sqt^{STOP}:sqt), venus (green) fused with *globin* 3'UTR (venus:glo) or *sqt* 3' UTR (venus:sqt). Expression of *gsc* at 30% epiboly (B-E) is expanded in embryos injected with sqt^{STOP}: sqt (C) and venus:sqt (E), but not with sqt^{STOP}: glo (B) or venus:glo (D). Dorsal expansion by the *sqt* UTR is transient and is not detected at 60% epiboly (F-I). Graph in J shows angle of *gsc* expansion in injected embryos at 30% epiboly. Each blue dot represents a single embryo. N indicates the number of injected embryos for each RNA, and μ(°) is the mean angle of *gsc*. Scale bar in B, 100μm.

3.3.2 Reverse transcriptase-quantitative PCR analysis of early DV genes in *sqt* 3'UTR-overexpressed embryos

To determine the role of *sqt* 3'UTR in influencing the dynamics of early dorsal and ventral gene expression, RT-qPCRs were performed to detect early expression of *sqt*, *dharma* (*dha*), *vox* and *vent* in lacZ:sqt-injected embryos versus control lacZ:glo-injected embryos. As sqt^{mut}:sqt RNA-injected embryos exhibited an increase in nuclear accumulation of β-catenin, I decided to examine the level of *dha* trancripts, whose expression is known to be downstream of activated β-catenin signalling (Yamanaka et al. 1998; Fekany et al. 1999). Genetic analysis indicates that dorsal-promoting Dharma/Bozozok functions by antagonizing the transcription of ventralizing homeobox genes *vox* and *vent* (Imai et al. 2001). Hence, I also looked at the dynamics of *vox* and *vent* transcript levels.

In lacZ:sqt-injected embryos, endogenous *sqt* and *dha* transcript levels increase about 2-fold transiently at sphere stages and revert to normal levels by 30% epiboly (Figure 3.3.2), as compared to control lacZ:glo-injected embryos. Conversely, *vox* and *vent* transcript levels are transiently reduced by about 50% and 70% respectively initially and subsequently returned back to normal (Figure 3.3.2). Therefore, *sqt* 3'UTR is both necessary and sufficient to transiently expand dorsal gene expression and reduce ventral gene expression.

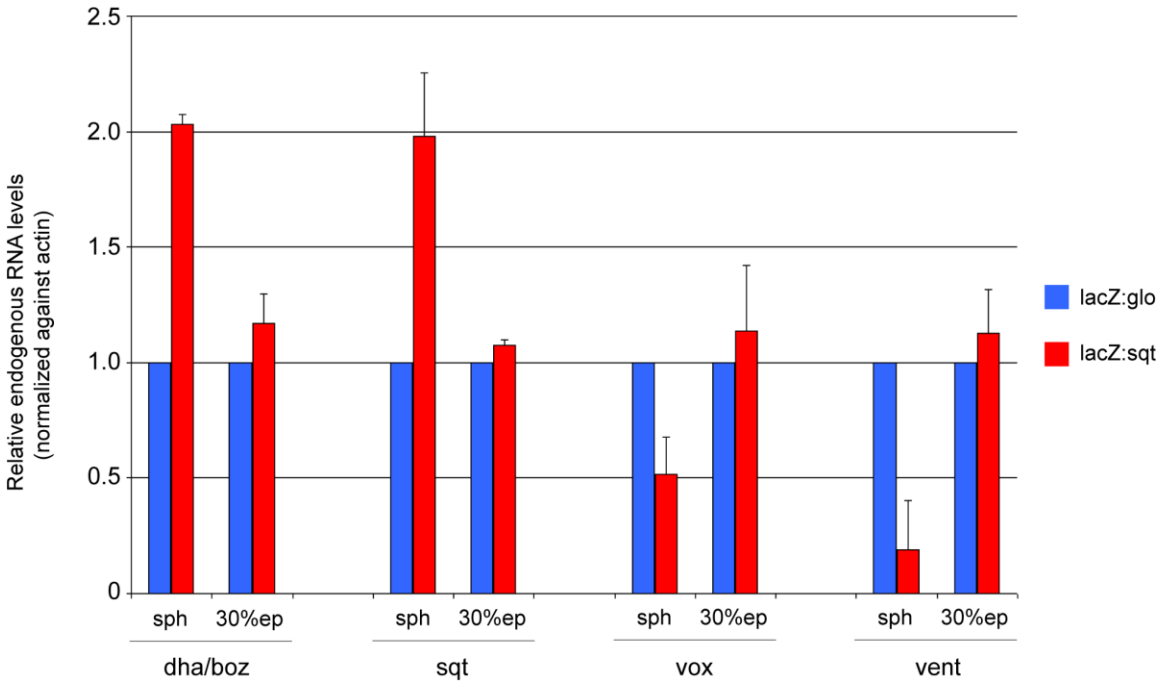

Figure 3.3.2 Overexpression of *sqt* UTR affects dymamics of endogenous *dha/boz*, *sqt*, *vox* and *vent* transcripts. Reverse transcriptase-quantitative PCR analysis of endogenous *dha/boz*, *sqt*, *vox* and *vent* transcripts in lacZ:glo and lacZ:sqt-injected embryos shows that *dha/boz* and *sqt* RNA levels transiently increase at sphere stage and return to normal levels at 30% epiboly. This transient increase is observed with a concomitant reduction in *vox* and *vent* expression at sphere, which subsequently revert to normal levels at 30% epiboly. Error bars indicate standard deviation between 2 independent experiments.

3.4 Functional relevance of *sqt* 3'UTR in DV specification

Overexpressing sqt^{mut}:sqt RNAs, and specifically, *sqt* 3'UTR, strikingly increases the nuclear accumulation of β-catenin (Figure 3.2.2.2C,D) and expands early dorsal gene expression (Figure 3.2.2.3F,G and 3.3.1C,E). However, the effect is only transient as dorsal gene expression revert to normal levels soon after (Figure 3.2.2.3J and 3.3.1G,I) and injected embryos look phenotypically normal at 24 hpf (Figure 3.2.2.1H). This raised the question of whether the dorsalizing activity we are reporting of *sqt* 3'UTR is of any developmental relevance to the embryo. To approach this issue, I used dorsal-deficient *ichabod* (*ich*) mutant embryos derived from homozygous *ich* mothers (Kelly et al. 2000). The *ich* mutation is closely linked to the zebrafish *ctnnb2* gene, and results in drastically reduced levels of *ctnnb2* transcripts (Bellipanni et al. 2006). As a result, embryos from mothers homozygous for the *ich* mutation fail to localize β-catenin (Ctnnb2) in dorsal nuclei (Kelly et al. 2000), and thus manifest severe dorsal deficiencies. These *ich* embryos can be rescued by *sqt* RNA injections (Kelly et al. 2000; Gore et al. 2005). And I compared the effect of *sqt* versus *globin* 3'UTR sequences on the ability of Sqt to rescue the dorsalized *ich* phenotypes.

3.4.1 sqt:sqt 3'UTR rescues *ichabod* phenotype efficiently

I synthesized and injected capped mRNA encoding Sqt fused to either *sqt* (sqt:sqt) or *globin* 3' UTR(sqt:glo) into *ich* embryos. All *ich* embryos used were derived from homozygous *ich* mothers that transmit 100% Class 1a radialized phenotypes (Figure 3.4.1A, (Kelly et al. 2000)). In these experiments, Sqt protein would be translated from both RNAs, hence, any difference in activity can be attributed to the different 3'UTRs. Interestingly, I observed that sqt:sqt rescues the dorsal deficiencies in *ich* mutant embryos more efficiently than sqt:glo. Approximately 70% of sqt:sqt-injected embryos display rescue of dorsal structures to varying extents (Figure 3.4.1B-E), with 15% showing complete rescue and 53% exhibiting partial rescue (n=100 embryos, Figure 3.4.1G). In striking contrast, only 37% of sqt:glo-injected *ich* mutant embryos (n=103 embryos, Figure 3.4.1G) show any rescue of dorsal structures. In addition, I noted that about 55% of sqt:glo-injected *ich* embryos arrest at early gastrula in comparison to only ~30% of sqt:sqt-injected *ich* embryos, probably due to ectopic Sqt signalling resulting from mislocalized sqt:glo, in contrast to localized Sqt from sqt:sqt (Figure 3.4.1F,G).

To rule out the influence of differential translation efficacies in the rescue efficiencies observed for sqt:sqt and sqt:glo, I decided to measure the amount of Sqt protein translated from the injected sqt:sqt and sqt:glo capped mRNA. As there is no good specific antibody against Sqt, I injected GFP fusions of sqt:sqt (sqtGFP:sqt) and sqt:glo (sqtGFP:glo), so that I could detect Sqt-GFP fusion protein using a polyclonal anti-GFP antibody. I collected sphere stage *ich* mutant embryos injected with either sqtGFP:sqt or sqtGFP:glo, and subjected the whole embryo lysates to SDS-PAGE. Immuno-blotting using anti-GFP antibody showed that the expression levels of Sqt from sqtGFP:sqt and sqtGFP:glo are similar (Figure 3.4.1H,I), indicating comparable translation efficacies.

Taken together, the results show that *sqt* 3'UTR confers more efficient activity to *sqt* in forming dorsal structures, and it has a biological function in dorsal specification that is distinct from that of Sqt protein.

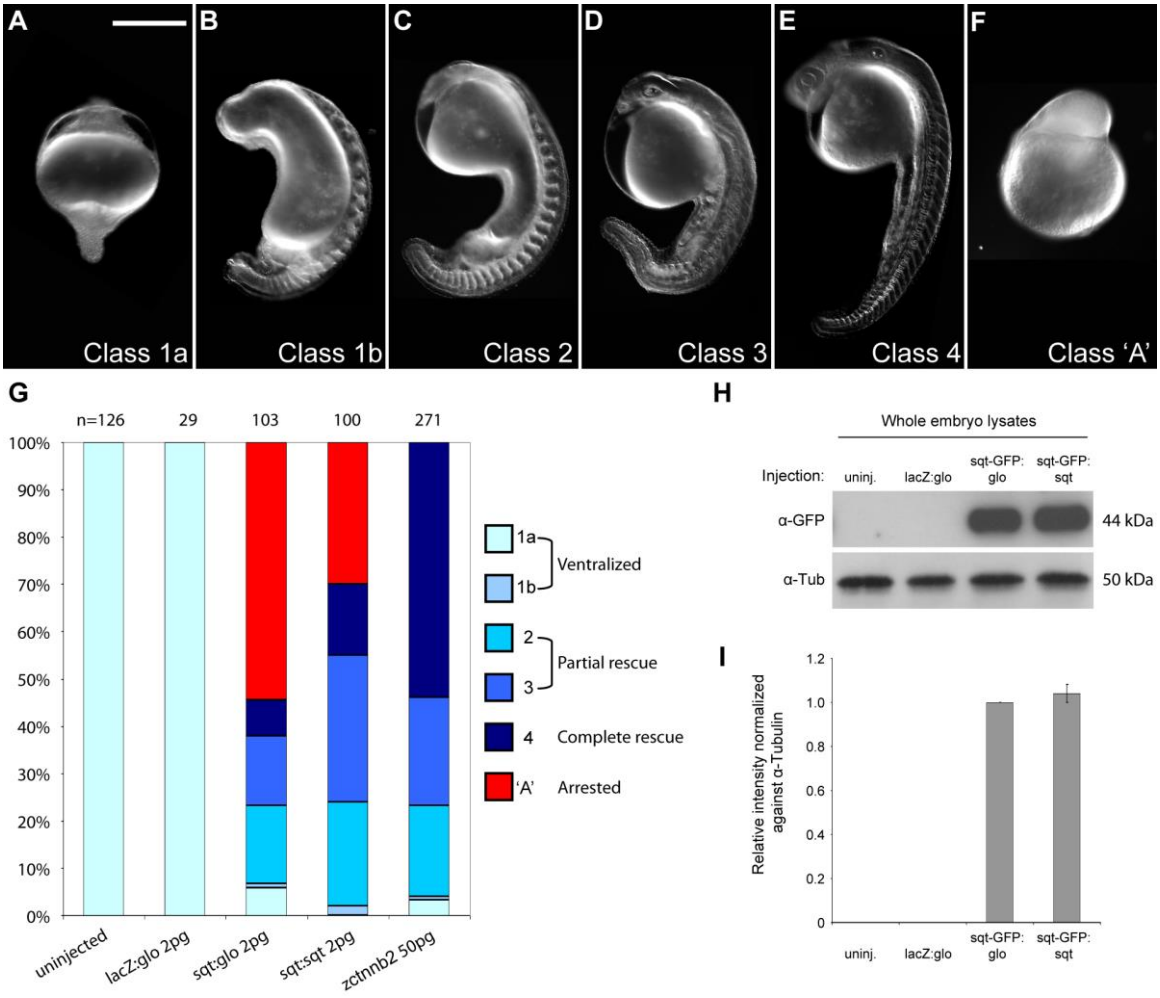

Figure 3.4.1 Rescue of *ichabod* embryos by Sqt is more effective with the *sqt* 3'UTR. Uninjected and lacZ:glo RNA injected *ichabod* embryos are completely radialized (A), whereas *sqt* or *zctnnb2* RNA injection rescues anterior and dorsal structures to varying extents (class 1b-class 4; B-E), or causes early arrest (class 'A'; F). Graph in G shows % embryos of each class. Injection of sqt:sqt and *ctnnb2* RNA is more effective in rescuing ich embryos than sqt:glo. H. Sqt-GFP protein (44 kD) expressed from embryos injected with sqt-GFP:sqt or sqt-GFP:glo, and lysates from uninjected embryos and lacZ:glo injected embryos as negative controls, are shown. Tubulin (50 kDa) is the loading control. I. Relative intensities of Sqt-GFP bands show that translation efficiency of sqt:sqt and sqt:glo in whole embryo lysates is comparable. Tubulin expression was used for normalization. Scale bar in A, 100 µm. Error bars in I indicate standard deviation between 2 independent experiments.

3.5 sqt^{mut}:sqt RNA can rescue *sqt* morphants

As shown earlier, *sqt* morphant embryos exhibit a loss of early gsc expression (Figure 3.1.1A, 3.1.2B and 3.5.1B) and at 24 hpf manifest a range of ventralized phenotypes (Gore et al. 2005), in contrast to control MO-injected and MZ*sqt* embryos (Figure 3.5.1A,D) Since earlier data supported that *sqt* 3'UTR harbours a dorsalizing activity, I decided to test if the UTR is competent in rescuing *sqt* morphant embryos.

3.5.1 Analysis of *gsc* expression in rescued *sqt* morphants

To assay for rescue of early dorsal gene expression in *sqt* morphants, I co-injected unactivated wild-type oocytes with cocktails of either *sqt* MO+sqt^{STOP}:sqt RNA or *sqt* MO+lacZ:sqt, and fix the embryos at 30% epiboly for *gsc* staining. As controls, I co-injected cocktails of either con MO+lacZ:glo or *sqt* MO+lacZ:glo and processed the embryos as above. Injected lacZ:sqt or sqt^{STOP}:sqt RNA was able to rescue early *gsc* expression in *sqt* MO1- or *sqt* MO2-injected embryos to varying extents (Figure 3.5.1C,E). 100% of embryos co-injected with *sqt* MO+sqt^{STOP}:sqt RNA or *sqt* MO+lacZ:sqt show rescue of early *gsc* expression (Total N = 94, Figure 3.5.1E), out of which approximately 30-40% show complete rescue to wild-type levels. In contrast, none of the embryos co-injected with lacZ:glo RNA and *sqt* morpholinos show restoration of *gsc* expression (N = 28, Figure 3.5.1E).

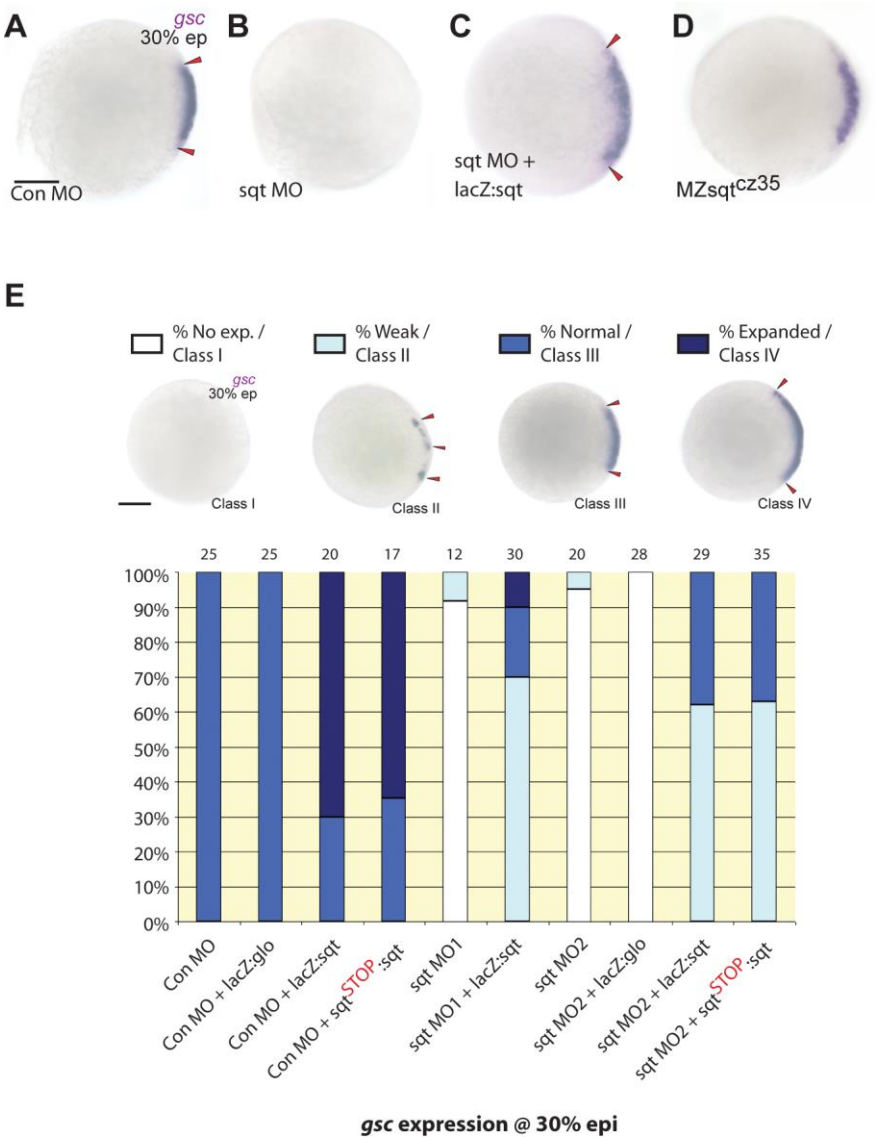

Figure 3.5.1 Loss of *gsc* expression by *sqt* morpholinos is rescued by the *sqt* 3'UTR. Early *gsc* expression is not detected in *sqt* MO-injected embryos (B), in contrast to Con MO-injected embryos (A) and MZ*sqt* embryos (D). Expression of *gsc* is rescued in *sqt* morphants by co-injection of lacZ:sqt (C), but not with lacZ:glo (E). (E) Histogram showing % embryos with dorsal gsc expression upon co-injection of *sqt* morpholinos with lacZ:glo, lacZ:sqt or sqt^{STOP}:sqt RNA. The number of embryos for each injection is shown on top. Embryo images show classification of *gsc* expression in injected embryos. Red arrowheads indicate the extent of *gsc* expression in the injected embryos. (A-D) Animal pole views, dorsal to the right; scale bar in A, 100µm.

3.5.2 Analysis of 24 hpf phenotypes in rescued *sqt* morphants

Since mutant *sqt* RNA, and more specifically *sqt* 3'UTR, demonstrated their ability in reinstating early dorsal *gsc* expression, I next asked if this early rescue was sufficient for *sqt* morphants to recover from severe ventralization. At 24 hpf stages, *sqt* morpholino-injected embryos manifest loss of anterior and dorsal structures (Figure 3.5.2B and (Gore et al. 2005)). Co-injections of the *sqt* MOs with sqt^{mut}:sqt RNA or lacZ:sqt RNA shifted the spectrum of ventralized phenotypes (V2, V3) to mild cyclopean phenotypes (V1/*sqt*) that strikingly resemble MZsqt^{cz35} mutant embryos (Figure 3.5.2A-E). Therefore, the rescue by the *sqt* UTR sequences is very significant.

Consistent with the observation that the rescue RNAs are incapable of translating wild-type Sqt protein (Figure 3.2.1), I did not observe a change in the occurrence of wild-type looking embryos in sqt MO+lacZ:sqt and sqt MO+sqt^{STOP}:sqt injections, compared to that of sqt MO+lacZ:glo. This indicates that mutant *sqt* RNAs cannot rescue the protein-coding role of Sqt. These set of rescue experiments indicate that it is the RNA form of maternal *sqt* that contributes to the initial establishment of dorsal and the biological activity of maternal *sqt* RNA in dorsal likely resides within its 3'UTR, independent of Sqt protein.

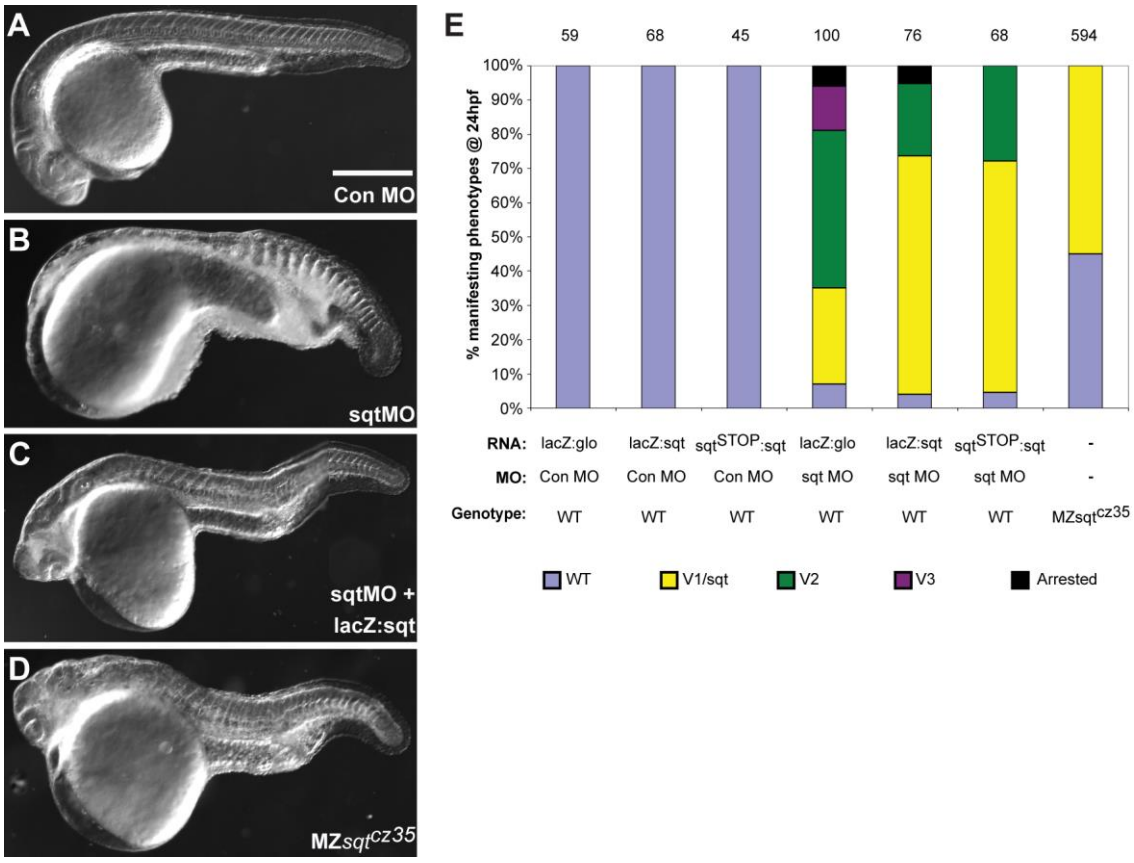

Figure 3.5.2 Loss of anterior and dorsal structures by *sqt* morpholinos is rescued by the *sqt* 3'UTR. *sqt* MO-injected embryos (B) display a ventralized phenotype in contrast to control MO-injected embryos (A). Embryos co-injected with *sqt* MO and either lacZ:sqt or sqt^{STOP}:sqt (C) are rescued partially, and are similar to MZ*sqt*^{cz35} mutant embryos (D). Embryo images in A-D were acquired in different focal planes for the rostral and caudal regions of the embryo and subsequently assembled. Graph in E shows extent of rescue of *sqt* MO-injected embryos by co-injection of lacZ:sqt or sqt^{STOP}:sqt, versus control lacZ:glo RNA. (A-D) Lateral views, anterior to the left. Scale bar in A is 100µm.

3.6 Deciphering the mode of action of maternal *sqt* RNA in dorsal initiation

In the previous sections, I discovered that *sqt*^{cz35} and *sqt*^{hi975} are not *bona fide* null alleles and hence, classical genetics using these mutant alleles may not reveal the maternal requirement of *sqt* in zebrafish embryonic development. Instead, using morpholino-mediated knockdown and RNA overexpression approaches, I uncovered a non-coding role for maternal *sqt* transcripts in initiating dorsal formation, contrary to published reports that maternal *sqt* is dispensable for DV patterning (Bennett et al. 2007; Pei et al. 2007). The next question that follows is how does *sqt* RNA function?

There have been other instances where a coding RNA also possess non-coding function(s). For example in *Drosophila*, *oskar* RNA and not Oskar protein is required for the normal progression of oogenesis (Jenny et al. 2006). Similarly, *Xenopus veg-T* RNA has a scaffolding role independent of the later functions of Veg-T protein in mesoderm induction and endoderm formation (Zhang and King 1996; Kloc et al. 2005). Therefore, there are numerous possibilities as to how maternal *sqt* RNA may act.

3.6.1 Is the activity of *sqt* mediated through a microRNA-based mechanism?

The 3'UTR of many RNAs is known to harbor target sites for microRNAs (miRNAs) that act to regulate the expression of their target RNA (Lee et al. 1993; Wightman et al. 1993; Reinhart et al. 2000; Johnston and Hobert 2003; Choi et al. 2007; Flynt et al. 2007; Thatcher et al. 2008; Qiu et al. 2009). One possibility is that the *sqt* UTR binds miRNAs that may function to negatively regulate dorsal determinants. Such a function has been described for some RNAs (Poliseno et al. 2010). If so, over-expressed mutant *sqt* RNA could act as a sink that binds to the miRNAs, thereby allowing a larger zone of dorsal (see model in Figure 3.6.1).

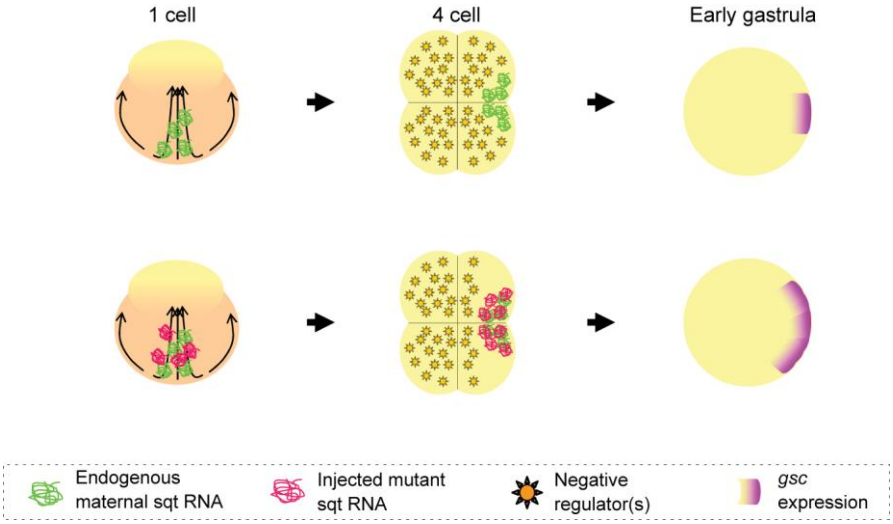

Figure 3.6.1 Model of *sqt* RNA acting as a sink to regulate dorsal formation. Model showing localization of *sqt* RNA (green) in 1-cell and 4-cell embryos, and expansion of dorsal *gsc* expression domain (purple arc) upon injection of mutant *sqt* RNA (magenta). Yellow asterisks indicate presumed negative regulators (for e.g. miRNAs) bound by the *sqt* UTR. The model proposes that if the *sqt* UTR binds miRNAs that may negatively regulate dorsal determinants, over-expressed mutant *sqt* RNA could act as a sink that binds to the miRNAs, allowing a larger zone of dorsal.

3.6.1.1 Presence of miR-430, miR-19a* and miR-152 target sites in *sqt* 3'UTR

Using various miRNA prediction programs (http://www.mirbase.org and http://www.ebi.ac.uk/enright-srv/microcosm/htdocs/targets/v5), I analyzed *sqt* 3'UTR sequences and identified targets that can be recognized by the following three miRNAs: miR-430 (Giraldez et al. 2005), miR-19a*, and miR-152 (Figure 3.6.1.1A). All three miRNA target sites belong to the "5' dominant (canonical)" class where 5′ dominant sites have sufficient complementarity to the miRNA 5′ end with minimal support pairing to the miRNA 3′ end (Brennecke et al. 2005).

3.6.1.2 Dorsal expansion by *sqt* 3'UTR is independent of miR-430, miR-19a* and miR-152

In order to determine the involvement of those miRNAs in *sqt* UTR-mediated dorsal expansion, I disrupted the binding of the miRNA to its target on injected *sqt* 3'UTR. To do this, there are two potential approaches. Firstly, I could use customized oligos termed "target protectors", which are complementary to the target site sequence, to compete with endogenous miRNA for binding to *sqt* 3'UTR. The second approach involves mutating the miRNA target site on injected *sqt* 3'UTR so that endogenous miRNA cannot bind it. As the latter approach exclusively targets the injected *sqt* 3'UTR, I decided to use it to address this question.

It has been demonstrated by several groups that mutations in the seed region of either miRNA target sites or the miRNAs themselves can lead to disruption of binding between the miRNA and its target (Choi et al. 2007; Mencia et al. 2009; Franzetti et al. 2012; Iliff et al. 2012). Hence, I generated two-base substitutions in the seed regions of miR-430 (Choi et al. 2007), miR-19a* and miR-152 target sites in venus:sqt (Figure 3.6.1.1A,B).

I injected synthetic capped mRNA encoding Venus reporter fused to the miRNA mutant *sqt* 3'UTRs into 1-cell embryos. Expression of the Venus reporter at 24 hpf confirmed the efficacy of the miRNA target site mutations (Figure 3.6.1.2F-J), and expression of *gsc* was examined at early gastrula stages. Mutations in target sites for miR-430, miR-19a*, or miR-152 do not affect the ability of *sqt* 3'UTR to expand *gsc* expression (Figure 3.6.1.2B-E). Furthermore, *gsc* expression still expands to ~98^{o} upon injection of reporter RNA with the *sqt*

3’UTR harboring mutations in the miRNA target sites (Figure 3.6.1.2K). These results suggest that the dorsal expanding activity of the *sqt* 3’UTR is not mediated via the above miRNAs.

3.6.1.3 Dorsal expansion by *sqt* 3’UTR is independent of *dicer*

To rule out the involvement of any other miRNAs in *sqt* 3’UTR-induced dorsal expansion phenomenon, I tested the activity of mutant *sqt* RNAs in the context of *dicer* mutants as Dicer protein is a central processing enzyme in the maturation of small RNAs (Carthew and Sontheimer 2009). Wienholds et al. 2003 reported that zygotic Dicer-deficient zebrafish do not survive past larval stage due to an overall cellular growth arrest (Wienholds et al. 2003). They also suggested that the presence of maternal Dicer allowed embryos to survive past early development. Indeed, embryos obtained from MZ*dicer* parents display severe morphogenesis defects at 24 hpf (Giraldez et al. 2005). Therefore, it was necessary to generate MZ*dicer* fish to eliminate all Dicer activity. Using homozygous *dicer* embryos as donors, I transplanted their primordial germ cells (PGCs) into wild-type host embryos that were depleted of their own germ cells (Ciruna et al. 2002). Then, I mated adult MZ*dicer* fish to obtain embryos devoid of maternal and zygotic contribution of Dicer.

Injection of lacZ:sqt RNA and sqt^{STOP}:sqt RNA in MZ*dicer* mutant embryos leads to expansion of dorsal gsc (mean arc of 90^{o}, Figure 3.6.1.3B-D), in comparison to MZ*dicer* embryos injected with the control lacZ:glo (mean arc of 70^{o}, Figure 3.6.1.3A,D). Therefore, dorsal activity of the *sqt* 3’UTR is not mediated by a Dicer-dependent mechanism.

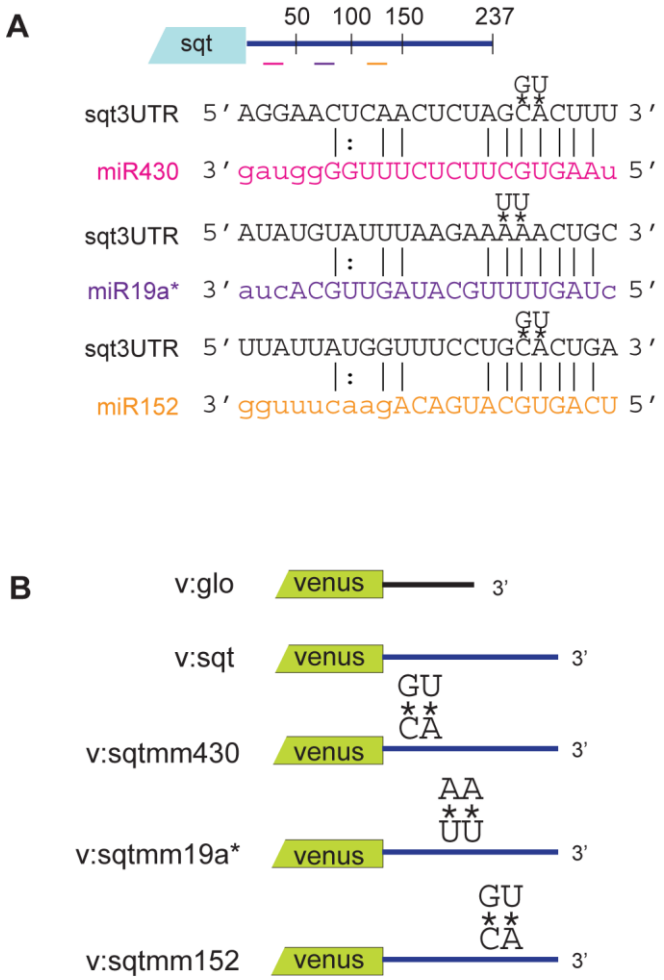

Figure 3.6.1.1 Predicted miRNA target sites in *sqt* 3'UTR and miRNA mutant *sqt* 3'UTR constructs. (A) Schematic showing predicted target sites (http://www.mirbase.org and http://www.ebi.ac.uk/enright-srv/microcosm/htdocs/targets/v5) for miR-430 (magenta bar), miR-19a* (purple bar) and miR-152 (orange bar) in the *sqt* UTR (blue line). Mutations in miRNA target sites are indicated with asterisks. (B) Schematic showing the Venus reporter (green box) fused to either *globin* UTR (v:glo), *sqt* UTR (v:sqt), or *sqt* UTR with the miRNA target site mutations illustrated in A (v:sqtmm430, v:sqtmm19a* and v:sqtmm152).

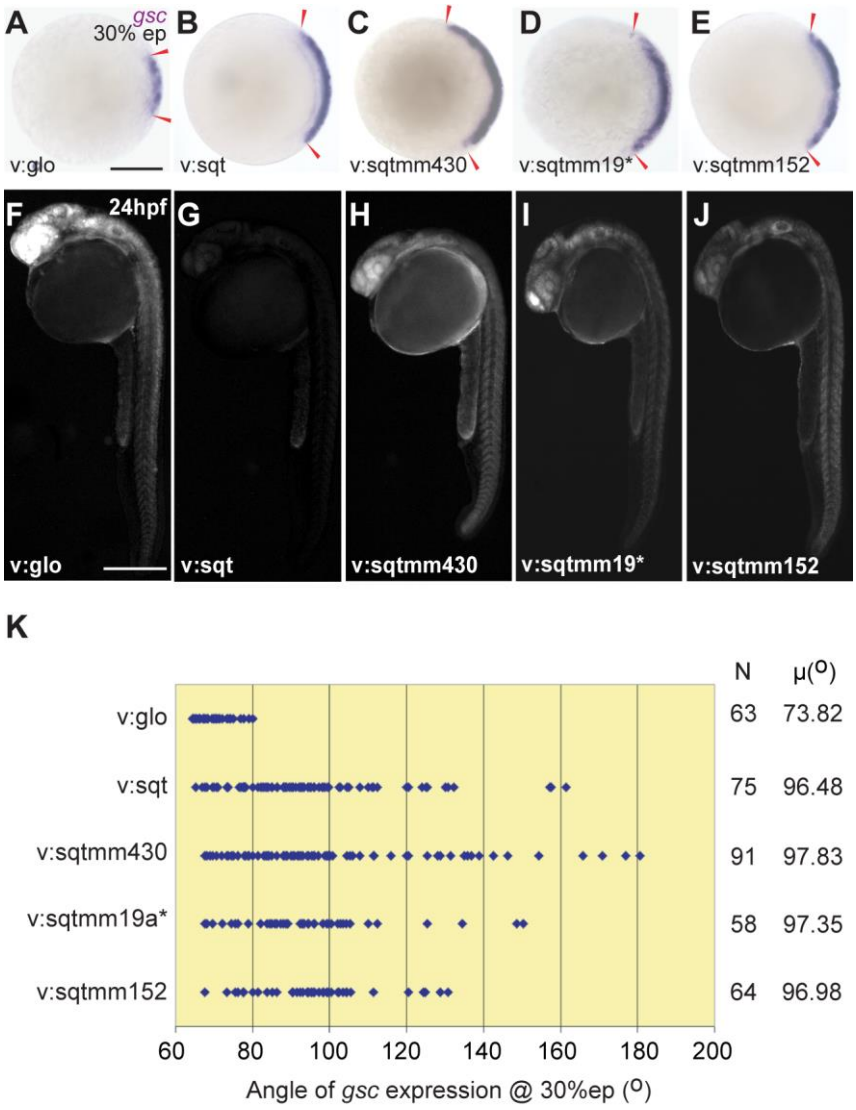

Figure 3.6.1.2 Dorsal expansion by *sqt* 3'UTR is independent of miR-430, miR-19a* and miR-152. (A) Normal expression of gsc at 30% epiboly when injected with control lacZ:glo. (C-E) Expression of *gsc* still expands upon injection of v:sqtmm430, v:sqtmm19a* and v:sqtmm152, similar to injection of v:sqt (B). (F-J) Expression of Venus protein at 24h shows the efficacy of the miRNA target site mutations. Venus expression is barely detected in v:sqt injected embryos (G), in comparison to v:glo (F), v:sqtmm430 (H), v:sqtmm19a* (I) and v:sqtmm152 (J) injected embryos. Graph in K shows angle of gsc expression in injected embryos at 30% epiboly. Each blue dot represents a single embryo. N indicates number of injected embryos, and μ(°) is the mean angle of *gsc*. (A-E) Animal pole views with dorsal to the right. (F-J), lateral views, dorsal to the right, anterior to the top. Red arrowheads in A-E mark the extent of *gsc* expression; scale bars in A and F, 100μm.

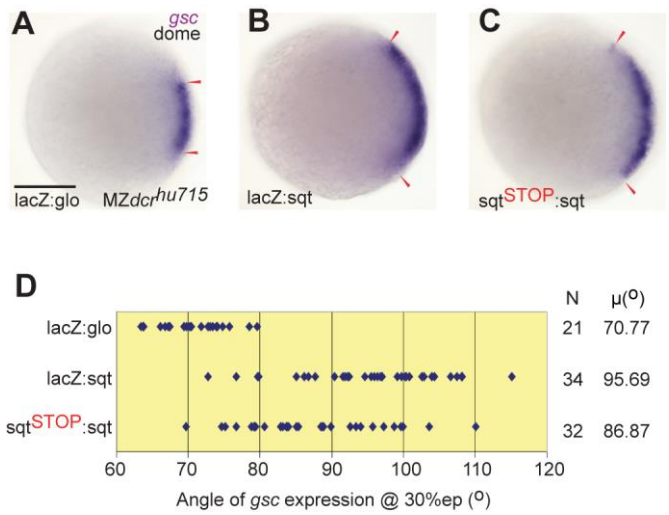

Figure 3.6.1.3 Dorsal expansion by *sqt* 3'UTR is independent of *dicer*. MZ*dicer* embryos injected with lacZ:sqt (B) and sqt^{STOP}:sqt RNA (C) show expanded dorsal gsc in comparison to MZ*dicer* embryos injected with lacZ:glo RNA (A). Therefore, dorsal activity of *sqt* 3'UTR is not mediated via *dicer*. Graph in D shows angle of *gsc* expression in injected embryos at 30% epiboly. Each blue dot represents a single embryo. N indicates number of injected embryos, and μ(°) is the mean angle of *gsc*. (A-C) Animal pole views with dorsal to the right. Red arrowheads in A-C mark the extent of *gsc* expression. Scale bar in A, 100μm.

3.6.2 Activity of maternal non-coding *sqt* does not require new protein synthesis

Maternal *sqt* RNA localizes asymmetrically in zebrafish embryos very early on in development (Gore et al. 2005). It is likely that *sqt* RNA exerts an influence on the initial embryonic dorsal establishment very soon after, because the effects of over-expressed mutant *sqt* RNAs are manifested as increased nuclear accumulation of β-catenin as early as the 512-cell stage (Figure 3.2.2.2C-E). Development during the in-between stages (4-cell to 512-cell) is largely dependent on the limited pool of maternal deposits (Schier 2007), although there may be some early zygotic transcripts being produced (Aanes et al. 2011).

To determine if the dorsal expansion by *sqt* RNA is direct, or whether it requires new protein synthesis, I injected wild-type embryos with sqt^{mut}:sqt RNAs, and treated with the translational inhibitor, Cycloheximide (CHX). I initially performed the experiments from 16-cell to oblong stage using 10 μg/ml of CHX, but prolonged treatments with CHX led to arrested embryonic development. Hence, I did transient CHX treatments from the 16- to 128-cell stage (schematic in Figure 3.6.2A). To determine efficacy of the CHX treatments, I examined the translation of endogenous Cyclin D1 protein (Figure 3.6.2K). If embryos were treated from 16-cell to oblong stage, protein translation is completely blocked. Although removing CHX after the 128-cell stage allowed translation to resume, protein synthesis between the 16-128 cell stage is effectively blocked (Figure 3.6.2K). Therefore, I made use of this strategy to address the requirement for new protein synthesis in the stages immediately after *sqt* RNA localization.

Treated embryos were washed, grown until the onset of gastrulation, and examined for expression of *gsc* (Figure 3.6.2B-J). Similar to control DMSO-treated mutant *sqt* RNA-injected embryos (Figure 3.6.2G,H,J), CHX-treated embryos injected with mutant *sqt* RNA also showed expansion of *gsc* expression (Figure 3.6.2C,D,J). In contrast, control lacZ:glo-injected embryos do not elicit an expansion in dorsal *gsc* expression domain when treated with either DMSO or CHX (Figure 3.6.2B,F,J). Embryos that were treated with CHX from 16-cell to oblong stage do not stain for *gsc* (Figure 3.6.2E), consistent with observations made by Leung et al., 2003 (Leung et al. 2003). Thus, the expansion of dorsal by *sqt* RNA appears to be independent of new protein synthesis between the 16-128 cell stages, and therefore, is likely to be a direct consequence of the localization of the RNA.

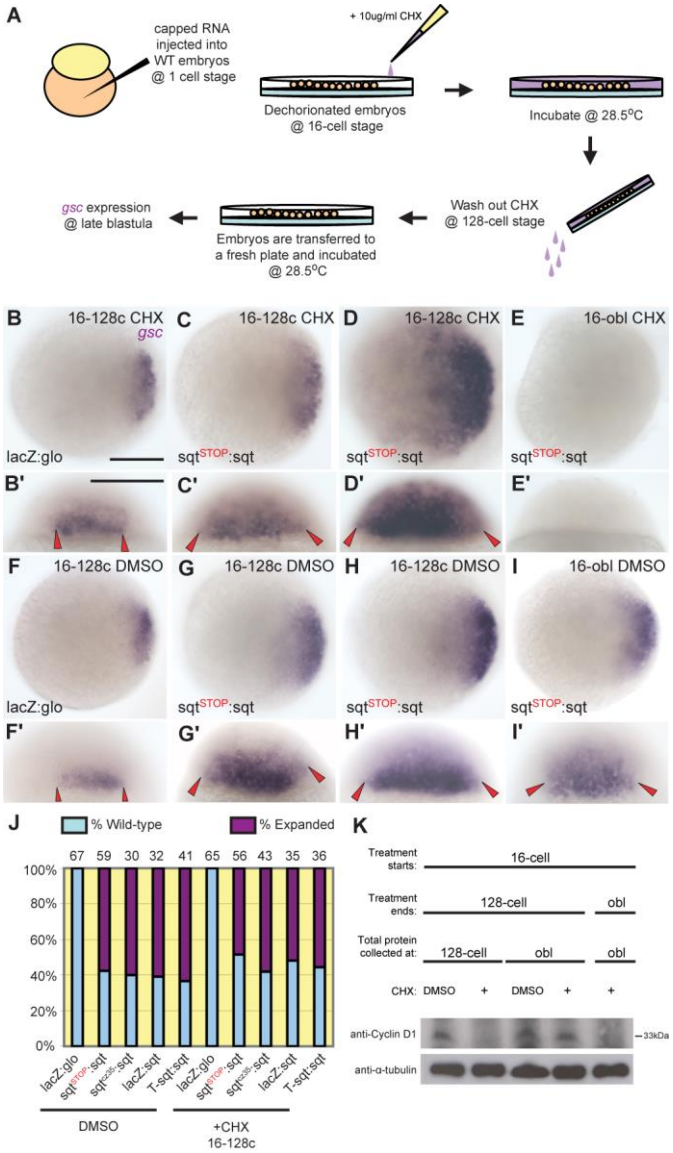

Figure 3.6.2 Dorsalizing activity of mutant *sqt* RNAs does not require new protein synthesis. (A) Schematic showing Cycloheximide (CHX) treatments to block new protein translation in injected embryos. Expression of *gsc* in oblong-stage embryos that were injected with lacZ:glo (B,B',F,F') or sqt^{STOP}: *sqt* RNA, and treated with CHX between 16 and 128 cell stages (C-E and C'-E') shows that sqt^{STOP}: *sqt* RNA injections expand dorsal (C,C',D,D') similar to those treated with DMSO (G-I and G'-I'). Embryos treated with CHX until oblong stages or later were arrested, and show no *gsc* expression (E,E'). Graph in J shows % embryos that manifest expansion of gsc expression with various *sqt* RNA injections and DMSO or CHX treatments. Total number of embryos for each RNA injection and treatment is shown on top. (K) Western blot to detect Cyclin D1 protein in embryo extracts to check the efficacy of CHX treatments. Tubulin was used as a loading control.

3.6.3 Activity is independent of Nodal/Oep signalling

From previous experiments, I have shown that *sqt* UTR but not wild-type Sqt protein is required for initiating dorsal formation in the early embryos. Sqt is a secreted morphogen (Jones et al. 1995; Chen and Schier 2001) that functions via activating cell surface Activin receptors (Shen and Schier 2000; Yeo and Whitman 2001). It is not known how the *sqt* UTR might function in this new role. For instance, does its activity require a functional Nodal signalling pathway?

Maternal and zygotic mutations affecting the Nodal co-receptor, One-eyed pinhead, (MZ*oep*), are thought to cause a complete lack of Nodal signaling in embryos (Gritsman et al. 1999). Although MZ*oep* embryos show reduced mesendoderm, the overall DV axis is still observable and initial dorsal *gsc* expression is present (Gritsman et al. 1999), similar to that observed in *cyc;sqt* double mutants (Dougan et al. 2003). I showed previously that early *gsc* expression is dependent on localized maternal *sqt* RNA (Figure 3.1.1, 3.1.2B). Moreover, the presence of *gsc* in MZ*oep* mutants suggests that the components *sqt* RNA require for dorsal expansion is intact in those embryos.

Nevertheless, I injected mutant *sqt* RNAs into MZ*oep* mutant embryos, and examined *gsc* expression at dome stages. MZ*oep* embryos injected with sqt^{cz35}:*sqt*, sqt^{STOP}:sqt, lacZ:sqt and Tsqt:sqt RNA show expanded *gsc* expression (Figure 3.6.3A-E, F), and the angle of *gsc* expression shows a range from 65^{o}-100^{o}, with a mean of ~88^{o}, in comparison to control lacZ:glo injected embryos which show *gsc* expression ranging from 63^{o}-70^{o}, and a mean angle of ~66^{o} (Figure 3.6.3F). Therefore, expansion of dorsal by *sqt* RNA does not require Nodal signaling, and this function of *sqt* is an Oep-independent function.

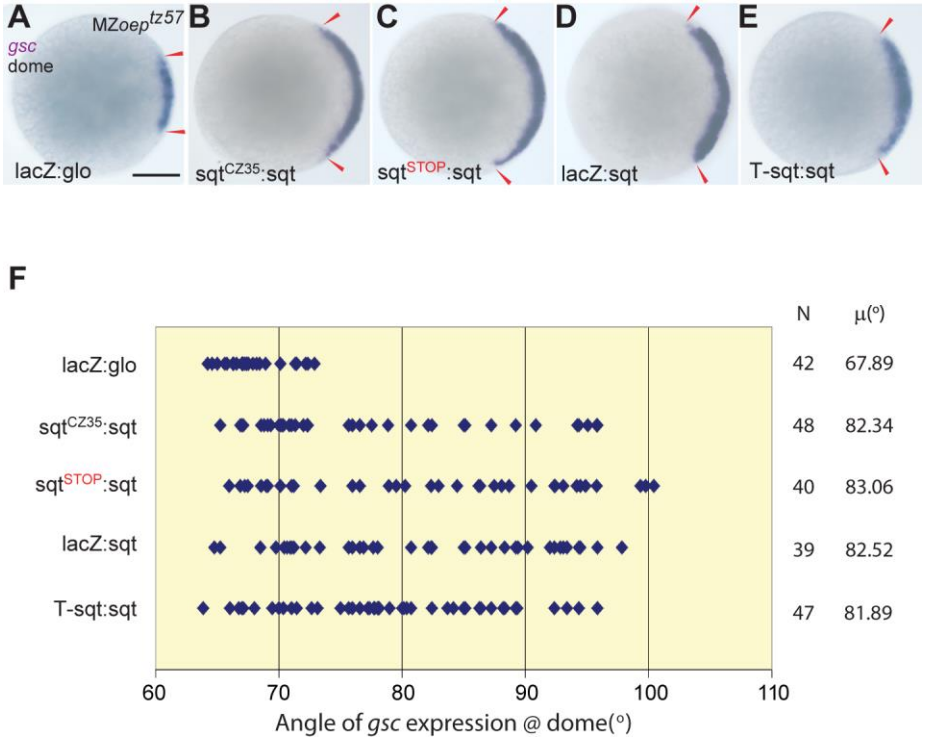

Figure 3.6.3 Dorsalizing activity of *sqt* is independent of Nodal/Oep signaling. Expression of *gsc* in dome stage MZ*oep* embryos (A-E) shows that in comparison to lacZ:glo RNA (A), injection of *sqt*^{cz35}:*sqt* (B), sqt^{STOP}:sqt (C), lacZ:sqt (D), or T-sqt:sqt RNA (E) expands dorsal. Graph in F shows the angle of *gsc* expansion in dome stage MZ*oep* embryos injected with various RNAs. Each blue dot represents a single embryo. N indicates the number of injected embryos for each RNA, and μ(°) is the mean angle of *gsc*. (A-E) Animal pole views, dorsal to the right. Red arrowheads in A-E mark the extent of *gsc* expression. Scale bar in A, 100μm.

3.6.4 Activity requires maternal canonical Wnt/β-catenin signalling

Nuclear accumulation of β-catenin is an early hallmark of dorsal and indicative of activated canonical Wnt signalling (Kelly et al. 2000). One intriguing observation I made was maternal *sqt* RNA functions ahead of nuclear accumulation of β-catenin, and mutant *sqt* RNA injections can increase the number of β-catenin-positive nuclei in both the blastoderm and YSL (Figure 3.2.2.2 C,D,E). This data suggests cross-talk between maternal *sqt* RNA and maternal Wnt signalling, with *sqt* RNA functioning upstream of Wnt/β-catenin signalling. This is surprising because a vast body of research in frogs, zebrafish and mammals has described canonical Wnt/β-catenin signalling-dependent regulation of *Nodal* genes as being essential for dorsal mesoderm formation (Conlon et al. 1994; Feldman et al. 1998; Osada and Wright 1999; Takahashi et al. 2000; Yang et al. 2002; Hilton et al. 2003; Zhang et al. 2003).

In frogs and fish, maternal Wnt/β-catenin signaling is essential for organizer formation and dorsal specification (Kelly et al. 2000; Tao et al. 2005). Embryos from mothers homozygous for mutations in the maternal effect gene, *ichabod* (*ich*), manifest dorsal deficiencies, and fail to localize β-catenin (Ctnnb2) in dorsal nuclei (Kelly et al. 2000). The *ichabod* mutation is closely linked to the zebrafish *ctnnb2* gene, and results in drastically reduced levels of *ctnnb2* transcripts (Bellipanni et al. 2006). To test if dorsal activity of *sqt* RNA is mediated via canonical Wnt signaling, I injected the various mutant *sqt* RNAs into *ich* mutant embryos, and examined *gsc* expression at early gastrula stages. Expression of *gsc* is not expanded in *ich* mutant embryos injected with *sqt* RNA (Figure 3.6.4.1A-E,K) in contrast to wild-type embryos injected with the mutant *sqt* RNAs (Figure 3.6.4.1F-K). At 24 hpf, mutant *sqt* RNA-injected wild-type embryos look phenotypically normal (Figure 3.6.4.2A,C,E,G,I), similar to previous observations (Figure 3.2.2.1H). I observed that the ventralized phenotypes of *ich* mutant embryos cannot be rescued by injection of mutant *sqt* RNAs (Figure 3.6.4.2B,D,F,H,J), unlike injection of wild-type *sqt* (Gore et al. 2005). Thus, expansion of dorsal by *sqt* RNA is dependent upon a functional Wnt/β-catenin signaling pathway.

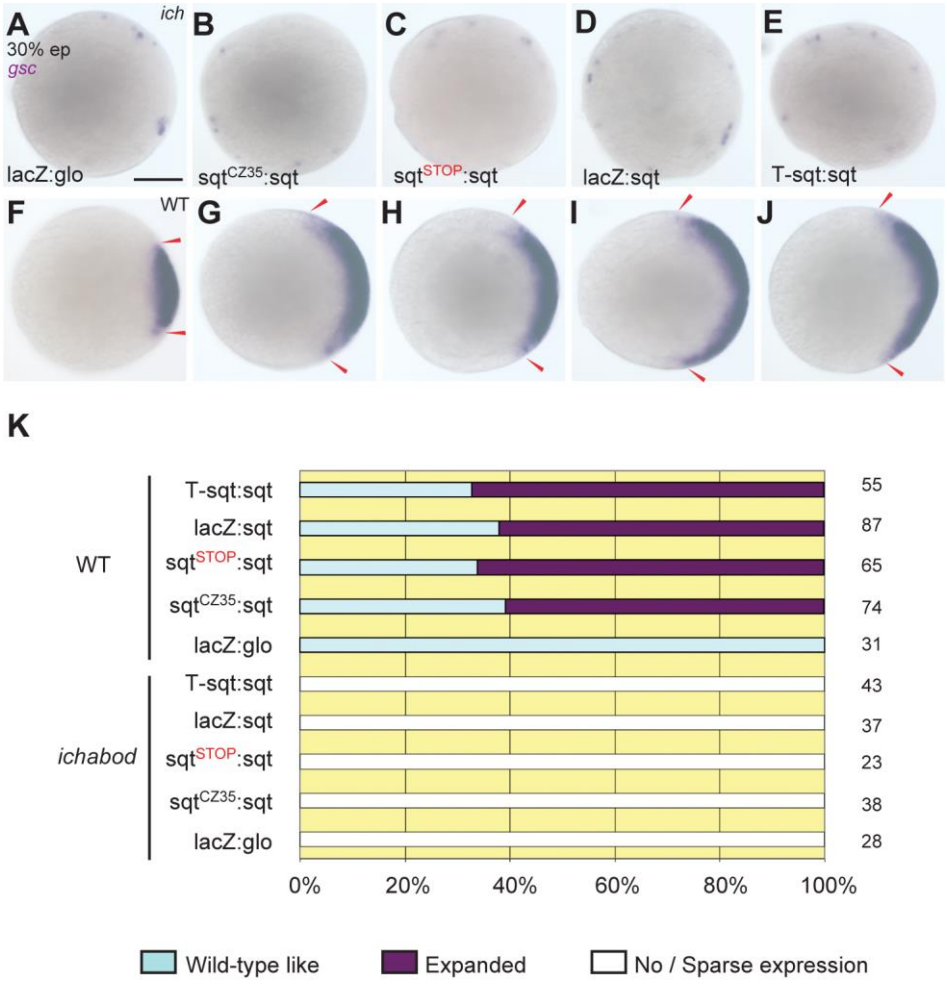

Figure 3.6.4.1 Dorsalizing activity of *sqt* requires canonical Wnt/β-catenin signalling. (A-E) *ich* mutant embryos show no or very sparse *gsc* expression for all injected mutant *sqt* RNAs, as well as control lacZ:glo RNA. (G-J) The same mutant *sqt* RNAs can expand dorsal *gsc* expression at comparable stages, in contrast to control lacZ:glo RNA (F). Graph in K shows % embryos that manifest expansion of *gsc* expression at 30% epiboly upon injection of various *sqt* RNAs in control or *ich* mutant embryos. (A-J) Animal pole views. (F-J) Dorsal to the right. Red arrowheads in F-J mark the extent of *gsc* expression. Scale bar in A, 100µm.

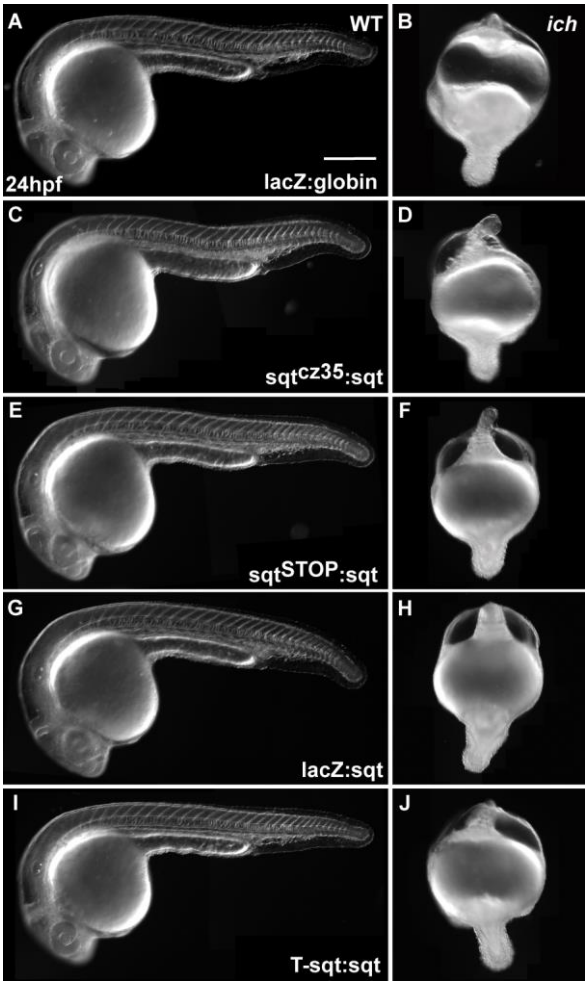

Figure 3.6.4.2 Injection of mutant *sqt* RNA does not rescue *ichabod* mutant embryos. Although mutant *sqt* RNAs (*sqt*^{cz35}:*sqt*, sqt^{STOP}:sqt, lacZ:sqt, and T-sqt:sqt) can expand early dorsal gene expression, at 24 hpf, mutant RNA injected embryos (C,E,G,I) were indistinguishable from control lacZ:globin injected embryos (A). (B,D,F,H,J) Furthermore, injection of the various mutant *sqt* RNAs failed to rescue dorsal structures in *ich* mutant embryos, unlike injection of *sqt*:*sqt* UTR RNA (Gore et al, 2005). (A,C,E,G,I) Lateral views, anterior to the left. (B,D,F,H,J) Lateral views, anterior to the top. Scale bar in A, 100µm.

3.7 Generation of RNA-null *sqt* mutant alleles

To unequivocally demonstrate that the maternal requirement of *sqt* RNAwhich has a non-coding role in the initial DV establishment, an RNA-null *sqt* mutant is essential. In zebrafish, large scale genetic screens have been carried out using the chemical mutagen, N-ethyl-N-nitrosourea (ENU) (Mullins et al. 1994; Solnica-Krezel et al. 1994; Riley and Grunwald 1995; Driever et al. 1996; Haffter et al. 1996). This chemical generates point mutations randomly in the genome, and although it is unlikely to disrupt gene transcription, it can potentially inactivate protein function due to the production of pre-mature stop codons. As I have shown earlier that a mutant *sqt* RNA harbouring a pre-mature stop signal (sqt^{STOP}:sqt) still possess dorsal-expanding activity (Figure 3.2.1, 3.2.2.2, 3.2.2.3, 3.3.1), an ENU-generated *sqt* lesion will most likely not assist in addressing the maternal non-coding role of *sqt* RNA. Indeed, despite screening through the European Union-funded FP6 Integrated Project ZF-MODELS collection of more than 7000 ENU mutagenized males, only three missense mutations in *sqt* was identified, and *sqt* RNAs carrying those mutations still possess activity upon overexpression.

However, targeted mutagenesis methods e.g. conditional whole gene knock-out technologies, that are widely used in embryonic stem cells and mice models (van der Weyden et al. 2002; Glaser et al. 2005), have only begun to show promise in zebrafish (Zu et al. 2013). Hence, I explored the possibility of using insertional mutagenesis methods e.g. transposons, to disable *sqt* transcription. Though non-targeting, it is possible that the transposon, if inserted into the transcription regulatory region of *sqt*, can generate a *sqt* RNA-null allele.

3.7.1 Remobilization of *Tol2* insertion in ET33-24

Transposons are mobile genetic elements that can integrate into the genome and potentially disrupt gene function (McClintock 1950; Kawakami et al. 1998; Kawakami and Shima 1999). These integrations are immobile in the absence of the transposase, and therefore can lead to establishment of stable transgenic lines. Due to a transposon's ability to integrate randomly at high efficiency, it has proven to be a useful reverse genetics tool. In zebrafish, several transposon systems e.g. *Sleeping Bea*uty (Davidson et al. 2003; Balciunas et al. 2004), *Tol2* (Kawakami et al. 2000; Kawakami et al. 2004; Parinov et al. 2004) and more recently *Ac-Ds* (Emelyanov et al. 2006; Parinov and Emelyanov 2007) have been

shown to be functional. Using these tools, large enhancer- and gene-trapping screens have been conducted and integration sites were identified using TAIL-PCRs, Inverse-PCRs and whole genome re-sequencing ((Trinh le et al. ; Kawakami et al. 2004; Urasaki et al. 2008; Kondrychyn et al. 2009; Clark et al. 2011) and Quach et al., unpublished data). However, after searching through the online public databases e.g. Zebrafish Enhancer TRAP lines database (ZETRAP 2.0, http://plover.imcb.a-star.edu.sg/webpages/home.html) and Zebrafish Gene Trap and Enhancer Trap Database (zTRAP, http://kawakami.lab.nig.ac.jp/ztrap/), I did not find any insertions in genomic *sqt* locus.

The Kawakami and Korzh laboratories (Garcia-Lecea et al. 2008; Urasaki et al. 2008) have reported the phenomenon of "local hopping" in their transposon re-mobilization experiments, where they introduce *tol2* transposase mRNA into stable transgenic lines that contain only one transposon insertion. This phenomenon seems to be a shared feature of "cut and paste" transposons. Hence, I decided to capitalize on this characteristic of *Tol2* to generate deletions which could potentially affect *sqt*, by remobilizing an insertion on zebrafish chromosome 21.

From a database collection of enhancer-trap lines from the Korzh laboratory (ZETRAP 2.0: Zebrafish Enhancer TRAP lines database http://plover.imcb.a-star.edu.sg/webpages/home.html), I identified an enhancer trap (ET) insertion, ET33-24, approximately 14 Mb away from *sqt* (chr21:19,838,794-19,840,960) (Figure 3.7.1.1A). The enhancer trap cassette, containing *keratin4* (*ker4*)-driven *egfp*, is inserted in a reverse orientation with respect to *sqt* (Figure 3.7.1.1A). To remobilize the ET cassette, I injected 100 pg of synthetic capped *tol2* mRNA into 1-cell stage embryos obtained from homozygous ET33-24 pairs. At this dosage, ~ 50% of *tol2*-injected embryos (n=87) showed embryonic lethality. All of the remaining embryos displayed speckled GFP expression (Figure 3.7.1.2B), distinct from the uniform epidermal expression in un-injected ET33-24 controls (Figure 3.7.1.2A), indicating occurence of *Tol2*-induced remobilization events.

Tol2-injected embryos were raised to adulthood and mated with MZ*sqt*^{cz35} to screen for non-complementation of the zygotic *sqt* phenotype (Figure 3.7.1.1B). At 28 hpf, each clutch showed a mixture of GFP+ and GFP- embryos, broadly indicative of ET excision in the founder's germline. Based on expression pattern changes at 28 hpf, 11 F0s transmitted an insertion distinct from the original site (Figure 3.7.1.2C,D,E,F). This number is likely to be

an underestimate of the actual re-mobilization frequency because visual GFP screening will not identify newly-located inserts that fail to trap enhancers. Although I have successfully remobilized the ET insert on chromosome 21, all embryos screened do not manifest *sqt* phenotypes. Hence, this suggests that the excised ET did not re-insert in a region that disrupts the genomic *sqt* locus.

It was generally observed in the past that *Tol2* transposon system functions via a "cut and paste" mechanism, and it creates no more than an 8 bp duplication at the target site. No complex DNA rearrangements or other modifications were reported (Kawakami et al. 2000). However, recent results from Kawakami lab showed that remobilization of a *Tol2* insert generates small (less than 100 bp) deletion surrounding the original integration site. This makes *Tol2*-based insert remobilization unsuitable for the generation of a *sqt* mutant, as a successful remobilization might in the process generate other mutations that will complicate mutant analysis. It is possible to use transposons to create a *sqt* mutant but to disrupt only *sqt*, the founder integration has to be inserted into *sqt* or its transcription regulatory regions. Given that transposon-based mutagenesis is random, the chance of finding a new *sqt* allele will be equivalent to other random mutagenesis methods e.g. ENU-based and will involve tedious screening of thousands of fish.

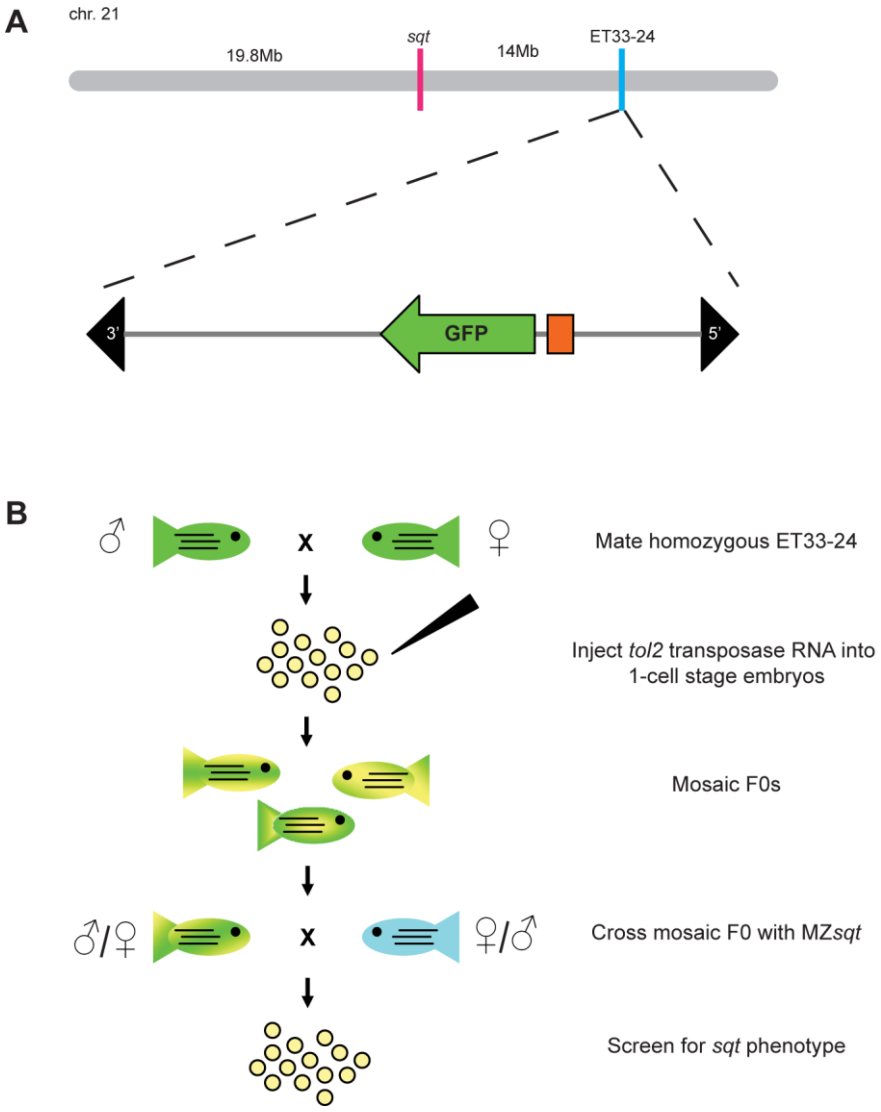

Figure 3.7.1.1 *Tol2*-mediated remobilization to disrupt *sqt*. (A) Schematic representation of Chromosome 21 and relative positions of *sqt* and ET33-24 insertion. The ET33-24 enhancer trap cassette is reversely-oriented with respect to *sqt*. Black triangles mark *Tol2* terminal inverted repeats. EGFP expression is driven by *keratin4* mini-promoter (orange box). (B) Screening scheme for *Tol2*-remobilized inserts. Mosaic *tol2*-injected F0s are crossed with MZ*sqt*^{cz35} and screened for non-complementation of zygotic *sqt* phenotype.

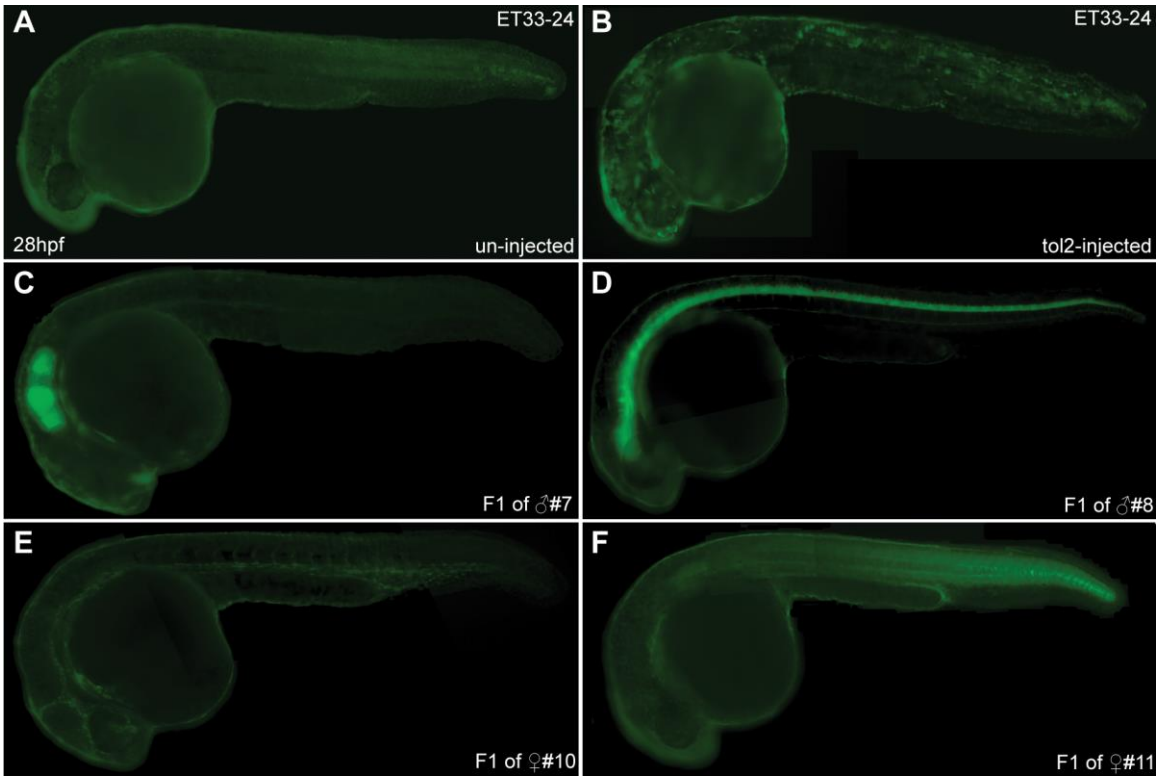

Figure 3.7.1.2 Tol2-mediated remobilization observed but *sqt* locus not disrupted. ET33-24 embryos injected with *Tol2* transposase RNA (B) showed speckled EGFP expression, in contrast to un-injected embryos (A), indicating excision of original ET33-24 insert. (C,D,E,F) F1embryos of *tol2*-injected F0s exhibited changes in EGFP expression, indicating re-integration of excised ET33-24 insert into new genomic regions.

3.7.2 Targeting nucleases

In recent years, the engineered nucleases technology has revolutionized the field of biology such that targeted mutagenesis or gene-replacement is no longer restricted to *in vitro* cell lines. Much to the advantage of zebrafish researchers, Zinc Finger Nucleases (ZFNs) and more recently, Transcription activator-like effector nucleases (TALENs) have been proven facile in targeted genome editing (Doyon et al. 2008; Meng et al. 2008; Huang et al. 2011; Dahlem et al. 2012). In contrast to previous mutagenesis methods e.g. N-ethyl-N-nitrosourea, gamma radiation, transposons etc., engineered nucleases offer more selectivity over target sites, with the possibility of a TALE-binding site occurring every 35 bp (Cermak et al. 2011).

For analyzing the function of maternal *sqt* RNA in dorso-ventral patterning, I surmised that the current *sqt* insertion mutant alleles that are not RNA nulls would not be the right tools. Instead, an appropriate *sqt* mutant would be one that either has the transcription start site (TSS) removed or the whole locus deleted. It has been demonstrated that mutagenic lesions of modest sizes can be achieved, with rare occurrence of large mutations, when a single ZFN- or TALEN-induced double-stranded breaks (DSBs) in the genome gets resolved by the error-prone non-homologous end-joining (NHEJ) DNA repair pathway (Bibikova et al. 2001; Beumer et al. 2006; Doyon et al. 2008; Meng et al. 2008; Huang et al. 2011; Dahlem et al. 2012) Indeed, in the transient assays of injected F0 embryos, I observed that *sqt*ZFN1 which targets *sqt* exon 2 gave rise to mutant alleles with small insertions/deletions/in-dels (Figure 3.7.2.1A). However, only 1/92 F0s screened transmitted through the germline, a 4 bp GGCC insertion at the target site (Table 3.7.2.3). Therefore, to increase the chances of deleting large regions accurately, I decided to harness the combinatorial action of multiple nucleases in removing either *sqt* TSS or whole *sqt* locus.

3.7.2.1 Target sites of *sqt* ZFNs and TALENs

ZFNs targeting the genomic *sqt* locus, *sqt*ZFN1 and *sqt*ZFN2, were selected and tested using the "OPEN" system (Maeder et al. 2008) by ToolGen Inc., Korea, for binding efficacy and activity. They target *sqt* exon 2 and *sqt* exon1 respectively (Figure 3.7.2.1A and Table 3.7.2.1). However, for my purpose of creating an RNA-null *sqt* mutant, the removal of the region intervening ZFN1 and ZFN2 is likely to be inutile. Therefore, I decided to generate TALENs with target sites at the 5' and 3'ends of genomic *sqt* locus.

As TALENs have single nucleotide resolution in their binding specificity (Mussolino et al. 2011; Dahlem et al. 2012), it is critical to tailor-make them according to the sequence of the wild-type fish stocks to be injected. Therefore, I fin-clipped 10 pairs of wild-type ABs, performed genomic PCR and sequenced an ~450 bp stretch at the 5' and 3' ends of *sqt* (yellow boxes in Figure 3.7.2.1A). From a multiple sequence alignment of the 20 fishes, I identified DNA stretches with no polymorphisms and further defined the TALEN target sites using an online tool TAL Effector Nucleotide Targeter, TALE-NT (https://tale-nt.cac.cornell.edu). The selected 5' and 3' *sqt* target sites (Figure 3.7.2.1A and Table 3.7.2.1, *sqt*5'TAL, chr21: 19,838,706-19,838,767; *sqt*3'TAL, chr21: 19,840,869-19,840,929; Zebrafish genome assembly Zv9) were blasted against the zebrafish genome assembly (Zv9) to check for uniqueness. Then, the TAL effector repeats were generated from 4 TAL effector single unit vectors (pA, pT, pG^{NN} and pC) using the "unit assembly" method (Huang et al. 2011).

Table 3.7.2.1. List of target sites for *sqt* TALENs and ZFNs

Target Gene	Targeting nuclease	Target site sequences (5’ to 3’)
sqt	*sqt*5’TAL	GCAAGTTTCTATAAGTgaacttagatgaccggccagcactcatgacATTCACTTTCCAGAGG
	*sqt*3’TAL	GCTATTATTGAAAGCTttgcgtgtttgccttatctgtaaatagtAGAGTATGTAAATTACC
	*sqt*ZFN1	TCACGCATCTACacctgaGTGTGAGAGAAG
	*sqt*ZFN2	CCTTGCTGGATTtcaagaGACCCTCAGGAA

Binding sites are in uppercase. Spacer sequences are in lowercase.

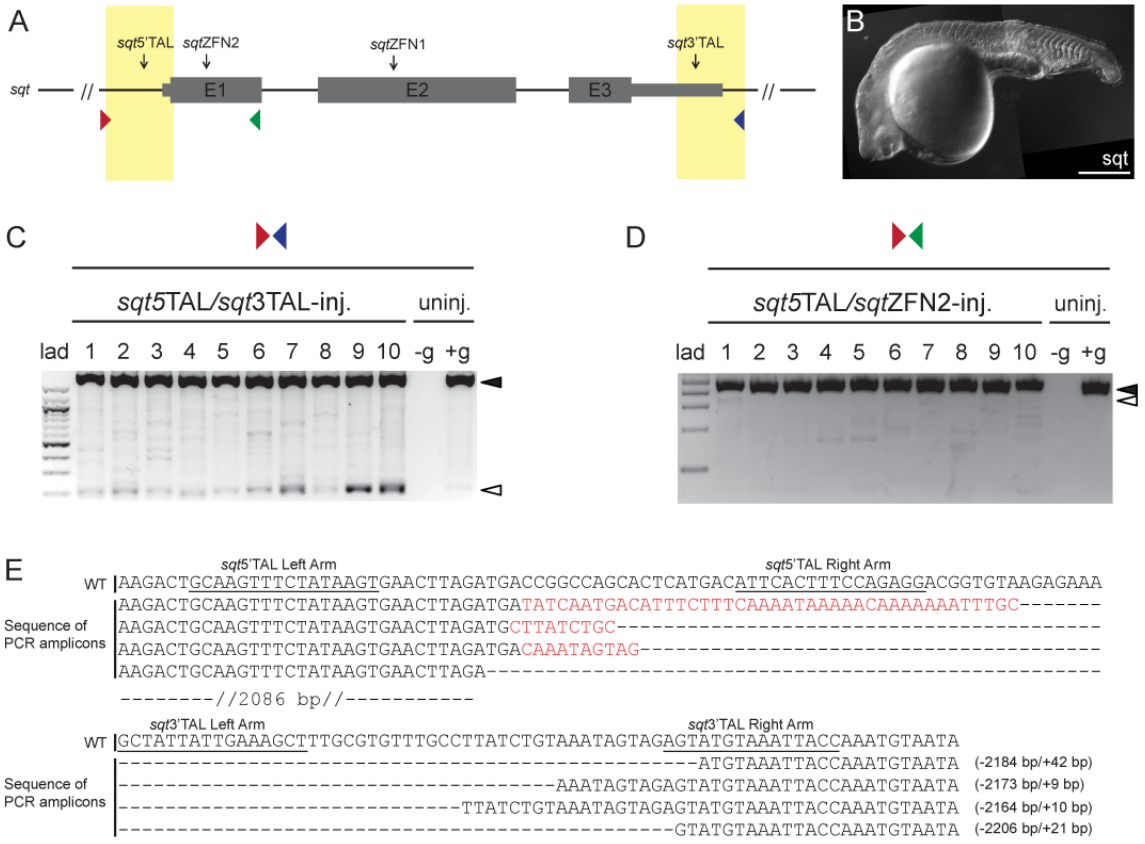

Figure 3.7.2.1 Targeted deletions in *sqt* by multiple TALEN and ZFN pairs. (A) Schematic representation of *sqt* locus, with positions of the TALEN targeting sites and ZFN targeting sites indicated by black arrows. E1, E2 and E3 indicate *sqt* exons 1-3. Colored triangles indicate the position of primers used for genotyping. (B) Phenotype of representative *sqt* nuclease-injected embryo manifesting cyclopia and midline defects. Scale bar, 100µm. (C) PCR with primers (red and blue triangles in A) spanning the *sqt* locus show a 2.4 kb product (black arrowhead) for the intact *sqt* locus, whereas individual embryos with TALEN deletions show a ~220 bp complete locus deletion product (white arrowhead) and several other intermediate sized products. No template control is indicated by –g. (D) PCR with primers spanning the *sqt* TSS site (red and green triangles in A) show a 478 bp full-length product for the wild type product (black arrowhead), whereas one embryo (#1) shows the expected ~300 bp deletion (white arrowhead). No template control is indicated by –g. (E) Alignment of wild type *sqt* sequences with some representative sequence from the PCR amplicons in C shows various deletions of ~ 2.2 kb between the targeting sites, accompanied by small insertions (red).

3.7.2.2 *sqt* ZFN and TALENs can induce lesions in *sqt*

To determine the optimal dosage for introducing lesions, I micro-injected various amounts of *sqt* TALEN and ZFN pairs into wild-type 1-cell stage zebrafish embryos individually and in combinations, and assessed cutting efficiency, phenotypes and survival at 24 hpf (Figure 3.7.2.1A,B and Table 3.7.2.2). Cyclopia and midline defects, similar to that observed in zygotic *sqt* mutants, were apparent in 15-25% of *sqt* nuclease-injected F0 embryos (Figure 3.7.2.1B and Table 3.7.2.2).The occurrence of characteristic zygotic *sqt* phenotypes in F0 embryos is indicative of bi-allelic mutations.

Next, to assess the efficacy of deletion mutations, I extracted genomic DNA from *sqt* nuclease-injected single 1 dpf embryos, and performed PCR and sequencing using *sqt*-specific primers (Figure 3.7.2.1C,D). Consistent with previous studies using single ZFN or TALEN pairs, alignment of the nuclease-induced lesions to wild-type *sqt* genomic sequence revealed that each nuclease pair by itself generated variable small insertions and deletions (Doyon et al. 2008; Meng et al. 2008; Huang et al. 2011). In contrast, PCR performed on embryos injected with either *sqt*5'TAL/*sqt*3'TAL or *sqt*5'TAL/*sqt*ZFN2 displayed both the wild-type PCR product (closed arrowhead, Figure 3.7.2.1C,D), as well as several smaller-sized products including one (open arrowhead, Figure 3.7.2.1C,D) that would be expected if intervening sequences were deleted totally. For the *sqt5*'TAL/*sqt*3'TAL combination, the deletions were confirmed by sequencing of the PCR products, and their alignment to wild-type *sqt* sequences showed that large deletions can be accompanied by insertions at both 5'and 3' targeting ends (3.7.2.1E). For *sqt5*'TAL/*sqt*ZFN2-injected embryos, the expected deleted product was detected at a low frequency and sequence analysis after T-cloning only identified wild-type *sqt* sequences.

To generate stable RNA-null *sqt* mutants, I raised *sqt5*'TAL/*sqt3*'TAL- and *sqt5*'TAL/*sqt*ZFN2-injected embryos to adulthood, and screened their progeny by PCR, using primers spanning the targeting sites (Figure 3.7.2.1A). I identified *sqt* whole-locus deletions in 3.3% to 9.5% F1 progeny of 6/56 *sqt5*'TAL/*sqt*3'TAL- injected F0s.

Amongst the *sqt5*'TAL/*sqt*ZFN2-injected F0s, I observed smaller 5'TSS deletions in 3.3% to 6.7% F1 embryos of 2/28 F0s (Figure 3.7.2.4 and Table 3.7.2.3). However, of the two founders transmitting *sqt* TSS deletions, PCR and sequencing revealed that only one appears to have resulted from combinatorial targeting by both *sqt5*'TAL and *sqt*ZFN2, whereas the other is likely produced from the activity of *sqt5*'TAL alone (Figure 3.7.2.4). After screening, selected founders positive for the whole locus deletion and *sqt* TSS deletion were propagated via crossing to wild-type, to obtain heterozygotes.

Table 3.7.2.2. Frequency of cyclopia and mid-line defects in *sqt* TAL and/or ZFN-injected embryos

Targeting Nuclease(s)	Wildtype	Cyclopia and midline defects	Abnormal	Dead	Total (N)
25pg *sqt*ZFN2	62 (53.0%)	25 (21.4%)	18 (15.4%)	12 (10.2%)	117
50pg *sqt*ZFN2	32 (29.1%)	26 (23.6%)	37 (33.6%)	15 (13.6%)	110
25pg *sqt*5TAL	22 (71.0%)	3 (9.7%)	0 (0.00%)	6 (19.3%)	31
50pg *sqt*5TAL	43 (45.7%)	15 (16.0%)	18 (19.1%)	18 (19.1%)	94
25pg *sqt*3TAL	18 (47.4%)	0 (0.00%)	5 (13.1%)	15 (39.5%)	38
50pg *sqt*3TAL	29 (38.2%)	12 (15.8%)	15 (19.7%)	20 (26.3%)	76
25pg *sqt*5TAL+*sqt*ZFN2	22 (29.3%)	17 (22.7%)	19 (25.3%)	17 (22.7%)	75
25pg *sqt*5TAL+*sqt*3TAL	30 (36.1%)	20 (24.1%)	15 (18.1%)	18 (21.7%)	83

Numbers were tabulated from at least 2 independent experiments.

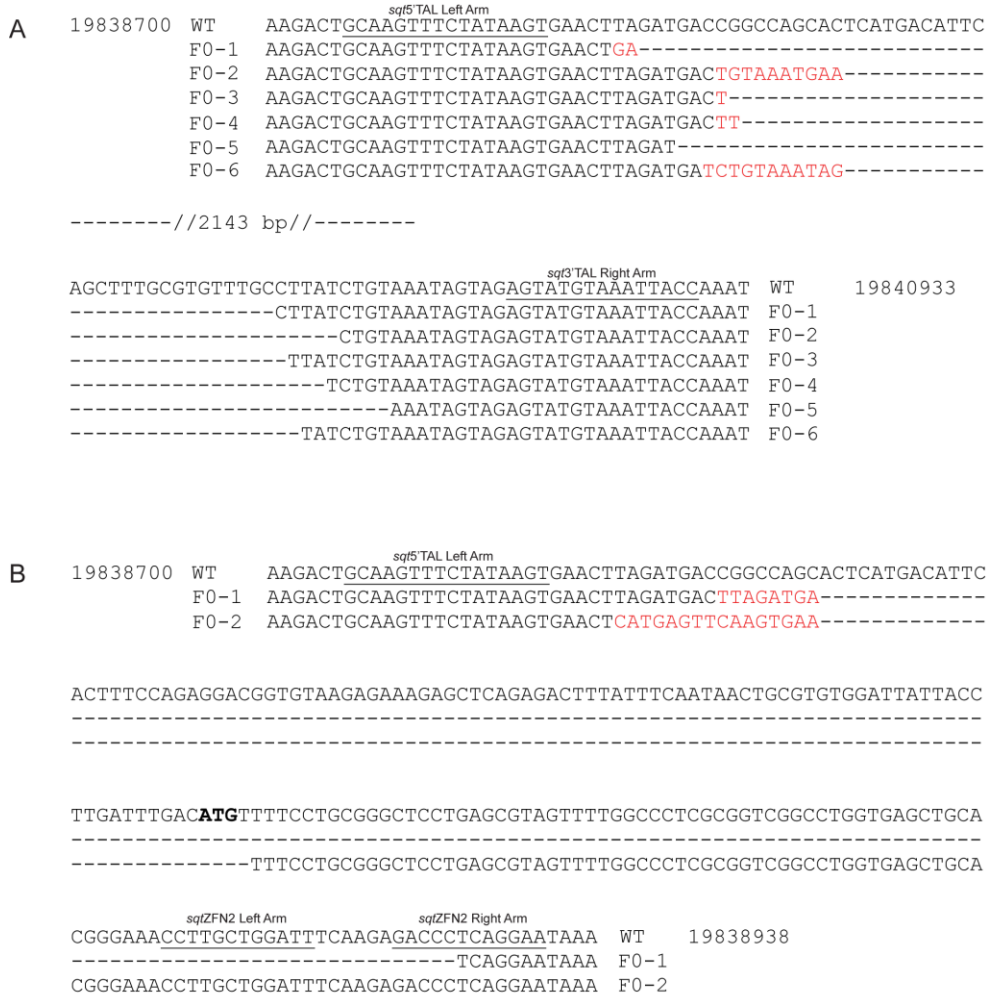

Figure 3.7.2.2 *sqt* ZFN and TALENs can induce heritable mutagenic lesions in *sqt*. (A) Alignment of *sqt* sequences showing the whole-locus and TSS deletions in embryos from F0 founders, compared to wild type *sqt*. Insertions are highlighted in red font, and gaps are indicated with dashed lines. All 6 founders for *sqt5*'TAL/*sqt3*'TAL showed embryos with the 2.1 kb whole locus deletion. (B) For *sqt5*'TAL/*sqt*ZFN2, founder 1 (F0-1) showed embryos with the intervening sequences excised, whereas founder 2 (F0-2) sequences indicate that only the 5'TAL was active. Genomic coordinates on chromosome 21 for wild type *sqt* are indicated for the regions shown. TALEN and ZFN target sites are indicated.

3.7.2.3 New *sqt* alleles are *bona fide sqt* RNA nulls

After breeding the new *sqt* mutant alleles to heterozygosity, I tested them for genetic complementation with the existing sqt^{cz35} insertion allele. I mated fish heterozygous for the ZFN-induced sqt^{sg7}, *sqt*5'TAL/*sqt*3'TAL-induced sqt^{sg32} whole-locus or *sqt*5'TAL/*sqt*ZFN2-induced sqt^{sg27} TSS deletion mutations with sqt^{cz35} insertion mutant carriers, and observed that 20-25% of the embryos manifest cyclopia and deficiencies in midline structures such as the notochord (Figure 3.7.2.4A-I). Therefore, the *sqt* TALEN and ZFN-induced mutations at the endogenous *sqt* locus do not complement the sqt^{cz35} insertion mutant phenotypes.

Finally, to ascertain if the *sqt* transcriptional start site and whole locus deletions actually abolish *sqt* RNA expression in mutant embryos, I performed semi-quantitative RT-PCR on sqt^{sg27} and sqt^{sg32} embryos. The zygotic expression of *sqt* peaks at 30% epiboly (Feldman et al. 1998; Rebagliati et al. 1998; Dougan et al. 2003; Gore et al. 2005). I collected single 30% epiboly embryos from pair-wise matings of heterozygous $sqt^{sg27/+}$ or $sqt^{sg32/+}$ fish, extracted both genomic DNA for genotyping, and total RNA for RT-PCR. In homozygotes for both the *sqt* TSS and whole *sqt* locus deletion, un-spliced and spliced forms of *sqt* RNA were not detected (Figure 3.7.2.5B,C). As predicted, the semi-quantitative RT-PCR results for the heterozygotes showed reduced amount of un-spliced and spliced *sqt* RT-PCR products in comparison to wild-type genotype, consistent with the heterozygous status. Therefore, my newly minted *sqt* alleles, sqt^{sg27} and sqt^{sg32}, are indeed *bona fide sqt* RNA-null mutants.

As sqt^{sg27} and sqt^{sg32} alleles are deletions in the genome, I also determined if adjacent genomic regions and elements were affected in these *sqt* mutants by examining expression of immediate flanking loci (*eif4ebp1*, *htr1ab*, and *rnf180*, Figure 3.7.2.3A) at appropriate stages. The *htr1ab* gene is located 5' to *sqt* in the same orientation, whereas *rnf180* and *eif4ebp1* genes are both oriented in the reverse direction to *sqt*, with the former located 5' upstream of *sqt* and the latter 3' downstream of *sqt*. Semi-quantitative RT-PCRs to detect expression of *eif4ebp1*, *htr1ab*, and *rnf180* show that their

transcription is unaffected in the *sqt*^{sg27} TSS deletion mutant embryos (Figure 3.7.2.3B). Similarly, flanking gene expression is not affected in homozygous *sqt*^{sg32} whole-locus deletion mutant embryos (Figure 3.7.2.3C). Thus, *sqt*^{sg27} and *sqt*^{sg32} lesions specifically affect *sqt* RNA transcription but do not affect neighboring transcriptional units.

Table 3.7.2.3. Germline transmission frequency of *sqt* TAL- and/or ZFN-induced lesions in zebrafish

Targeting nuclease(s)	No. of F_0 screened	No. of mutant F_0s
*sqt*5'TAL + *sqt*3'TAL	56	6 (whole locus deleted)
*sqt*5'TAL + *sqt*ZFN2	28	2 (TSS deletions)
*sqt*ZFN1	92	1 (small insertion)

For each founder (F_0), at least 30 F1 embryos were analysed individually.

Figure 3.7.2.3 Sequences of new *sqt* alleles. Alignment of *sqt* sequences showing the *sqt*^{sg27} TSS deletion (A), *sqt* ^{sg32} whole-locus deletion (B), and *sqt*^{sg7} ZFN (C) mutations in comparison to wild type *sqt*. Insertions are highlighted in red font, and gaps are indicated with dashed lines. TALEN and ZFN target sites are indicated.

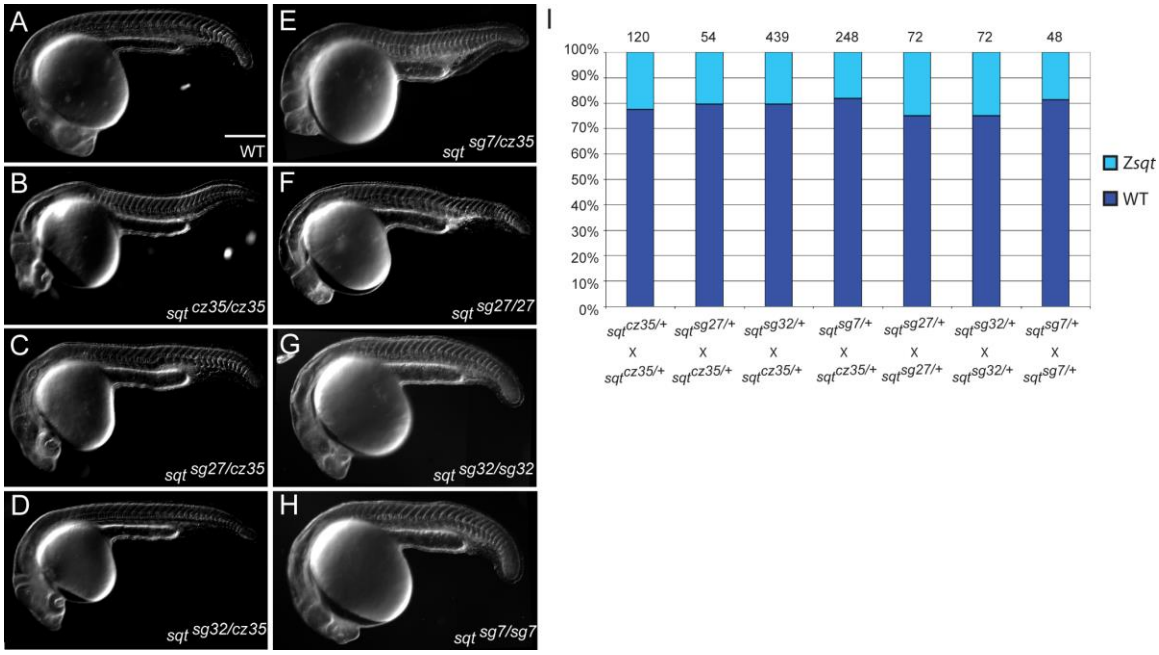

Figure 3.7.2.4 New *sqt* alleles do not complement *sqt*^{cz35} allele. DIC images of 24 h wild type (A), *sqt*$^{cz35/cz35}$ (B), *sqt*$^{sg27/cz35}$ (C), *sqt*$^{sg32/cz35}$ (D), *sqt*$^{sg7/cz35}$ (E), *sqt*$^{sg27/sg27}$ (F), *sqt*$^{sg32/sg32}$ (G), and *sqt*$^{sg7/sg7}$ (H) embryos; scale bar in A, 100µm. (I) % embryos with *sqt* mutant phenotypes in *sqt* $^{cz35/+}$, *sqt* $^{sg27/+,}$ *sqt* $^{sg32/+}$ and *sqt* $^{sg7/+}$ in-crosses and mating of *sqt* $^{cz35/+}$ with *sqt* $^{sg27/+}$, *sqt* $^{sg32/+}$ and *sqt* $^{sg7/+}$. The *cz35* allele is a ~1.9kb insertion in *sqt* exon 1; the *sg27* allele is a 98 bp deletion of *sqt* TSS sequences; *sg32* allele is a whole locus deletion of *sqt*; the *sg7* ZFN allele harbors a GGCC insertion in *sqt* exon 2.

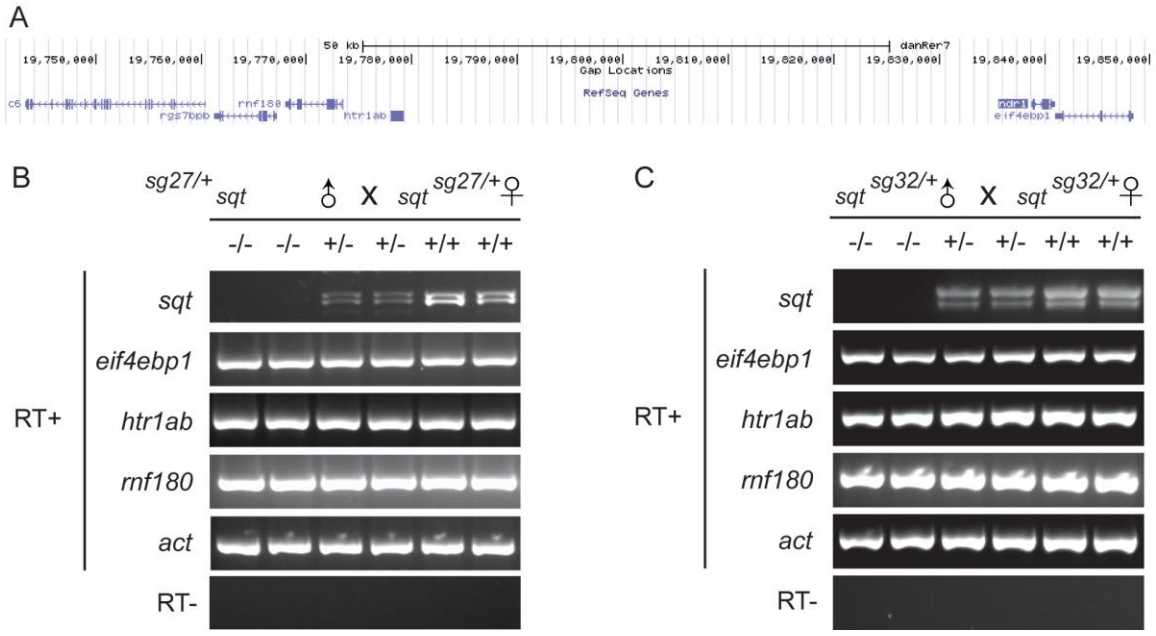

Figure 3.7.2.5 New *sqt* alleles are *bona fide sqt* RNA nulls. (A). UCSC genome browser view of the *sqt* locus and neighboring genomic region. RT-PCR with primers to detect expression of *sqt* RNA and transcripts of neighboring genes, *eif4bp1*, *rnf180*, and *htr1ab* shows lack of *sqt* RNA expression in *sqt* $^{sg27/sg27}$ (B) and *sqt* $^{sg32/sg32}$ (C) embryos whereas all neighboring gene transcripts are expressed at wild-type levels. Actin expression was used as control. In contrast both un-spliced and spliced *sqt* RNA is detected in wild-type and heterozygous embryos.

CHAPTER IV: DISCUSSION

4.1 Maternal *sqt* RNA has a non-coding role in early dorsal axis specification

As a fertilized embryo begins its life, one of the earliest and most important decisions it makes is to decide where to form its dorsal, ventral, anterior and posterior structures. In many organisms including humans, the process of embryonic axes specification consists of a multitude of precisely controlled events that are initiated by maternally-deposited factors (Denegre et al. 1997; Riechmann and Ephrussi 2001; Jorgensen and Mango 2002; Pelegri 2003; Dosch et al. 2004; Wagner et al. 2004; Nishida 2005; Schier 2007; Bastock and St Johnston 2008; Li et al. 2010; Langdon and Mullins 2011). These factors activate various signalling pathways to establish the body plan in the developing organism. To identify the maternal factors and understand the precise mechanisms by which they specify the dorso-ventral (DV) axis, I use zebrafish, a vertebrate, as a model organism.

In frogs, flies and fish, a common tactical approach used to break egg symmetry is the asymmetric positioning of maternal determinants. For example in frogs, DV axis is determined by a Wnt pathway component, *Xwnt11* RNA, which is localized to two dorsal vegetal blastomeres by the 8-cell stage, and blocking canonical Wnt signalling pathway results in embryos lacking dorsal structures (Tao et al. 2005). In zebrafish, the asymmetric localization of *sqt* RNA (or *nodal-related 1*) to the presumptive dorsal cells at early cleavage stages shows that dorso-ventral asymmetry in the blastoderm is established prior to the onset of zygotic transcription (Gore et al. 2005). Maternal *sqt* transcripts localize to two cells by the 4-cell stage in a microtubule-driven and 3' un-translated region (UTR)-dependent process. Disruption of proper *sqt* RNA localization, as well as, the knockdown of *sqt* using anti-sense oligonucleotides (morpholinos) or by cell ablation techniques give rise to embryos manifesting severe dorsal deficiencies (loss of head and spinal structures). Therefore, it was proposed that asymmetrically localized *sqt* RNA and associated factors may function to specify dorsal. However, embryos derived from mothers that are homozygous for insertion mutations in *sqt*, sqt^{cz35} and sqt^{hi975}, only exhibit mild dorsal-deficient phenotypes, suggesting that early specification of the dorso-ventral axis might not require the activity of maternal Sqt (Aoki et al. 2002;

Bennett et al. 2007; Pei et al. 2007). In addition, Nodal signalling-deficient mutants such as one-eyed pinhead (MZ*oep*) and zygotic *cyc;sqt* double mutants also do not completely lack dorsal structures (Dougan et al. 2003). Hence, the function of maternal *sqt* in dorsal specification is paradoxical (Bennett et al. 2007; Gore et al. 2007).

Contrary to general belief, sqt^{cz35} and sqt^{hi975} insertion alleles are not maternal transcript nulls: sqt^{cz35} RNA is expressed in MZ*sqt* at similar levels to *sqt* in wild-type embryos at early stages and also localizes to two cells in 4- and 8-cell stage embryos. In the MZ*sqt* mutants, I also observed a reduction in *sqt* RNA levels during gastrulation, consistent with a previous report of reduced *sqt* mutant transcripts in late blastula embryos (Bennett et al. 2007).

One may ask, why are *sqt* mutant RNAs, containing numerous premature translation-termination codons (PTCs), not targeted for degradation by the eukaryotic nonsense-mediated RNA decay (NMD) pathway? The NMD pathway selectively eliminates nonsense transcripts in order to prevent accumulation of potentially deleterious truncated proteins (Culbertson 1999; Wagner and Lykke-Andersen 2002; Baker and Parker 2004; Belostotsky and Sieburth 2009; Huntzinger and Izaurralde 2011). It has been demonstrated that the position of the PTC relative to the exon-exon junction is critical in eliciting NMD (Nagy and Maquat 1998), and both splicing and translation are required for detection of PTCs and recruitment of UPF proteins that trigger NMD (Ishigaki et al. 2001; Lejeune et al. 2004). Similar to wildtype *sqt* RNA, maternal mutant *sqt* RNAs in the MZ*sqt* genetic mutants are un-spliced. They also possess an intact DLE element in their 3'UTR, thus presumably translationally repressed by Ybx1 (Kumari et al. 2013). Hence, mutant *sqt* RNAs in the MZ*sqt* genetic mutants might have escaped the cell's surveillance program due to a composite of factors.

Using a variety of mutations that disrupt Sqt protein, I found that *sqt* RNA has functions in initiation of embryonic dorsal, independent of Sqt protein. Notably, mutant *sqt* RNAs, including sqt^{cz35} RNA, can expand dorsal gene expression, with a concomitant reduction in ventral gene expression. Interestingly, we never detected any ectopic sites of

gsc or *chd* expression in the mutant *sqt* RNA-injected embryos, unlike those injected with wild-type *sqt* RNA (Erter et al. 1998; Rebagliati et al. 1998). Thus, although mutant *sqt* RNAs and the *sqt* 3'UTR can expand the endogenous dorsal domain, these *sqt* sequences do not induce dorsal at ectopic locations, presumably because these RNAs harbour the dorsal localization element (DLE). I also observed slight expansion of *no tail*, a pan-mesodermal gene, expression, suggesting that sqt 3'UTR might have implications in mesoderm induction as well, a phenomenon that is thought to arise from the syncytial layer (Mizuno et al. 1996).

Dorsal expansion induced by mutant *sqt* RNA is not sustained, and by mid-gastrula stages, the embryos appear to have regulated dorsal gene expression levels back to that observed in control embryos. This transient expansion is consistent with the normal *gsc* expression observed at 60% epiboly by Bennett et al., (2007) in T-sqt injected embryos. It is unlikely that the transient dorsal expansion is due to a morphological delay as the embryos are not generally delayed. Moreover, the expansion of *gsc*-expressing domain is restricted to the gastrula margin and does not extend animally, in contrast to the broad *gsc* expression domain reported in early embryos (Schulte-Merker et al. 1994). In addition to expanded *gsc*, I also observed expansion of *chd* and substantially increased numbers of β-catenin-positive nuclei in embryos injected with non-coding *sqt* RNA. In sqt^{mut}:sqt RNA injected embryos, *dha* and endogenous *sqt* transcript levels transiently increase, with a concomitant reduction in *vox* and *vent* transcripts, providing the basis for the transient increase in *chd*, *gsc* and *ntl* and reduction in ventral expression of *gata2* (Hammerschmidt et al. 1996; Erter et al. 1998; Rebagliati et al. 1998; Yamanaka et al. 1998; Imai et al. 2001; Gilardelli et al. 2004). As dorsal expansion by non-coding *sqt* RNA is transient, sqt^{mut}:sqt-injected wild-type embryos look phenotypically similar to wild-type embryos. This is not a standalone case because it has been reported that extra copies of *bicoid+* in *Drosophila* can lead to transient oversized head regions in embryos, which develop into apparently normal adults (Berleth et al. 1988). In 1997, Namba et al. explained that up-regulation and down-regulation of apoptosis, in the enlarged and compromised body regions respectively, have roles in generating such tissue plasticity in early embryonic development (Namba et al. 1997). Hence, it is possible that the zebrafish

embryo has an ability to self-regulate such that changes in early patterning do not lead to overt later consequences, in the absence of active mechanism(s) to reinforce/maintain such changes.

In the course of my study, I also found that although mutant *sqt* RNA can expand dorsal gene expression even in MZ*oep* embryos that lack all Nodal signalling (Gritsman et al. 1999), the expansion is not sustained. Initiation of dorsal *gsc* expression and its subsequent loss has been reported previously in *cyc*;*sqt* compound mutant embryos (Dougan et al. 2003). Therefore, maintenance of *gsc* expression during gastrulation requires Nodal signalling. Although *sqt* RNA can initiate and expand dorsal gene expression independently of *Sqt* protein or Oep-dependent Nodal signaling, the sustenance of dorsal gene expression requires the signaling functions of Sqt mediated via Oep. Thus, *sqt* RNA mediates the early dorsal activity of maternal *sqt*, independent of Sqt protein and its later signaling functions.

So, what may be the reason for the discrepancy between the mild dorsal deficiencies observed in MZ*sqt* insertion mutants and the severe loss of anterior and dorsal structures observed in *sqt* morphants? I observed that injection of non-coding *sqt* RNA into *sqt* morphants can phenocopy MZ*sqt* insertion mutant embryos. Taken together, these findings suggest that it is the activity of the mutant *sqt* transcripts in the maternal *sqt* insertion mutants that leads to initial dorsal expression in mutant embryos, hence providing the reason why MZ*sqt* mutants do not exhibit the severe loss of dorsal identity manifested by *sqt* morphants in which maternal *sqt* RNA localization and activity are both disrupted.

4.2 Proposed model of *sqt* RNA acting as a scaffold

The non-coding function of *sqt* RNA is evident since the *sqt* 3'UTR fused to reporter genes such as *lacZ* or *venus* is sufficient to expand dorsal gene expression, as well as rescue early dorsal gene expression in *sqt* morphant embryos. As miRNA target sites are frequently located in 3' UTR of RNAs (Lee et al. 1993; Wightman et al. 1993;

Reinhart et al. 2000; Johnston and Hobert 2003; Choi et al. 2007; Flynt et al. 2007; Thatcher et al. 2008; Qiu et al. 2009), it is possible that *sqt* 3'UTR may bind negative regulators of dorsal that are in the form of miRNAs. However, I found that the activity of miRNAs is unlikely to be involved in *sqt* RNA-mediated dorsal induction since *sqt* 3'UTR with mutations in the target site sequences of the three predicted microRNAs still expand dorsal. It remains possible that there are other small RNA targets in the *sqt* 3'UTR, which have not been identified yet. Nevertheless, my experiments show that the *sqt* 3'UTR functions independent of the miRNAs tested.

In development, there are some instances where coding RNA also possess a non-coding function. For example in Drosophila, the well-characterized maternal *oskar* (*osk*) transcripts was found to have a non-coding function discovered via genetic mutant analysis. In wild-type, maternal *osk* mRNA is deposited into the oocyte by nurse cells, and becomes accumulated at the posterior end of the oocyte during mid-oogenesis. Then, translation is de-repressed and *osk* mRNA is further processed into two isoforms, long and short Osk, that have functions in posterior polarity determination and primordial germ cell fate specification (Lehmann and Ephrussi 1994; Gunkel et al. 1998). In 2006, Jenny et al. described a new translation-independent role for *osk* mRNA after discovering that mutants (osk^{A87} and osk^{187}) that do not produce *osk* mRNA display oogenesis arrest, whereas Osk protein-null but mRNA-producing mutant females are fertile (Jenny et al. 2006). The eggless phenotype of the osk^{A87} and osk^{187} mutants can be rescued by *osk* 3'UTR but not *osk* CDS, suggesting that it is indeed the function of the mRNA that effect early oogenesis in Drosophila.

RNAs are associated with a wide array of regulatory proteins in ribonucleoprotein complexes throughout their lifespan (Baltz et al. 2012). Staufen, an RNA-binding protein, showed a change in distribution in the *osk* RNA-null mutant, but it does not seem to have a role in early oocyte development. Hence, Jenny et al. discussed the possibility of *osk* RNA performing a scaffolding function for yet unidentified proteins or RNAs essential for oocyte maturation. An alternative hypothesis for *osk* 3'UTR function suggests that *osk* RNA might bind and sequester negative regulator(s) of egg chamber development,

and the identification of such determinants is pertinent to the full understanding of *osk* RNA's mode of action and mechanism.

Another example of a coding RNA with a non-coding function is *vegT* RNA in Xenopus. It encodes a T box transcription factor with functions in mesodermal patterning along the Xenopus's DV and AP axis at different stages of development (Zhang and King 1996). During oogenesis, initially uniformly distributed *vegT* transcripts accumulate at the vegetal hemisphere of the oocyte, together with several other RNAs, and remain there till ovulation (Rebagliati et al. 1985; Bashirullah et al. 1998; King et al. 1999; Palacios and St Johnston 2001; Kloc et al. 2002). Interestingly, antisense oligonucleotide-based knockdown of *vegT* RNA resulted in the release of other RNAs e.g. *vg1* RNA. Cytoskeletal stainings revealed that *vegT* RNA knockdown resulted in the collapse of the oocyte's cytokeratin cytoskeletal network. Surprisingly, exogenous *vegT* transcripts can re-constitute the cytoskeletal architecture when supplied. Hence, *vegT* RNA is suggested to have a function in maintaining the structural integrity of the cytoskeleton, which is important for the proper anchorage of other localized RNAs and/or protein (Kloc et al. 2005).

So, could *sqt* RNA be assuming a structural scaffolding role like *osk* or *vegT* RNA? I found that inhibiting protein translation does not affect the dorsal expanding activity of non-coding *sqt*, suggesting that the activity of *sqt* RNA is direct, and independent of protein translation. In addition, *sqt* 3'UTR harbours the sequence and structural element (Dorsal localization element, DLE) essential for its asymmetric localization (Gilligan et al. 2011) and can bind different proteins in in vitro assays (Kumari et al. 2013). These observations, together with my results, support a function for *sqt* RNA in perhaps translocating some factor/protein(s) that bind the *sqt* UTR, to the future dorsal side. *sqt* RNA is normally present in limiting amounts in early embryos (Rebagliati et al. 1998; Gore et al. 2005). Therefore, even small increases in the amount of *sqt* UTR, which may harbor docking sites for the protein(s), could lead to increased levels of this factor (see model in Figure 4.2) in the future embryonic dorsal side where *sqt* RNA accumulates. This factor is likely to function via the canonical Wnt/β-catenin

pathway, since the *sqt* UTR is unable to expand dorsal in the context of *ich* mutant embryos, which are deficient in β-catenin signalling (Kelly et al. 2000). It is possible that the factor(s) binding to the *sqt* UTR are components of the Wnt/β-catenin pathway.

In Xenopus, dorsally-localized *Xwnt11* RNA activates downstream signalling via β-catenin (Tao et al. 2005). However, the factors that bind and localize *Xwnt11* RNA have not been identified yet. In zebrafish, embryos from homozygous *ich* mutant mothers show that maternal β-catenin function is required for dorsal specification, but for many years, the Wnt that activates the canonical signaling pathway was unknown (Nojima et al. 2010), and the mechanism that generates asymmetric dorsal accumulation of nuclear β-catenin is unclear. Recently, Lu et al. reported that asymmetrically localized maternal *wnt8a* RNA at the vegetal cortex is likely to activate canonical Wnt/β-catenin signalling (Lu et al. 2011). However, given the broad expression domain of *wnt8a* trancripts, maternal Wnt8 signal from the yolk, which is likely to be diffusible, can potentially access at least one-fifth of the blastoderm margin (Tran et al. 2012). Also, it is noteworthy that *wnt8a* transcripts are at the same time uniformly distributed throughout the blastoderm (Lu et al. 2011). However, I observed that nuclear β-catenin is only found in a small cluster of dorsal-fated cells, consistent with a previous report (Dougan et al. 2003). Thus, there is potentially a mechanism to spatially limit Wnt8 activity in the blastoderm, in order to restrict nuclear β-catenin accumulation. Based on antisense knockdown experiments, Lu et al. suggested two likely candidates, Sfrp1a and Frzb, to be involved in negatively regulating Wnt8. However, maternal expression of *sfrp1a* and *frzb* transcripts is not spatially restricted (B. Thisse and C. Thisse, personal communication). These transcripts encode secreted Wnt antagonists, which are freely diffusible (Lin et al. 1997; Wang et al. 1997; Pera and De Robertis 2000; Lee et al. 2006; Mii and Taira 2009; Ploper et al. 2011). Thus, it is unclear whether a uniform maternal Sfrp1a and Frzb activity is sufficient to limit the response to a broadly expressed Wnt8 signal, to a few marginal cells.

Since both overexpression of *sqt* UTR and knockdown of *sqt* RNA have effects on early nuclear β-catenin accumulation, localized maternal *sqt* RNA in the blastoderm

can be a candidate for the molecule that functions to limit the range of maternal Wnt8 activity and to spatially restrict nuclear β-catenin accumulation to future dorsal cells. Given its ability to bind proteins (Kumari et al. 2013), I propose that maternal *sqt* RNA may act as a scaffold to bind and deliver/sequester maternal factors, that are likely to be intra-cellular component(s) of the Wnt pathway.

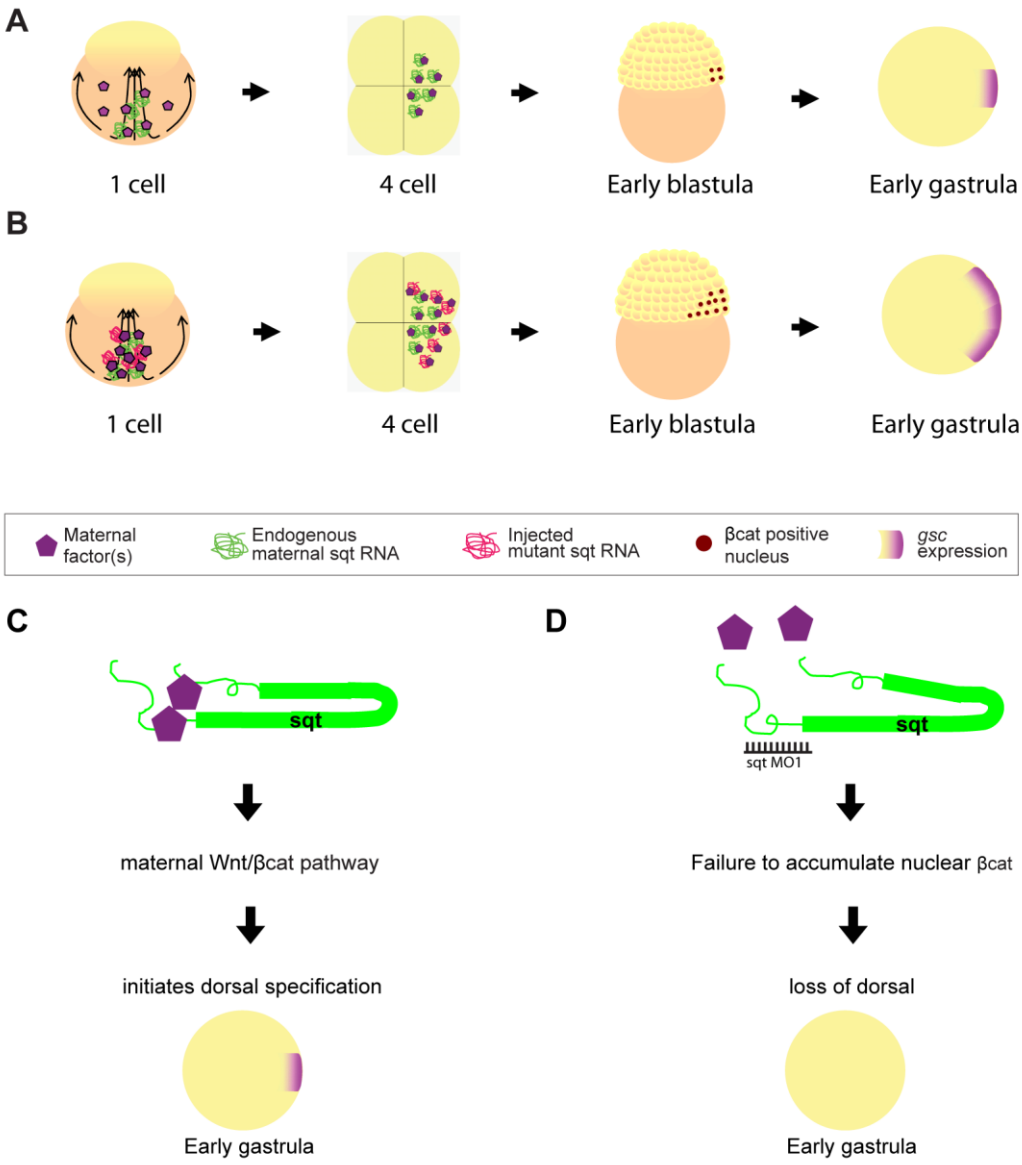

Figure 4.2. Model of *sqt* RNA as a scaffold. (A) In wild-type embryos, *sqt* RNA (green) localizes to dorsal, and delivers/sequesters maternal factors (purple polygons) bound to it, to specify dorsal (red β-Catenin positive nuclei and purple arc of *gsc* expression). (B) Upon over-expression of *sqt* RNA (magenta), the localized RNA and the factors it binds increases, thereby increasing the number of β-Catenin positive nuclei in the blastoderm and YSL, and expanding *gsc* expression in dorsal. (C) *sqt* RNA likely acts as a scaffold that binds and delivers maternal factor(s), initiating dorsal specification in a maternal Wnt/ β -Catenin-dependent manner. (D) In *sqt* MO-injected embryos injected, maternal *sqt* RNA and the factors fail to localize to dorsal, β-Catenin does not accumulate in dorsal nuclei, eventually leading to a lack of dorsal gene expression.

4.3 The role of functional long non-coding RNAs in development and disease

The RNA world hypothesis supports RNA as the primordial molecule responsible for early life. It can store genetic information like DNA, and catalyzes some chemical reactions like protein e.g. ribosomes, ribozymes etc. However, through evolution, RNA has been relegated in status to being the messenger between DNA and protein due to its weaker stability and lack in enzymatic versatility. It is also believed to evolve the slowest as core components of the cellular translation and splicing machinery are composed almost entirely of RNA. In recent years, with increasing understanding of the cell's transcriptomic landscape, the concept of central dogma of molecular biology i.e. the flow of genetic information from DNA to RNA to protein, has been challenged for its accuracy. Unbiased high-throughput genomics approaches revealed the identities of non-coding RNAs transcribed in a developmentally-regulated fashion and also hinted at the mechanisms responsible for their biogenesis and processing.

Amongst the non-coding RNAs that comprise a multifarious collection of transcripts such as housekeeping ribosomal RNA, transfer RNA, small nuclear RNA, microRNA etc., there is a fast-expanding class of long transcripts, termed long non-coding RNAs (lncRNAs) that act as functional RNAs, rather than encode protein. These lncRNAs are generally defined as transcripts longer than 200 nucleotides. Some well-known mammalian examples of this class of RNA include *H19*, *Xist/Tsix* and *HOTAIR* (Brannan et al. 1990; Brockdorff et al. 1992; Rinn et al. 2007). The degree of lncRNA transcript existence was first revealed by Okazaki et al. in a study using large-scale sequencing of cDNA libraries in the mouse (Okazaki et al. 2002). Okazaki et al. reported that a large proportion of the mammalian transcriptome does not encode proteins. Recent technical advances, such as tilling arrays and RNA deep sequencing (RNA-seq) have made it possible to pry into the dark matter of the genomic universe (Okazaki et al. 2002; Carninci et al. 2005; Kapranov et al. 2005; Denoeud et al. 2007; Kapranov et al. 2007a; Kapranov et al. 2007b; Ponjavic et al. 2007; Core et al. 2008; Preker et al. 2008; Seila et al. 2008; Fejes-Toth et al. 2009; Guttman et al. 2009; Neil et al. 2009; Xu et al. 2009; Guttman et al. 2010; Cabili et al. 2011). These studies unequivocally demonstrated that

the genomes of mammals, as well as other organisms such as zebrafish, produce copious amounts of long transcripts that lack significant protein-coding capacity.

Long ncRNAs have been found to be involved in high-order chromosomal dynamics (Rinn et al. 2007; Nagano et al. 2008; Pandey et al. 2008; Zhao et al. 2008; Guttman et al. 2009; Khalil et al. 2009; Huarte et al. 2010; Tian et al. 2010; Tsai et al. 2010; Zhao et al. 2010; Wang et al. 2011), suggesting that lncRNAs are important for organization of the genome and transcriptional regulation of gene expression. Recent reports also describe the involvement of lncRNAs in the sequestration of miRNAs (Poliseno et al. 2010) and proteins (Tripathi et al. 2010; Hung et al. 2011). Apart from their roles in development, dysregulation of some lncRNAs have been linked to human diseases e.g. leukaemia (Calin et al. 2007a; Calin et al. 2007b), hepatocellular carcinoma (Calin et al. 2007a; Lin et al. 2007), psoriasis (Sonkoly et al. 2005), ischaemic heart disease (Ishii et al. 2006), Alzheimer's disease (Faghihi et al. 2008) etc. In the context of cancers, an emerging mechanistic basis of these lncRNAs involve regulating the expression of a tumour suppressor or oncogene through epigenetic modifications, failing which lead to oncogenesis.

However, unlike microRNAs or proteins, current understanding of lncRNAs does not allow for easy and confident functional annotation, owing to the diversity of lncRNAs described to date. In addition, many lncRNAs function via their conserved secondary structures and not their sequence (Khalil et al. 2009; Guttman et al. 2011; Khalil and Rinn 2011). In the budding yeast, Saccharomyces cerevisiae, Kertesz et al. reported the development of a new technique called parallel analysis of RNA structure (PARS) to profile the secondary structure of mRNAs at single nucleotide resolution (Kertesz et al. 2010). Briefly, it involves treating RNAs with structure-specific enzymes such as RNase V1 or S1 nuclease independently, followed by deep sequencing. A similar approach, termed FragSeq, using single-strand specific nuclease P1 and high-throughput sequencing was applied to mouse non-coding RNAs in two cell types (Underwood et al. 2010). Next, the selective 2'-hydroxyl acylation analyzed by primer extension (SHAPE) chemistry, together with next generation sequencing (SHAPE-Seq), was proven adept in measuring

the structures of a mixed pool of RNAs (Lucks et al. 2011). Data from these procedures can be assimilated using bioinformatics approaches e.g. SeqFold, to provide better secondary structure predictions (Ouyang et al. 2012). And possibly, combined with large-scale spatial and temporal profiling of the lncRNAs' expression signatures (Cabili et al. 2011; Pauli et al. 2011), we may be able to predict their roles in generating cellular identities, mediating spatial organization in multi-cellular organisms, as well as maintaining the non-disease status of cells, tissues and organs. For ncRNAs associated with diseases, the understanding of their functions will potentially help identify new biomarkers that can improve prognosis and serve as targets for development of future therapeutics.

Lastly, bulk of the past lncRNA research describes RNA that strictly functions in its RNA-form and do not code for proteins. In recent years, however, researchers have reported on a subset of non-coding RNAs that also have protein-coding functions. In fact, these RNAs were first characterized for their corresponding protein roles before their non-coding RNA functions were deciphered. For example in humans, the tumor suppressor *p53* mRNA region encoding the Mdm2-binding site interacts directly with the RING domain of Mdm2, leading to the impairment of the E3 ligase activity of Mdm2, thereby promoting *p53* mRNA translation (Candeias et al. 2008). In *Drosophila* and *Xenopus*, *osk* and *vegT* RNA possess both essential non-coding and coding functions at different stages of embryonic development (Kloc et al. 2005; Jenny et al. 2006). Now, in zebrafish, I uncovered a novel non-coding role of *sqt* RNA in mediating early dorsal induction, through overexpression and knockdown studies. These discoveries further increase the spectrum of gene function and it seems that this mechanistic theme is likely to be conserved across organisms. With gigantic transcriptomic and proteomic datasets being churned out so rapidly, the identification of more RNAs with both non-coding and coding capacities seem achievable in the near future.

4.4 Targeting nucleases --- a key tool for studying functional RNAs

It is challenging to assess the requirement as well as determine the biological activities of lncRNAs, or any other functional RNAs for that matter, because traditional mutagenesis methods e.g. ENU, gamma rays, transposons etc. have their fair share of short-comings in this context. For example, ENU causes point mutations which frequently lead to the generation of classical genetic mutants that are protein nulls (Mullins et al. 1994; Solnica-Krezel et al. 1994; Riley and Grunwald 1995; Driever et al. 1996; Haffter et al. 1996). However, those mutants may not have defective transcription at the mutated loci. On the other hand, gamma rays-mediated mutagenesis often result in complex chromosomal rearrangements that affect multiple loci, thus complicating the functional analysis of specific genes (Feldman et al. 1998; Brault et al. 2006). As for transposons, different systems have different preferences for their insertion sites. Although Tol2 prefers to insert in the 5' region of genes, the insertion may or may not disrupt the transcription regulatory region (Kawakami et al. 2000; Kawakami 2004; Kawakami et al. 2004; Parinov et al. 2004). Also, these reverse genetics approaches involve tedious target gene identification methods e.g. Targeting Induced Local Lesions in Genomes (TILLING), Thermal Asymmetric Interlace-PCR (TAIL-PCR), inverse PCR etc. Hence, to study functional RNAs, a rapid and facile method to generate whole-locus or transcript-specific deletion is much needed.

In the mid 1990s, researchers at Johns Hopkins University first build the zinc finger nucleases (ZFNs), a genome-editing tool whose basis serve as a blueprint for the flurry of subsequent tools developed e.g. TALENs, CRISPR-CAS. All these tools have the ability to recognize DNA sequences and create double-stranded breaks (DSBs) that eventually lead to mutations due to the error-prone non-homologous end-joining (NHEJ) DSB DNA repair pathway. Both ZFNs and TALENs consist of a DNA-binding domain that bind DNA with a modular and predictable architecture, and a *Fok*I nuclease domain. Each zinc finger DNA recognition helix generally binds three base pairs (Klug 2010), and typically arrays of 3-6 helices are combined to create a DNA-binding domain with specificity to 9-18 base pairs. However, it was soon discovered that the reality is more

complex than what it seems theoretically. It was difficult to engineer ZFNs with the desired binding affinities because sequence recognition specificity of the combined zinc finger modules cannot be predicted accurately based on the specificity of individual module (Ramirez et al. 2008; Lam et al. 2011). It was then necessary to test and select for the best ZFN combinations, but even with the Oligomerized Pool Engineering (OPEN) method of refining selections, a ZFN targeting site can only be found at 200 base pairs intervals at best, more typically every 500 bases, in a random genomic sequence (Maeder et al. 2008; Sander et al. 2011a).

TALENs, on the other hand, bind DNA through a long stretch of tandem repeats, each consisting of typically 34 amino acids. Each repeat has DNA recognition capability of single nucleotide resolution (Boch et al. 2009; Moscou and Bogdanove 2009; Boch and Bonas 2010). It was reported that TALEN-binding sites are expected to occur about once every 35 base pairs based on the criteria set by analysing naturally occurring TALEs (Cermak et al. 2011). Thus, TALENs quickly became far more attractive than ZFNs for editing genomes.

The ZFN and TALEN technologies have been used successfully in many organisms to generate small insertion and deletion mutations of specific gene loci (Huang et al. 2011; Wood et al. 2011; Dahlem et al. 2012; Mercer et al. 2012). However, to study the functions of non-coding RNAs, it is necessary to generate RNA null mutant alleles by either deleting a gene's transcriptional regulatory region or by deleting the entire gene. Large chromosomal deletions and inversions have been shown in cell lines using ZFNs, and deletions using two pairs of TALENs have been generated in silkworm, swine fibroblasts and zebrafish (Sollu et al. 2010; Carlson et al. 2012; Ma et al. 2012; Gupta et al. 2013). However, so far, heritable chromosomal deletions that specifically abolish expression of a transcript have not been reported with these nucleases in any organism.

In the process of generating a *sqt* RNA null genetic mutant, I injected two pairs of *sqt*-specific TALENs and TALENs/ZFNs combinations into wild-type zebrafish embryos, and successfully created zebrafish carrying germ-line transmissible mutagenic

lesions of a whole *sqt* locus deletion and a deletion of the 5' transcriptional start site (5' TSS). The zygotic sqt^{sg27} and sqt^{sg32} deletion mutant embryos manifest phenotypes that are consistent with the previously identified *sqt* mutations. And the sqt^{sg27} TSS deletion that is predicted to excise the transcriptional start site elements and sqt^{sg32} whole-locus deletion indeed result in mutant embryos that are *sqt* RNA-null. Thus, I have demonstrated that it is feasible to leverage on the combinatorial action of multiple nucleases to delete specific genes from the genome. In fact, data from my study revealed that the usage of multiple nucleases can generate defined deletions at desired locations with high efficacy. Even with the emergence of improvements in nuclease variants e.g. "GoldyTALEN" system (Bedell et al. 2012) and the RNA-guide mediated CRISPR-Cas system (Cong et al. 2013; Hwang et al. 2013; Mali et al. 2013), the multiple-nuclease strategy can potentially still be harnessed to investigate the roles of all "functional" RNAs in the genome.

CHAPTER V:
CONCLUSION AND FUTURE DIRECTIONS

From my study, three major conclusions I came to are 1) *sqt* 3'UTR is necessary and sufficient for the dorsal-inducing activity of *sqt* RNA, 2) *sqt* RNA interacts with canonical Wnt/β-catenin pathway in early embryonic DV axis specification and the 3) combinatorial action of multiple nucleases can delete whole transcriptional units. To decipher the precise mechanism by which *squint/nodal-related-1* (*sqt*/ndr-1) RNA works in dorso-ventral (DV) patterning, it is essential to identify the machinery involved in this intricate process.

The dorsal-inducing activity of *sqt* clearly resides within its non-protein-coding UTR. In development, there are numerous instances of presence of RNA *cis*-acting signals that function in RNA localization, translational control etc. (Bashirullah et al. 1998; Johnstone and Lasko 2001; Kindler et al. 2005; Sossin and DesGroseillers 2006; Jambhekar and Derisi 2007). And these *cis*-acting signals can exist as sequence and/or structural motifs. The region of maternal *sqt* 3'UTR responsible for its own asymmetric translocation has been identified by sequential deletion of the *sqt* 3'UTR (Gilligan et al. 2011). Using the same approach and by assaying for extent of dorsal gene expression, it is possible to broadly define specific regions of the 3'UTR that are critical for the dorsal-inducing activity of *sqt* RNA. The identification of these functional element(s) within *sqt* UTR will allow me to check Nodal genes in other vertebrates for similar element(s), and possibily identify parallels in their functions in various cellular/developmental contexts.

Next, en-route to deciphering the mechanism of maternal *sqt* RNA in dorsal axis induction, the identification of trans-acting partners of *sqt* 3'UTR is of equal importance to finding the cis-acting signals. Using RNA mobility shift assays, my colleagues have observed the binding of different proteins to distinct segments of *sqt* 3'UTR (Kumari et al. 2013). Therefore, it is likely that *sqt* RNA interacts physically with certain proteins, thus bringing about dorsal specification. To identify these proteins in *sqt* RNA-containing RNP complexes, one strategy involves immunoprecipitation (IP) using anti-Ybx1 antibody (Ybx1, *sqt* DLE-binding protein, (Kumari et al. 2013)). It has been shown that this method can result in the identification of the bound proteins or interacting RNAs (Niranjanakumari et al. 2002; Gilbert and Svejstrup 2006; Keene et al. 2006; Jonson et al.

2007). Alternatively, short sequence tags (aptamers) can be embedded in exogenously expressed RNA and through subsequent affinity purification steps, bound factors can be enriched and identified (Bachler et al. 1999; Srisawat and Engelke 2002; Beach and Keene 2008; Slobodin and Gerst 2010).

However, biochemical approaches can be technically challenging due to binding specificity issues. Hence, a relatively easy and straight-forward candidate approach can be used in parallel to identify *sqt* RNA's *trans*-acting partners in dorsal induction. In this study, I observed crosstalk between maternal *sqt* RNA and the canonical Wnt/β-catenin pathway. As many components of the canonical Wnt/β-catenin pathway are known and antibodies against proteins in the pathway are readily available, whole mount immuno-staining at early cleavage stages using those antibodies can be performed to identify maternal deposition of those proteins as well as their distribution within the embryo. In general, any of the Wnt pathway-related proteins that share a similar asymmetric localization as maternal *sqt* RNA is of interest.

Eventually, the identification of both the minimal binding motif(s) on *sqt* RNA and the binding protein(s) will help to decipher *sqt* RNA's role in dorsal specification. More importantly, the results may provide fresh insights on how Nodal and Wnt pathway components can interact and also serve as reference for possible Nodal and Wnt interactions in other cellular contexts e.g. tumorigenesis.

CHAPTER VI: REFERENCES

Aanes H, Winata CL, Lin CH, Chen JP, Srinivasan KG, Lee SG, Lim AY, Hajan HS, Collas P, Bourque G et al. 2011. Zebrafish mRNA sequencing deciphers novelties in transcriptome dynamics during maternal to zygotic transition. *Genome research* **21**: 1328-1338.

Adams MD Celniker SE Holt RA Evans CA Gocayne JD Amanatides PG Scherer SE Li PW Hoskins RA Galle RF et al. 2000. The genome sequence of Drosophila melanogaster. *Science (New York, NY* **287**: 2185-2195.

Amiri A, Keiper BD, Kawasaki I, Fan Y, Kohara Y, Rhoads RE, Strome S. 2001. An isoform of eIF4E is a component of germ granules and is required for spermatogenesis in C. elegans. *Development* **128**: 3899-3912.

Amsterdam A, Nissen RM, Sun Z, Swindell EC, Farrington S, Hopkins N. 2004. Identification of 315 genes essential for early zebrafish development. *Proceedings of the National Academy of Sciences of the United States of America* **101**: 12792-12797.

Aoki TO, Mathieu J, Saint-Etienne L, Rebagliati MR, Peyrieras N, Rosa FM. 2002. Regulation of nodal signalling and mesendoderm formation by TARAM-A, a TGFbeta-related type I receptor. *Developmental biology* **241**: 273-288.

Bachler M, Schroeder R, von Ahsen U. 1999. StreptoTag: a novel method for the isolation of RNA-binding proteins. *Rna* **5**: 1509-1516.

Baker KE, Parker R. 2004. Nonsense-mediated mRNA decay: terminating erroneous gene expression. *Current opinion in cell biology* **16**: 293-299.

Balciunas D, Davidson AE, Sivasubbu S, Hermanson SB, Welle Z, Ekker SC. 2004. Enhancer trapping in zebrafish using the Sleeping Beauty transposon. *BMC genomics* **5**: 62.

Baltz AG, Munschauer M, Schwanhausser B, Vasile A, Murakawa Y, Schueler M, Youngs N, Penfold-Brown D, Drew K, Milek M et al. 2012. The mRNA-bound proteome and its global occupancy profile on protein-coding transcripts. *Molecular cell* **46**: 674-690.

Barker DD, Wang C, Moore J, Dickinson LK, Lehmann R. 1992. Pumilio is essential for function but not for distribution of the Drosophila abdominal determinant Nanos. *Genes & development* **6**: 2312-2326.

Basham SE, Rose LS. 1999. Mutations in ooc-5 and ooc-3 disrupt oocyte formation and the reestablishment of asymmetric PAR protein localization in two-cell Caenorhabditis elegans embryos. *Developmental biology* **215**: 253-263.

Bashirullah A, Cooperstock RL, Lipshitz HD. 1998. RNA localization in development. *Annual review of biochemistry* **67**: 335-394.

Bastock R, St Johnston D. 2008. Drosophila oogenesis. *Curr Biol* **18**: R1082-1087.

Bates WR, Jeffery WR. 1987. Alkaline phosphatase expression in ascidian egg fragments and andromerogons. *Developmental biology* **119**: 382-389.

Baumeister HG. 1973. Lampbrush chromosomes and RNA-synthesis during early oogenesis of Brachydanio rerio (Cyprinidae, Teleostei). *Z Zellforsch Mikrosk Anat* **145**: 145-150.

Bayer TA, Campos-Ortega JA. 1992. A transgene containing lacZ is expressed in primary sensory neurons in zebrafish. *Development* **115**: 421-426.

Beach DL, Keene JD. 2008. Ribotrap : targeted purification of RNA-specific RNPs from cell lysates through immunoaffinity precipitation to identify regulatory proteins and RNAs. *Methods in molecular biology (Clifton, NJ* **419**: 69-91.

Beck S, Le Good JA, Guzman M, Ben Haim N, Roy K, Beermann F, Constam DB. 2002. Extraembryonic proteases regulate Nodal signalling during gastrulation. *Nature cell biology* **4**: 981-985.

Bedell VM, Wang Y, Campbell JM, Poshusta TL, Starker CG, Krug RG, 2nd, Tan W, Penheiter SG, Ma AC, Leung AY et al. 2012. In vivo genome editing using a high-efficiency TALEN system. *Nature* **491**: 114-118.

Bellen HJ, Levis RW, Liao G, He Y, Carlson JW, Tsang G, Evans-Holm M, Hiesinger PR, Schulze KL, Rubin GM et al. 2004. The BDGP gene disruption project: single transposon insertions associated with 40% of Drosophila genes. *Genetics* **167**: 761-781.

Bellipanni G, Varga M, Maegawa S, Imai Y, Kelly C, Myers AP, Chu F, Talbot WS, Weinberg ES. 2006. Essential and opposing roles of zebrafish beta-catenins in the formation of dorsal axial structures and neurectoderm. *Development* **133**: 1299-1309.

Belostotsky DA, Sieburth LE. 2009. Kill the messenger: mRNA decay and plant development. *Current opinion in plant biology* **12**: 96-102.

Bennett JT, Stickney HL, Choi WY, Ciruna B, Talbot WS, Schier AF. 2007. Maternal nodal and zebrafish embryogenesis. *Nature* **450**: E1-2; discussion E2-4.

Berleth T, Burri M, Thoma G, Bopp D, Richstein S, Frigerio G, Noll M, Nusslein-Volhard C. 1988. The role of localization of bicoid RNA in organizing the anterior pattern of the Drosophila embryo. *The EMBO journal* **7**: 1749-1756.

Beumer K, Bhattacharyya G, Bibikova M, Trautman JK, Carroll D. 2006. Efficient gene targeting in Drosophila with zinc-finger nucleases. *Genetics* **172**: 2391-2403.

Bibikova M, Carroll D, Segal DJ, Trautman JK, Smith J, Kim YG, Chandrasegaran S. 2001. Stimulation of homologous recombination through targeted cleavage by chimeric nucleases. *Molecular and cellular biology* **21**: 289-297.

Boch J, Bonas U. 2010. Xanthomonas AvrBs3 family-type III effectors: discovery and function. *Annual review of phytopathology* **48**: 419-436.

Boch J, Scholze H, Schornack S, Landgraf A, Hahn S, Kay S, Lahaye T, Nickstadt A, Bonas U. 2009. Breaking the code of DNA binding specificity of TAL-type III effectors. *Science (New York, NY* **326**: 1509-1512.

Bourbon HM, Gonzy-Treboul G, Peronnet F, Alin MF, Ardourel C, Benassayag C, Cribbs D, Deutsch J, Ferrer P, Haenlin M et al. 2002. A P-insertion screen identifying novel X-linked essential genes in Drosophila. *Mechanisms of development* **110**: 71-83.

Bowerman B, Shelton CA. 1999. Cell polarity in the early Caenorhabditis elegans embryo. *Current opinion in genetics & development* **9**: 390-395.

Brannan CI, Dees EC, Ingram RS, Tilghman SM. 1990. The product of the H19 gene may function as an RNA. *Molecular and cellular biology* **10**: 28-36.

Brault V, Pereira P, Duchon A, Herault Y. 2006. Modeling chromosomes in mouse to explore the function of genes, genomic disorders, and chromosomal organization. *PLoS genetics* **2**: e86.

Brendza RP, Serbus LR, Duffy JB, Saxton WM. 2000. A function for kinesin I in the posterior transport of oskar mRNA and Staufen protein. *Science (New York, NY* **289**: 2120-2122.

Brennecke J, Stark A, Russell RB, Cohen SM. 2005. Principles of microRNA-target recognition. *PLoS biology* **3**: e85.

Brockdorff N, Ashworth A, Kay GF, McCabe VM, Norris DP, Cooper PJ, Swift S, Rastan S. 1992. The product of the mouse Xist gene is a 15 kb inactive X-specific transcript containing no conserved ORF and located in the nucleus. *Cell* **71**: 515-526.

Cabili MN, Trapnell C, Goff L, Koziol M, Tazon-Vega B, Regev A, Rinn JL. 2011. Integrative annotation of human large intergenic noncoding RNAs reveals global properties and specific subclasses. *Genes & development* **25**: 1915-1927.

Calin GA, Liu CG, Ferracin M, Hyslop T, Spizzo R, Sevignani C, Fabbri M, Cimmino A, Lee EJ, Wojcik SE et al. 2007a. Ultraconserved regions encoding ncRNAs are altered in human leukemias and carcinomas. *Cancer cell* **12**: 215-229.

Calin GA, Pekarsky Y, Croce CM. 2007b. The role of microRNA and other non-coding RNA in the pathogenesis of chronic lymphocytic leukemia. *Best practice & research* **20**: 425-437.

Candeias MM, Malbert-Colas L, Powell DJ, Daskalogianni C, Maslon MM, Naski N, Bourougaa K, Calvo F, Fahraeus R. 2008. P53 mRNA controls p53 activity by managing Mdm2 functions. *Nature cell biology* **10**: 1098-1105.

Carlson DF, Tan W, Lillico SG, Stverakova D, Proudfoot C, Christian M, Voytas DF, Long CR, Whitelaw CB, Fahrenkrug SC. 2012. Efficient TALEN-mediated gene knockout in livestock. *Proceedings of the National Academy of Sciences of the United States of America* **109**: 17382-17387.

Carninci P Kasukawa T Katayama S Gough J Frith MC Maeda N Oyama R Ravasi T Lenhard B Wells C et al. 2005. The transcriptional landscape of the mammalian genome. *Science (New York, NY* **309**: 1559-1563.

Carthew RW, Sontheimer EJ. 2009. Origins and Mechanisms of miRNAs and siRNAs. *Cell* **136**: 642-655.

Cermak T, Doyle EL, Christian M, Wang L, Zhang Y, Schmidt C, Baller JA, Somia NV, Bogdanove AJ, Voytas DF. 2011. Efficient design and assembly of custom TALEN and other TAL effector-based constructs for DNA targeting. *Nucleic acids research* **39**: e82.

Cha BJ, Koppetsch BS, Theurkauf WE. 2001. In vivo analysis of Drosophila bicoid mRNA localization reveals a novel microtubule-dependent axis specification pathway. *Cell* **106**: 35-46.

Chan SK, Struhl G. 1997. Sequence-specific RNA binding by bicoid. *Nature* **388**: 634.

Chen Y, Schier AF. 2001. The zebrafish Nodal signal Squint functions as a morphogen. *Nature* **411**: 607-610.

Cheng NN, Kirby CM, Kemphues KJ. 1995. Control of cleavage spindle orientation in Caenorhabditis elegans: the role of the genes par-2 and par-3. *Genetics* **139**: 549-559.

Choi WY, Giraldez AJ, Schier AF. 2007. Target protectors reveal dampening and balancing of Nodal agonist and antagonist by miR-430. *Science (New York, NY* **318**: 271-274.

Ciruna B, Weidinger G, Knaut H, Thisse B, Thisse C, Raz E, Schier AF. 2002. Production of maternal-zygotic mutant zebrafish by germ-line replacement. *Proceedings of the National Academy of Sciences of the United States of America* **99**: 14919-14924.

Clark KJ, Urban MD, Skuster KJ, Ekker SC. 2011. Transgenic zebrafish using transposable elements. *Methods in cell biology* **104**: 137-149.

Collignon J, Varlet I, Robertson EJ. 1996. Relationship between asymmetric nodal expression and the direction of embryonic turning. *Nature* **381**: 155-158.

Cong L, Ran FA, Cox D, Lin S, Barretto R, Habib N, Hsu PD, Wu X, Jiang W, Marraffini LA et al. 2013. Multiplex genome engineering using CRISPR/Cas systems. *Science (New York, NY* **339**: 819-823.

Conlon FL, Lyons KM, Takaesu N, Barth KS, Kispert A, Herrmann B, Robertson EJ. 1994. A primary requirement for nodal in the formation and maintenance of the primitive streak in the mouse. *Development* **120**: 1919-1928.

Core LJ, Waterfall JJ, Lis JT. 2008. Nascent RNA sequencing reveals widespread pausing and divergent initiation at human promoters. *Science (New York, NY* **322**: 1845-1848.

Cove D, Hope I, Quatrano R. 1999. Polarity in Biological Systems. in *Development*, pp. 507-524. Springer Berlin Heidelberg.

Culbertson MR. 1999. RNA surveillance. Unforeseen consequences for gene expression, inherited genetic disorders and cancer. *Trends Genet* **15**: 74-80.

Dahlem TJ, Hoshijima K, Jurynec MJ, Gunther D, Starker CG, Locke AS, Weis AM, Voytas DF, Grunwald DJ. 2012. Simple methods for generating and detecting locus-specific mutations induced with TALENs in the zebrafish genome. *PLoS genetics* **8**: e1002861.

Davidson AE, Balciunas D, Mohn D, Shaffer J, Hermanson S, Sivasubbu S, Cliff MP, Hackett PB, Ekker SC. 2003. Efficient gene delivery and gene expression in zebrafish using the Sleeping Beauty transposon. *Developmental biology* **263**: 191-202.

Dawid IB, Sargent TD. 1988. Xenopus laevis in developmental and molecular biology. *Science (New York, NY* **240**: 1443-1448.

Denegre JM, Ludwig ER, Mowry KL. 1997. Localized maternal proteins in Xenopus revealed by subtractive immunization. *Developmental biology* **192**: 446-454.

Denoeud F, Kapranov P, Ucla C, Frankish A, Castelo R, Drenkow J, Lagarde J, Alioto T, Manzano C, Chrast J et al. 2007. Prominent use of distal 5' transcription start sites and discovery of a large number of additional exons in ENCODE regions. *Genome research* **17**: 746-759.

DeTolla LJ, Srinivas S, Whitaker BR, Andrews C, Hecker B, Kane AS, Reimschuessel R. 1995. Guidelines for the Care and Use of Fish in Research. *ILAR journal / National Research Council, Institute of Laboratory Animal Resources* **37**: 159-173.

Donald DL. 1997. *C. elegans II*. Cold Spring Harbor Laboratory Press, New York, NY.

Dosch R, Wagner DS, Mintzer KA, Runke G, Wiemelt AP, Mullins MC. 2004. Maternal control of vertebrate development before the midblastula transition: mutants from the zebrafish I. *Developmental cell* **6**: 771-780.

Dougan ST, Warga RM, Kane DA, Schier AF, Talbot WS. 2003. The role of the zebrafish nodal-related genes squint and cyclops in patterning of mesendoderm. *Development* **130**: 1837-1851.

Doyon Y, McCammon JM, Miller JC, Faraji F, Ngo C, Katibah GE, Amora R, Hocking TD, Zhang L, Rebar EJ et al. 2008. Heritable targeted gene disruption in zebrafish using designed zinc-finger nucleases. *Nature biotechnology* **26**: 702-708.

Driever W, Nusslein-Volhard C. 1989. The bicoid protein is a positive regulator of hunchback transcription in the early Drosophila embryo. *Nature* **337**: 138-143.

Driever W, Solnica-Krezel L, Schier AF, Neuhauss SC, Malicki J, Stemple DL, Stainier DY, Zwartkruis F, Abdelilah S, Rangini Z et al. 1996. A genetic screen for mutations affecting embryogenesis in zebrafish. *Development* **123**: 37-46.

Elinson RP, Rowning B. 1988. A transient array of parallel microtubules in frog eggs: potential tracks for a cytoplasmic rotation that specifies the dorso-ventral axis. *Developmental biology* **128**: 185-197.

Emelyanov A, Gao Y, Naqvi NI, Parinov S. 2006. Trans-kingdom transposition of the maize dissociation element. *Genetics* **174**: 1095-1104.

Erter CE, Solnica-Krezel L, Wright CV. 1998. Zebrafish nodal-related 2 encodes an early mesendodermal inducer signaling from the extraembryonic yolk syncytial layer. *Developmental biology* **204**: 361-372.

Etemad-Moghadam B, Guo S, Kemphues KJ. 1995. Asymmetrically distributed PAR-3 protein contributes to cell polarity and spindle alignment in early C. elegans embryos. *Cell* **83**: 743-752.

Evans TC, Crittenden SL, Kodoyianni V, Kimble J. 1994. Translational control of maternal glp-1 mRNA establishes an asymmetry in the C. elegans embryo. *Cell* **77**: 183-194.

Faghihi MA, Modarresi F, Khalil AM, Wood DE, Sahagan BG, Morgan TE, Finch CE, St Laurent G, 3rd, Kenny PJ, Wahlestedt C. 2008. Expression of a noncoding RNA is elevated in Alzheimer's disease and drives rapid feed-forward regulation of beta-secretase. *Nature medicine* **14**: 723-730.

Farr GH, 3rd, Ferkey DM, Yost C, Pierce SB, Weaver C, Kimelman D. 2000. Interaction among GSK-3, GBP, axin, and APC in Xenopus axis specification. *The Journal of cell biology* **148**: 691-702.

Fejes-Toth K, Sotirova V, Sachidanandam R, Assaf G, Hannon GJ, Kapranov P, Foissac S, Willingham AT, Duttagupta R, Dumais E et al. 2009. Post-transcriptional processing generates a diversity of 5'-modified long and short RNAs. *Nature* **457**: 1028-1032.

Fekany K, Yamanaka Y, Leung T, Sirotkin HI, Topczewski J, Gates MA, Hibi M, Renucci A, Stemple D, Radbill A et al. 1999. The zebrafish bozozok locus encodes Dharma, a homeodomain protein essential for induction of gastrula organizer and dorsoanterior embryonic structures. *Development* **126**: 1427-1438.

Feldman B, Gates MA, Egan ES, Dougan ST, Rennebeck G, Sirotkin HI, Schier AF, Talbot WS. 1998. Zebrafish organizer development and germ-layer formation require nodal-related signals. *Nature* **395**: 181-185.

Feldman B, Stemple DL. 2001. Morpholino phenocopies of sqt, oep, and ntl mutations. *Genesis* **30**: 175-177.

Ferrandon D, Elphick L, Nusslein-Volhard C, St Johnston D. 1994. Staufen protein associates with the 3'UTR of bicoid mRNA to form particles that move in a microtubule-dependent manner. *Cell* **79**: 1221-1232.

Flynt AS, Li N, Thatcher EJ, Solnica-Krezel L, Patton JG. 2007. Zebrafish miR-214 modulates Hedgehog signaling to specify muscle cell fate. *Nature genetics* **39**: 259-263.

Forlani S, Ferrandon D, Saget O, Mohier E. 1993. A regulatory function for K10 in the establishment of dorsoventral polarity in the Drosophila egg and embryo. *Mechanisms of development* **41**: 109-120.

Franzetti GA, Laud-Duval K, Bellanger D, Stern MH, Sastre-Garau X, Delattre O. 2012. MiR-30a-5p connects EWS-FLI1 and CD99, two major therapeutic targets in Ewing tumor. *Oncogene*.

Funayama N, Fagotto F, McCrea P, Gumbiner BM. 1995. Embryonic axis induction by the armadillo repeat domain of beta-catenin: evidence for intracellular signaling. *The Journal of cell biology* **128**: 959-968.

Garcia-Lecea M, Kondrychyn I, Fong SH, Ye ZR, Korzh V. 2008. In vivo analysis of choroid plexus morphogenesis in zebrafish. *PloS one* **3**: e3090.

Gerhard GS, Kauffman EJ, Wang X, Stewart R, Moore JL, Kasales CJ, Demidenko E, Cheng KC. 2002. Life spans and senescent phenotypes in two strains of Zebrafish (Danio rerio). *Experimental gerontology* **37**: 1055-1068.

Gerhart J, Danilchik M, Doniach T, Roberts S, Rowning B, Stewart R. 1989. Cortical rotation of the Xenopus egg: consequences for the anteroposterior pattern of embryonic dorsal development. *Development* **107 Suppl**: 37-51.

Gilardelli CN, Pozzoli O, Sordino P, Matassi G, Cotelli F. 2004. Functional and hierarchical interactions among zebrafish vox/vent homeobox genes. *Dev Dyn* **230**: 494-508.

Gilbert C, Svejstrup JQ. 2006. RNA immunoprecipitation for determining RNA-protein associations in vivo. *Current protocols in molecular biology / edited by Frederick M Ausubel [et al]* **Chapter 27**: Unit 27 24.

Gilligan PC, Kumari P, Lim S, Cheong A, Chang A, Sampath K. 2011. Conservation defines functional motifs in the squint/nodal-related 1 RNA dorsal localization element. *Nucleic acids research* **39**: 3340-3349.

Giraldez AJ, Cinalli RM, Glasner ME, Enright AJ, Thomson JM, Baskerville S, Hammond SM, Bartel DP, Schier AF. 2005. MicroRNAs regulate brain morphogenesis in zebrafish. *Science (New York, NY* **308**: 833-838.

Glaser S, Anastassiadis K, Stewart AF. 2005. Current issues in mouse genome engineering. *Nature genetics* **37**: 1187-1193.

Goldstein B, Hird SN. 1996. Specification of the anteroposterior axis in Caenorhabditis elegans. *Development* **122**: 1467-1474.

Golling G, Amsterdam A, Sun Z, Antonelli M, Maldonado E, Chen W, Burgess S, Haldi M, Artzt K, Farrington S et al. 2002. Insertional mutagenesis in zebrafish rapidly identifies genes essential for early vertebrate development. *Nature genetics* **31**: 135-140.

Gore AV, Cheong A, Gilligan PC, Sampath K. 2007. Gore et al. reply to J. T. Bennett et al. Nature 450, doi: 10.1038/nature06314. *Nature* **450**: E2-E4.

Gore AV, Maegawa S, Cheong A, Gilligan PC, Weinberg ES, Sampath K. 2005. The zebrafish dorsal axis is apparent at the four-cell stage. *Nature* **438**: 1030-1035.
Gore AV, Sampath K. 2002. Localization of transcripts of the zebrafish morphogen Squint is dependent on egg activation and the microtubule cytoskeleton. *Mechanisms of development* **112**: 153-156.
Gritsman K, Talbot WS, Schier AF. 2000. Nodal signaling patterns the organizer. *Development* **127**: 921-932.
Gritsman K, Zhang J, Cheng S, Heckscher E, Talbot WS, Schier AF. 1999. The EGF-CFC protein one-eyed pinhead is essential for nodal signaling. *Cell* **97**: 121-132.
Gunkel N, Yano T, Markussen FH, Olsen LC, Ephrussi A. 1998. Localization-dependent translation requires a functional interaction between the 5' and 3' ends of oskar mRNA. *Genes & development* **12**: 1652-1664.
Guo S, Kemphues KJ. 1996. Molecular genetics of asymmetric cleavage in the early Caenorhabditis elegans embryo. *Current opinion in genetics & development* **6**: 408-415.
Gupta A, Hall VL, Kok FO, Shin M, McNulty JC, Lawson ND, Wolfe SA. 2013. Targeted Chromosomal Deletions and Inversions in Zebrafish. *Genome research*.
Guttman M, Amit I, Garber M, French C, Lin MF, Feldser D, Huarte M, Zuk O, Carey BW, Cassady JP et al. 2009. Chromatin signature reveals over a thousand highly conserved large non-coding RNAs in mammals. *Nature* **458**: 223-227.
Guttman M, Donaghey J, Carey BW, Garber M, Grenier JK, Munson G, Young G, Lucas AB, Ach R, Bruhn L et al. 2011. lincRNAs act in the circuitry controlling pluripotency and differentiation. *Nature* **477**: 295-300.
Guttman M, Garber M, Levin JZ, Donaghey J, Robinson J, Adiconis X, Fan L, Koziol MJ, Gnirke A, Nusbaum C et al. 2010. Ab initio reconstruction of cell type-specific transcriptomes in mouse reveals the conserved multi-exonic structure of lincRNAs. *Nature biotechnology* **28**: 503-510.
Haffter P, Granato M, Brand M, Mullins MC, Hammerschmidt M, Kane DA, Odenthal J, van Eeden FJ, Jiang YJ, Heisenberg CP et al. 1996. The identification of genes with unique and essential functions in the development of the zebrafish, Danio rerio. *Development* **123**: 1-36.
Hammerschmidt M, Serbedzija GN, McMahon AP. 1996. Genetic analysis of dorsoventral pattern formation in the zebrafish: requirement of a BMP-like ventralizing activity and its dorsal repressor. *Genes & development* **10**: 2452-2461.
Hart D, Donovan M. 1983. The structure of the chorion and site of sperm entry in the egg of Brachydanio. *J exp Zool* 277-296.
Heasman J, Crawford A, Goldstone K, Garner-Hamrick P, Gumbiner B, McCrea P, Kintner C, Noro CY, Wylie C. 1994. Overexpression of cadherins and underexpression of beta-catenin inhibit dorsal mesoderm induction in early Xenopus embryos. *Cell* **79**: 791-803.
Higashijima S, Okamoto H, Ueno N, Hotta Y, Eguchi G. 1997. High-frequency generation of transgenic zebrafish which reliably express GFP in whole muscles or the whole body by using promoters of zebrafish origin. *Developmental biology* **192**: 289-299.

Hill DP, Strome S. 1990. Brief cytochalasin-induced disruption of microfilaments during a critical interval in 1-cell C. elegans embryos alters the partitioning of developmental instructions to the 2-cell embryo. *Development* **108**: 159-172.
Hilton E, Rex M, Old R. 2003. VegT activation of the early zygotic gene Xnr5 requires lifting of Tcf-mediated repression in the Xenopus blastula. *Mechanisms of development* **120**: 1127-1138.
Hino S, Michiue T, Asashima M, Kikuchi A. 2003. Casein kinase I epsilon enhances the binding of Dvl-1 to Frat-1 and is essential for Wnt-3a-induced accumulation of beta-catenin. *The Journal of biological chemistry* **278**: 14066-14073.
Hird SN, Paulsen JE, Strome S. 1996. Segregation of germ granules in living Caenorhabditis elegans embryos: cell-type-specific mechanisms for cytoplasmic localisation. *Development* **122**: 1303-1312.
Hird SN, White JG. 1993. Cortical and cytoplasmic flow polarity in early embryonic cells of Caenorhabditis elegans. *The Journal of cell biology* **121**: 1343-1355.
Houliston E, Elinson RP. 1991a. Evidence for the involvement of microtubules, ER, and kinesin in the cortical rotation of fertilized frog eggs. *The Journal of cell biology* **114**: 1017-1028.
-. 1991b. Patterns of microtubule polymerization relating to cortical rotation in Xenopus laevis eggs. *Development* **112**: 107-117.
Howley C, Ho RK. 2000. mRNA localization patterns in zebrafish oocytes. *Mechanisms of development* **92**: 305-309.
Huang P, Xiao A, Zhou M, Zhu Z, Lin S, Zhang B. 2011. Heritable gene targeting in zebrafish using customized TALENs. *Nature biotechnology* **29**: 699-700.
Huarte M, Guttman M, Feldser D, Garber M, Koziol MJ, Kenzelmann-Broz D, Khalil AM, Zuk O, Amit I, Rabani M et al. 2010. A large intergenic noncoding RNA induced by p53 mediates global gene repression in the p53 response. *Cell* **142**: 409-419.
Hung T, Wang Y, Lin MF, Koegel AK, Kotake Y, Grant GD, Horlings HM, Shah N, Umbricht C, Wang P et al. 2011. Extensive and coordinated transcription of noncoding RNAs within cell-cycle promoters. *Nature genetics* **43**: 621-629.
Huntzinger E, Izaurralde E. 2011. Gene silencing by microRNAs: contributions of translational repression and mRNA decay. *Nature reviews* **12**: 99-110.
Hwang WY, Fu Y, Reyon D, Maeder ML, Tsai SQ, Sander JD, Peterson RT, Yeh JR, Joung JK. 2013. Efficient genome editing in zebrafish using a CRISPR-Cas system. *Nature biotechnology* **31**: 227-229.
Iliff BW, Riazuddin SA, Gottsch JD. 2012. A single-base substitution in the seed region of miR-184 causes EDICT syndrome. *Investigative ophthalmology & visual science* **53**: 348-353.
Imai Y, Gates MA, Melby AE, Kimelman D, Schier AF, Talbot WS. 2001. The homeobox genes vox and vent are redundant repressors of dorsal fates in zebrafish. *Development* **128**: 2407-2420.
Ishigaki Y, Li X, Serin G, Maquat LE. 2001. Evidence for a pioneer round of mRNA translation: mRNAs subject to nonsense-mediated decay in mammalian cells are bound by CBP80 and CBP20. *Cell* **106**: 607-617.
Ishii N, Ozaki K, Sato H, Mizuno H, Saito S, Takahashi A, Miyamoto Y, Ikegawa S, Kamatani N, Hori M et al. 2006. Identification of a novel non-coding RNA,

MIAT, that confers risk of myocardial infarction. *Journal of human genetics* **51**: 1087-1099.
Jambhekar A, Derisi JL. 2007. Cis-acting determinants of asymmetric, cytoplasmic RNA transport. *Rna* **13**: 625-642.
Jenny A, Hachet O, Zavorszky P, Cyrklaff A, Weston MD, Johnston DS, Erdelyi M, Ephrussi A. 2006. A translation-independent role of oskar RNA in early Drosophila oogenesis. *Development* **133**: 2827-2833.
Jesuthasan S, Stahle U. 1997. Dynamic microtubules and specification of the zebrafish embryonic axis. *Curr Biol* **7**: 31-42.
Johnson SL, Midson CN, Ballinger EW, Postlethwait JH. 1994. Identification of RAPD primers that reveal extensive polymorphisms between laboratory strains of zebrafish. *Genomics* **19**: 152-156.
Johnston RJ, Hobert O. 2003. A microRNA controlling left/right neuronal asymmetry in Caenorhabditis elegans. *Nature* **426**: 845-849.
Johnstone O, Lasko P. 2001. Translational regulation and RNA localization in Drosophila oocytes and embryos. *Annual review of genetics* **35**: 365-406.
Jones CM, Kuehn MR, Hogan BL, Smith JC, Wright CV. 1995. Nodal-related signals induce axial mesoderm and dorsalize mesoderm during gastrulation. *Development* **121**: 3651-3662.
Jonson L, Vikesaa J, Krogh A, Nielsen LK, Hansen T, Borup R, Johnsen AH, Christiansen J, Nielsen FC. 2007. Molecular composition of IMP1 ribonucleoprotein granules. *Molecular & cellular proteomics : MCP* **6**: 798-811.
Jorgensen EM, Mango SE. 2002. The art and design of genetic screens: caenorhabditis elegans. *Nature reviews* **3**: 356-369.
Kandler-Singer I, Kalthoff K. 1976. RNase sensitivity of an anterior morphogenetic determinant in an insect egg (Smittia sp., Chironomidae, Diptera). *Proceedings of the National Academy of Sciences of the United States of America* **73**: 3739-3743.
Kapranov P, Cheng J, Dike S, Nix DA, Duttagupta R, Willingham AT, Stadler PF, Hertel J, Hackermuller J, Hofacker IL et al. 2007a. RNA maps reveal new RNA classes and a possible function for pervasive transcription. *Science (New York, NY* **316**: 1484-1488.
Kapranov P, Drenkow J, Cheng J, Long J, Helt G, Dike S, Gingeras TR. 2005. Examples of the complex architecture of the human transcriptome revealed by RACE and high-density tiling arrays. *Genome research* **15**: 987-997.
Kapranov P, Willingham AT, Gingeras TR. 2007b. Genome-wide transcription and the implications for genomic organization. *Nature reviews* **8**: 413-423.
Kawakami K. 2004. Transgenesis and gene trap methods in zebrafish by using the Tol2 transposable element. *Methods in cell biology* **77**: 201-222.
Kawakami K, Koga A, Hori H, Shima A. 1998. Excision of the tol2 transposable element of the medaka fish, Oryzias latipes, in zebrafish, Danio rerio. *Gene* **225**: 17-22.
Kawakami K, Shima A. 1999. Identification of the Tol2 transposase of the medaka fish Oryzias latipes that catalyzes excision of a nonautonomous Tol2 element in zebrafish Danio rerio. *Gene* **240**: 239-244.
Kawakami K, Shima A, Kawakami N. 2000. Identification of a functional transposase of the Tol2 element, an Ac-like element from the Japanese medaka fish, and its

transposition in the zebrafish germ lineage. *Proceedings of the National Academy of Sciences of the United States of America* **97**: 11403-11408.
Kawakami K, Takeda H, Kawakami N, Kobayashi M, Matsuda N, Mishina M. 2004. A transposon-mediated gene trap approach identifies developmentally regulated genes in zebrafish. *Developmental cell* **7**: 133-144.
Kawamura K, Fujiwara S. 1994. Transdifferentiation of pigmented multipotent epithelium during morphallactic development of budding tunicates. *The International journal of developmental biology* **38**: 369-377.
Keene JD, Komisarow JM, Friedersdorf MB. 2006. RIP-Chip: the isolation and identification of mRNAs, microRNAs and protein components of ribonucleoprotein complexes from cell extracts. *Nature protocols* **1**: 302-307.
Kelly C, Chin AJ, Leatherman JL, Kozlowski DJ, Weinberg ES. 2000. Maternally controlled (beta)-catenin-mediated signaling is required for organizer formation in the zebrafish. *Development* **127**: 3899-3911.
Kemphues KJ, Kusch M, Wolf N. 1988. Maternal-effect lethal mutations on linkage group II of Caenorhabditis elegans. *Genetics* **120**: 977-986.
Kemphues KJ, Strome S. 1997. Fertilization and Establishment of Polarity in the Embryo.
Kenyon C. 1988. The nematode Caenorhabditis elegans. *Science (New York, NY* **240**: 1448-1453.
Kertesz M, Wan Y, Mazor E, Rinn JL, Nutter RC, Chang HY, Segal E. 2010. Genome-wide measurement of RNA secondary structure in yeast. *Nature* **467**: 103-107.
Kessel RG, Beams HW, Tung HN. 1984. Relationships between annulate lamellae and filament bundles in oocytes of the zebrafish, Brachydanio rerio. *Cell and tissue research* **236**: 725-727.
Kessel RG, Tung HN, Roberts R, Beams HW. 1985. The presence and distribution of gap junctions in the oocyte-follicle cell complex of the zebrafish, Brachydanio rerio. *Journal of submicroscopic cytology* **17**: 239-253.
Khalil AM, Guttman M, Huarte M, Garber M, Raj A, Rivea Morales D, Thomas K, Presser A, Bernstein BE, van Oudenaarden A et al. 2009. Many human large intergenic noncoding RNAs associate with chromatin-modifying complexes and affect gene expression. *Proceedings of the National Academy of Sciences of the United States of America* **106**: 11667-11672.
Khalil AM, Rinn JL. 2011. RNA-protein interactions in human health and disease. *Seminars in cell & developmental biology* **22**: 359-365.
Kimmel CB, Ballard WW, Kimmel SR, Ullmann B, Schilling TF. 1995. Stages of embryonic development of the zebrafish. *Dev Dyn* **203**: 253-310.
Kimmel CB, Law RD. 1985. Cell lineage of zebrafish blastomeres. II. Formation of the yolk syncytial layer. *Developmental biology* **108**: 86-93.
Kindler S, Wang H, Richter D, Tiedge H. 2005. RNA transport and local control of translation. *Annual review of cell and developmental biology* **21**: 223-245.
King ML, Zhou Y, Bubunenko M. 1999. Polarizing genetic information in the egg: RNA localization in the frog oocyte. *Bioessays* **21**: 546-557.
Kirby C, Kusch M, Kemphues K. 1990. Mutations in the par genes of Caenorhabditis elegans affect cytoplasmic reorganization during the first cell cycle. *Developmental biology* **142**: 203-215.

Kloc M, Dougherty MT, Bilinski S, Chan AP, Brey E, King ML, Patrick CW, Jr., Etkin LD. 2002. Three-dimensional ultrastructural analysis of RNA distribution within germinal granules of Xenopus. *Developmental biology* **241**: 79-93.

Kloc M, Wilk K, Vargas D, Shirato Y, Bilinski S, Etkin LD. 2005. Potential structural role of non-coding and coding RNAs in the organization of the cytoskeleton at the vegetal cortex of Xenopus oocytes. *Development* **132**: 3445-3457.

Klug A. 2010. The discovery of zinc fingers and their applications in gene regulation and genome manipulation. *Annual review of biochemistry* **79**: 213-231.

Knaut H, Pelegri F, Bohmann K, Schwarz H, Nusslein-Volhard C. 2000. Zebrafish vasa RNA but not its protein is a component of the germ plasm and segregates asymmetrically before germline specification. *The Journal of cell biology* **149**: 875-888.

Kondrychyn I, Garcia-Lecea M, Emelyanov A, Parinov S, Korzh V. 2009. Genome-wide analysis of Tol2 transposon reintegration in zebrafish. *BMC genomics* **10**: 418.

Koprunner M, Thisse C, Thisse B, Raz E. 2001. A zebrafish nanos-related gene is essential for the development of primordial germ cells. *Genes & development* **15**: 2877-2885.

Kumari P, Gilligan PC, Lim S, Tran LD, Winkler S, Philp R, Sampath K. 2013. An essential role for maternal control of Nodal signaling. *eLife* **2**: e00683.

Lam KN, van Bakel H, Cote AG, van der Ven A, Hughes TR. 2011. Sequence specificity is obtained from the majority of modular C2H2 zinc-finger arrays. *Nucleic acids research* **39**: 4680-4690.

Langdon YG, Mullins MC. 2011. Maternal and zygotic control of zebrafish dorsoventral axial patterning. *Annual review of genetics* **45**: 357-377.

Le Good JA, Joubin K, Giraldez AJ, Ben-Haim N, Beck S, Chen Y, Schier AF, Constam DB. 2005. Nodal stability determines signaling range. *Curr Biol* **15**: 31-36.

Lee E, Salic A, Kirschner MW. 2001. Physiological regulation of [beta]-catenin stability by Tcf3 and CK1epsilon. *The Journal of cell biology* **154**: 983-993.

Lee HX, Ambrosio AL, Reversade B, De Robertis EM. 2006. Embryonic dorsal-ventral signaling: secreted frizzled-related proteins as inhibitors of tolloid proteinases. *Cell* **124**: 147-159.

Lee RC, Feinbaum RL, Ambros V. 1993. The C. elegans heterochronic gene lin-4 encodes small RNAs with antisense complementarity to lin-14. *Cell* **75**: 843-854.

Lehmann R, Ephrussi A. 1994. Germ plasm formation and germ cell determination in Drosophila. *Ciba Foundation symposium* **182**: 282-296; discussion 296-300.

Lehmann R, Nusslein-Volhard C. 1986. Abdominal segmentation, pole cell formation, and embryonic polarity require the localized activity of oskar, a maternal gene in Drosophila. *Cell* **47**: 141-152.

Lejeune F, Ranganathan AC, Maquat LE. 2004. eIF4G is required for the pioneer round of translation in mammalian cells. *Nature structural & molecular biology* **11**: 992-1000.

Leung T, Bischof J, Soll I, Niessing D, Zhang D, Ma J, Jackle H, Driever W. 2003. bozozok directly represses bmp2b transcription and mediates the earliest dorsoventral asymmetry of bmp2b expression in zebrafish. *Development* **130**: 3639-3649.

Levin M, Johnson RL, Stern CD, Kuehn M, Tabin C. 1995. A molecular pathway determining left-right asymmetry in chick embryogenesis. *Cell* **82**: 803-814.
Li L, Yuan H, Weaver CD, Mao J, Farr GH, 3rd, Sussman DJ, Jonkers J, Kimelman D, Wu D. 1999. Axin and Frat1 interact with dvl and GSK, bridging Dvl to GSK in Wnt-mediated regulation of LEF-1. *The EMBO journal* **18**: 4233-4240.
Li L, Zheng P, Dean J. 2010. Maternal control of early mouse development. *Development* **137**: 859-870.
Lin K, Wang S, Julius MA, Kitajewski J, Moos M, Jr., Luyten FP. 1997. The cysteine-rich frizzled domain of Frzb-1 is required and sufficient for modulation of Wnt signaling. *Proceedings of the National Academy of Sciences of the United States of America* **94**: 11196-11200.
Lin R, Maeda S, Liu C, Karin M, Edgington TS. 2007. A large noncoding RNA is a marker for murine hepatocellular carcinomas and a spectrum of human carcinomas. *Oncogene* **26**: 851-858.
Long Q, Meng A, Wang H, Jessen JR, Farrell MJ, Lin S. 1997. GATA-1 expression pattern can be recapitulated in living transgenic zebrafish using GFP reporter gene. *Development* **124**: 4105-4111.
Lowe LA, Supp DM, Sampath K, Yokoyama T, Wright CV, Potter SS, Overbeek P, Kuehn MR. 1996. Conserved left-right asymmetry of nodal expression and alterations in murine situs inversus. *Nature* **381**: 158-161.
Lu FI, Thisse C, Thisse B. 2011. Identification and mechanism of regulation of the zebrafish dorsal determinant. *Proceedings of the National Academy of Sciences of the United States of America* **108**: 15876-15880.
Lucks JB, Mortimer SA, Trapnell C, Luo S, Aviran S, Schroth GP, Pachter L, Doudna JA, Arkin AP. 2011. Multiplexed RNA structure characterization with selective 2'-hydroxyl acylation analyzed by primer extension sequencing (SHAPE-Seq). *Proceedings of the National Academy of Sciences of the United States of America* **108**: 11063-11068.
Ma S, Zhang S, Wang F, Liu Y, Xu H, Liu C, Lin Y, Zhao P, Xia Q. 2012. Highly efficient and specific genome editing in silkworm using custom TALENs. *PloS one* **7**: e45035.
Maeder ML, Thibodeau-Beganny S, Osiak A, Wright DA, Anthony RM, Eichtinger M, Jiang T, Foley JE, Winfrey RJ, Townsend JA et al. 2008. Rapid "open-source" engineering of customized zinc-finger nucleases for highly efficient gene modification. *Molecular cell* **31**: 294-301.
Makabe KW, Kawashima T, Kawashima S, Minokawa T, Adachi A, Kawamura H, Ishikawa H, Yasuda R, Yamamoto H, Kondoh K et al. 2001. Large-scale cDNA analysis of the maternal genetic information in the egg of Halocynthia roretzi for a gene expression catalog of ascidian development. *Development* **128**: 2555-2567.
Mali P, Yang L, Esvelt KM, Aach J, Guell M, DiCarlo JE, Norville JE, Church GM. 2013. RNA-guided human genome engineering via Cas9. *Science (New York, NY* **339**: 823-826.
Mango SE, Thorpe CJ, Martin PR, Chamberlain SH, Bowerman B. 1994. Two maternal genes, apx-1 and pie-1, are required to distinguish the fates of equivalent blastomeres in the early Caenorhabditis elegans embryo. *Development* **120**: 2305-2315.

Mayden RL, Tang KL, Conway KW, Freyhof J, Chamberlain S, Haskins M, Schneider L, Sudkamp M, Wood RM, Agnew M et al. 2007. Phylogenetic relationships of Danio within the order Cypriniformes: a framework for comparative and evolutionary studies of a model species. *Journal of experimental zoology* **308**: 642-654.

McClintock B. 1950. The origin and behavior of mutable loci in maize. *Proceedings of the National Academy of Sciences of the United States of America* **36**: 344-355.

Mello CC, Draper BW, Priess JR. 1994. The maternal genes apx-1 and glp-1 and establishment of dorsal-ventral polarity in the early C. elegans embryo. *Cell* **77**: 95-106.

Mencia A, Modamio-Hoybjor S, Redshaw N, Morin M, Mayo-Merino F, Olavarrieta L, Aguirre LA, del Castillo I, Steel KP, Dalmay T et al. 2009. Mutations in the seed region of human miR-96 are responsible for nonsyndromic progressive hearing loss. *Nature genetics* **41**: 609-613.

Meng X, Noyes MB, Zhu LJ, Lawson ND, Wolfe SA. 2008. Targeted gene inactivation in zebrafish using engineered zinc-finger nucleases. *Nature biotechnology* **26**: 695-701.

Meno C, Gritsman K, Ohishi S, Ohfuji Y, Heckscher E, Mochida K, Shimono A, Kondoh H, Talbot WS, Robertson EJ et al. 1999. Mouse Lefty2 and zebrafish antivin are feedback inhibitors of nodal signaling during vertebrate gastrulation. *Molecular cell* **4**: 287-298.

Mercer AC, Gaj T, Fuller RP, Barbas CF, 3rd. 2012. Chimeric TALE recombinases with programmable DNA sequence specificity. *Nucleic acids research* **40**: 11163-11172.

Mickey KM, Mello CC, Montgomery MK, Fire A, Priess JR. 1996. An inductive interaction in 4-cell stage C. elegans embryos involves APX-1 expression in the signalling cell. *Development* **122**: 1791-1798.

Mii Y, Taira M. 2009. Secreted Frizzled-related proteins enhance the diffusion of Wnt ligands and expand their signalling range. *Development* **136**: 4083-4088.

Miller JR, Rowning BA, Larabell CA, Yang-Snyder JA, Bates RL, Moon RT. 1999. Establishment of the dorsal-ventral axis in Xenopus embryos coincides with the dorsal enrichment of dishevelled that is dependent on cortical rotation. *The Journal of cell biology* **146**: 427-437.

Mizuno T, Yamaha E, Kuroiwa A, Takeda H. 1999. Removal of vegetal yolk causes dorsal deficencies and impairs dorsal-inducing ability of the yolk cell in zebrafish. *Mechanisms of development* **81**: 51-63.

Mizuno T, Yamaha E, Wakahara M, Kuroiwa A, Takeda H. 1996. Mesoderm induction in zebrafish. *Nature* **383**: 131-132.

Morton DG, Roos JM, Kemphues KJ. 1992. par-4, a gene required for cytoplasmic localization and determination of specific cell types in Caenorhabditis elegans embryogenesis. *Genetics* **130**: 771-790.

Moscou MJ, Bogdanove AJ. 2009. A simple cipher governs DNA recognition by TAL effectors. *Science (New York, NY* **326**: 1501.

Moskowitz IP, Gendreau SB, Rothman JH. 1994. Combinatorial specification of blastomere identity by glp-1-dependent cellular interactions in the nematode Caenorhabditis elegans. *Development* **120**: 3325-3338.

Mullins MC, Hammerschmidt M, Haffter P, Nusslein-Volhard C. 1994. Large-scale mutagenesis in the zebrafish: in search of genes controlling development in a vertebrate. *Curr Biol* **4**: 189-202.

Mullins MC, Hammerschmidt M, Kane DA, Odenthal J, Brand M, van Eeden FJ, Furutani-Seiki M, Granato M, Haffter P, Heisenberg CP et al. 1996. Genes establishing dorsoventral pattern formation in the zebrafish embryo: the ventral specifying genes. *Development* **123**: 81-93.

Munro E, Nance J, Priess JR. 2004. Cortical flows powered by asymmetrical contraction transport PAR proteins to establish and maintain anterior-posterior polarity in the early C. elegans embryo. *Developmental cell* **7**: 413-424.

Mussolino C, Morbitzer R, Lutge F, Dannemann N, Lahaye T, Cathomen T. 2011. A novel TALE nuclease scaffold enables high genome editing activity in combination with low toxicity. *Nucleic acids research* **39**: 9283-9293.

Nagano T, Mitchell JA, Sanz LA, Pauler FM, Ferguson-Smith AC, Feil R, Fraser P. 2008. The Air noncoding RNA epigenetically silences transcription by targeting G9a to chromatin. *Science (New York, NY* **322**: 1717-1720.

Nagy E, Maquat LE. 1998. A rule for termination-codon position within intron-containing genes: when nonsense affects RNA abundance. *Trends in biochemical sciences* **23**: 198-199.

Nakamura Y, Makabe KW, Nishida H. 2003. Localization and expression pattern of type I postplasmic mRNAs in embryos of the ascidian Halocynthia roretzi. *Gene Expr Patterns* **3**: 71-75.

Namba R, Pazdera TM, Cerrone RL, Minden JS. 1997. Drosophila embryonic pattern repair: how embryos respond to bicoid dosage alteration. *Development* **124**: 1393-1403.

Nasevicius A, Ekker SC. 2000. Effective targeted gene 'knockdown' in zebrafish. *Nature genetics* **26**: 216-220.

Neil H, Malabat C, d'Aubenton-Carafa Y, Xu Z, Steinmetz LM, Jacquier A. 2009. Widespread bidirectional promoters are the major source of cryptic transcripts in yeast. *Nature* **457**: 1038-1042.

Neuman-Silberberg FS, Schupbach T. 1993. The Drosophila dorsoventral patterning gene gurken produces a dorsally localized RNA and encodes a TGF alpha-like protein. *Cell* **75**: 165-174.

Niessing D, Driever W, Sprenger F, Taubert H, Jackle H, Rivera-Pomar R. 2000. Homeodomain position 54 specifies transcriptional versus translational control by Bicoid. *Molecular cell* **5**: 395-401.

Niranjanakumari S, Lasda E, Brazas R, Garcia-Blanco MA. 2002. Reversible cross-linking combined with immunoprecipitation to study RNA-protein interactions in vivo. *Methods* **26**: 182-190.

Nishida H. 1994. Localization of determinants for formation of the anterior-posterior axis in eggs of the ascidian Halocynthia roretzi. *Development* **120**: 3093-3104.

-. 1996. Vegetal egg cytoplasm promotes gastrulation and is responsible for specification of vegetal blastomeres in embryos of the ascidian Halocynthia roretzi. *Development* **122**: 1271-1279.

-. 2005. Specification of embryonic axis and mosaic development in ascidians. *Dev Dyn* **233**: 1177-1193.

Nojima H, Rothhamel S, Shimizu T, Kim CH, Yonemura S, Marlow FL, Hibi M. 2010. Syntabulin, a motor protein linker, controls dorsal determination. *Development* **137**: 923-933.
Nusslein-Volhard C, Wieschaus E. 1980. Mutations affecting segment number and polarity in Drosophila. *Nature* **287**: 795-801.
Ober EA, Schulte-Merker S. 1999. Signals from the yolk cell induce mesoderm, neuroectoderm, the trunk organizer, and the notochord in zebrafish. *Developmental biology* **215**: 167-181.
Okazaki Y Furuno M Kasukawa T Adachi J Bono H Kondo S Nikaido I Osato N Saito R Suzuki H et al. 2002. Analysis of the mouse transcriptome based on functional annotation of 60,770 full-length cDNAs. *Nature* **420**: 563-573.
Olsen LC, Aasland R, Fjose A. 1997. A vasa-like gene in zebrafish identifies putative primordial germ cells. *Mechanisms of development* **66**: 95-105.
Oppenheimer JM. 1936. Transplantation experiments on developing teleosts (Fundulus and Perca). *J Exp Zool*: 409-437.
Orr WC, Galanopoulos VK, Romano CP, Kafatos FC. 1989. A female sterile screen of the Drosophila melanogaster X chromosome using hybrid dysgenesis: identification and characterization of egg morphology mutants. *Genetics* **122**: 847-858.
Osada SI, Wright CV. 1999. Xenopus nodal-related signaling is essential for mesendodermal patterning during early embryogenesis. *Development* **126**: 3229-3240.
Ouyang Z, Snyder MP, Chang HY. 2012. SeqFold: genome-scale reconstruction of RNA secondary structure integrating high-throughput sequencing data. *Genome research* **23**: 377-387.
Palacios IM, St Johnston D. 2001. Getting the message across: the intracellular localization of mRNAs in higher eukaryotes. *Annual review of cell and developmental biology* **17**: 569-614.
Pandey RR, Mondal T, Mohammad F, Enroth S, Redrup L, Komorowski J, Nagano T, Mancini-Dinardo D, Kanduri C. 2008. Kcnq1ot1 antisense noncoding RNA mediates lineage-specific transcriptional silencing through chromatin-level regulation. *Molecular cell* **32**: 232-246.
Parinov S, Emelyanov A. 2007. Transposable elements in fish functional genomics: technical challenges and perspectives. *Genome biology* **8 Suppl 1**: S6.
Parinov S, Kondrichin I, Korzh V, Emelyanov A. 2004. Tol2 transposon-mediated enhancer trap to identify developmentally regulated zebrafish genes in vivo. *Dev Dyn* **231**: 449-459.
Pauli A, Valen E, Lin MF, Garber M, Vastenhouw NL, Levin JZ, Fan L, Sandelin A, Rinn JL, Regev A et al. 2011. Systematic identification of long noncoding RNAs expressed during zebrafish embryogenesis. *Genome research* **22**: 577-591.
Pei W, Williams PH, Clark MD, Stemple DL, Feldman B. 2007. Environmental and genetic modifiers of squint penetrance during zebrafish embryogenesis. *Developmental biology* **308**: 368-378.
Pelegri F. 2003. Maternal factors in zebrafish development. *Dev Dyn* **228**: 535-554.
Pelegri F, Mullins MC. 2004. Genetic screens for maternal-effect mutations. *Methods in cell biology* **77**: 21-51.

Pera EM, De Robertis EM. 2000. A direct screen for secreted proteins in Xenopus embryos identifies distinct activities for the Wnt antagonists Crescent and Frzb-1. *Mechanisms of development* **96**: 183-195.

Pichler S, Gonczy P, Schnabel H, Pozniakowski A, Ashford A, Schnabel R, Hyman AA. 2000. OOC-3, a novel putative transmembrane protein required for establishment of cortical domains and spindle orientation in the P(1) blastomere of C. elegans embryos. *Development* **127**: 2063-2073.

Ploper D, Lee HX, De Robertis EM. 2011. Dorsal-ventral patterning: Crescent is a dorsally secreted Frizzled-related protein that competitively inhibits Tolloid proteases. *Developmental biology* **352**: 317-328.

Pogoda HM, Solnica-Krezel L, Driever W, Meyer D. 2000. The zebrafish forkhead transcription factor FoxH1/Fast1 is a modulator of nodal signaling required for organizer formation. *Curr Biol* **10**: 1041-1049.

Poliseno L, Salmena L, Zhang J, Carver B, Haveman WJ, Pandolfi PP. 2010. A coding-independent function of gene and pseudogene mRNAs regulates tumour biology. *Nature* **465**: 1033-1038.

Ponjavic J, Ponting CP, Lunter G. 2007. Functionality or transcriptional noise? Evidence for selection within long noncoding RNAs. *Genome research* **17**: 556-565.

Preker P, Nielsen J, Kammler S, Lykke-Andersen S, Christensen MS, Mapendano CK, Schierup MH, Jensen TH. 2008. RNA exosome depletion reveals transcription upstream of active human promoters. *Science (New York, NY* **322**: 1851-1854.

Prodon F, Yamada L, Shirae-Kurabayashi M, Nakamura Y, Sasakura Y. 2007. Postplasmic/PEM RNAs: a class of localized maternal mRNAs with multiple roles in cell polarity and development in ascidian embryos. *Dev Dyn* **236**: 1698-1715.

Qiu R, Liu K, Liu Y, Mo W, Flynt AS, Patton JG, Kar A, Wu JY, He R. 2009. The role of miR-124a in early development of the Xenopus eye. *Mechanisms of development* **126**: 804-816.

Ramirez CL, Foley JE, Wright DA, Muller-Lerch F, Rahman SH, Cornu TI, Winfrey RJ, Sander JD, Fu F, Townsend JA et al. 2008. Unexpected failure rates for modular assembly of engineered zinc fingers. *Nature methods* **5**: 374-375.

Rebagliati MR, Toyama R, Fricke C, Haffter P, Dawid IB. 1998. Zebrafish nodal-related genes are implicated in axial patterning and establishing left-right asymmetry. *Developmental biology* **199**: 261-272.

Rebagliati MR, Weeks DL, Harvey RP, Melton DA. 1985. Identification and cloning of localized maternal RNAs from Xenopus eggs. *Cell* **42**: 769-777.

Reinhart BJ, Slack FJ, Basson M, Pasquinelli AE, Bettinger JC, Rougvie AE, Horvitz HR, Ruvkun G. 2000. The 21-nucleotide let-7 RNA regulates developmental timing in Caenorhabditis elegans. *Nature* **403**: 901-906.

Riechmann V, Ephrussi A. 2001. Axis formation during Drosophila oogenesis. *Current opinion in genetics & development* **11**: 374-383.

Riley BB, Grunwald DJ. 1995. Efficient induction of point mutations allowing recovery of specific locus mutations in zebrafish. *Proceedings of the National Academy of Sciences of the United States of America* **92**: 5997-6001.

Rinn JL, Kertesz M, Wang JK, Squazzo SL, Xu X, Brugmann SA, Goodnough LH, Helms JA, Farnham PJ, Segal E et al. 2007. Functional demarcation of active and

silent chromatin domains in human HOX loci by noncoding RNAs. *Cell* **129**: 1311-1323.
Roegiers F, McDougall A, Sardet C. 1995. The sperm entry point defines the orientation of the calcium-induced contraction wave that directs the first phase of cytoplasmic reorganization in the ascidian egg. *Development* **121**: 3457-3466.
Roth S, Stein D, Nusslein-Volhard C. 1989. A gradient of nuclear localization of the dorsal protein determines dorsoventral pattern in the Drosophila embryo. *Cell* **59**: 1189-1202.
Rowning BA, Wells J, Wu M, Gerhart JC, Moon RT, Larabell CA. 1997. Microtubule-mediated transport of organelles and localization of beta-catenin to the future dorsal side of Xenopus eggs. *Proceedings of the National Academy of Sciences of the United States of America* **94**: 1224-1229.
Rushlow CA, Han K, Manley JL, Levine M. 1989. The graded distribution of the dorsal morphogen is initiated by selective nuclear transport in Drosophila. *Cell* **59**: 1165-1177.
Saito T, Fujimoto T, Maegawa S, Inoue K, Tanaka M, Arai K, Yamaha E. 2006. Visualization of primordial germ cells in vivo using GFP-nos1 3'UTR mRNA. *The International journal of developmental biology* **50**: 691-699.
Salic A, Lee E, Mayer L, Kirschner MW. 2000. Control of beta-catenin stability: reconstitution of the cytoplasmic steps of the wnt pathway in Xenopus egg extracts. *Molecular cell* **5**: 523-532.
Sampath K, Cheng AM, Frisch A, Wright CV. 1997. Functional differences among Xenopus nodal-related genes in left-right axis determination. *Development* **124**: 3293-3302.
Sampath K, Rubinstein AL, Cheng AM, Liang JO, Fekany K, Solnica-Krezel L, Korzh V, Halpern ME, Wright CV. 1998. Induction of the zebrafish ventral brain and floorplate requires cyclops/nodal signalling. *Nature* **395**: 185-189.
Sander JD, Dahlborg EJ, Goodwin MJ, Cade L, Zhang F, Cifuentes D, Curtin SJ, Blackburn JS, Thibodeau-Beganny S, Qi Y et al. 2011a. Selection-free zinc-finger-nuclease engineering by context-dependent assembly (CoDA). *Nature methods* **8**: 67-69.
Sander JD, Yeh JR, Peterson RT, Joung JK. 2011b. Engineering zinc finger nucleases for targeted mutagenesis of zebrafish. *Methods in cell biology* **104**: 51-58.
Sasakura Y, Ogasawara M, Makabe KW. 1998a. HrWnt-5: a maternally expressed ascidian Wnt gene with posterior localization in early embryos. *The International journal of developmental biology* **42**: 573-579.
-. 1998b. Maternally localized RNA encoding a serine/threonine protein kinase in the ascidian, Halocynthia roretzi. *Mechanisms of development* **76**: 161-163.
Sawada T, Schatten G. 1989. Effects of cytoskeletal inhibitors on ooplasmic segregation and microtubule organization during fertilization and early development in the ascidian Molgula occidentalis. *Developmental biology* **132**: 331-342.
Schier AF. 2007. The maternal-zygotic transition: death and birth of RNAs. *Science (New York, NY* **316**: 406-407.
Schier AF, Shen MM. 2000. Nodal signalling in vertebrate development. *Nature* **403**: 385-389.

Schier AF, Talbot WS. 2001. Nodal signaling and the zebrafish organizer. *The International journal of developmental biology* **45**: 289-297.
Schilling TF. 2002. The morphology of larval and adult zebrafish. In Zebrafish: A Practical Approach. Oxford Univ. Press.
Schneider S, Steinbeisser H, Warga RM, Hausen P. 1996. Beta-catenin translocation into nuclei demarcates the dorsalizing centers in frog and fish embryos. *Mechanisms of development* **57**: 191-198.
Schulte-Merker S, Hammerschmidt M, Beuchle D, Cho KW, De Robertis EM, Nusslein-Volhard C. 1994. Expression of zebrafish goosecoid and no tail gene products in wild-type and mutant no tail embryos. *Development* **120**: 843-852.
Schupbach T. 1987. Germ line and soma cooperate during oogenesis to establish the dorsoventral pattern of egg shell and embryo in Drosophila melanogaster. *Cell* **49**: 699-707.
Schupbach T, Wieschaus E. 1986. Germline autonomy of maternal-effect mutations altering the embryonic body pattern of Drosophila. *Developmental biology* **113**: 443-448.
-. 1989. Female sterile mutations on the second chromosome of Drosophila melanogaster. I. Maternal effect mutations. *Genetics* **121**: 101-117.
-. 1991. Female sterile mutations on the second chromosome of Drosophila melanogaster. II. Mutations blocking oogenesis or altering egg morphology. *Genetics* **129**: 1119-1136.
Seila AC, Calabrese JM, Levine SS, Yeo GW, Rahl PB, Flynn RA, Young RA, Sharp PA. 2008. Divergent transcription from active promoters. *Science (New York, NY* **322**: 1849-1851.
Selman K, Wallace RA, Sarka A, Qi X. 1993. Stages of oocyte development in the zebrafish, Brachydanio rerio. *Journal of Morphology* **218**: 203-224.
Shen MM, Schier AF. 2000. The EGF-CFC gene family in vertebrate development. *Trends Genet* **16**: 303-309.
Shimizu T, Yamanaka Y, Ryu SL, Hashimoto H, Yabe T, Hirata T, Bae YK, Hibi M, Hirano T. 2000. Cooperative roles of Bozozok/Dharma and Nodal-related proteins in the formation of the dorsal organizer in zebrafish. *Mechanisms of development* **91**: 293-303.
Sirotkin HI, Gates MA, Kelly PD, Schier AF, Talbot WS. 2000. Fast1 is required for the development of dorsal axial structures in zebrafish. *Curr Biol* **10**: 1051-1054.
Slobodin B, Gerst JE. 2010. A novel mRNA affinity purification technique for the identification of interacting proteins and transcripts in ribonucleoprotein complexes. *Rna* **16**: 2277-2290.
Smith P, Leung-Chiu WM, Montgomery R, Orsborn A, Kuznicki K, Gressman-Coberly E, Mutapcic L, Bennett K. 2002. The GLH proteins, Caenorhabditis elegans P granule components, associate with CSN-5 and KGB-1, proteins necessary for fertility, and with ZYX-1, a predicted cytoskeletal protein. *Developmental biology* **251**: 333-347.
Sollu C, Pars K, Cornu TI, Thibodeau-Beganny S, Maeder ML, Joung JK, Heilbronn R, Cathomen T. 2010. Autonomous zinc-finger nuclease pairs for targeted chromosomal deletion. *Nucleic acids research* **38**: 8269-8276.

Solnica-Krezel L, Schier AF, Driever W. 1994. Efficient recovery of ENU-induced mutations from the zebrafish germline. *Genetics* **136**: 1401-1420.
Sonkoly E, Bata-Csorgo Z, Pivarcsi A, Polyanka H, Kenderessy-Szabo A, Molnar G, Szentpali K, Bari L, Megyeri K, Mandi Y et al. 2005. Identification and characterization of a novel, psoriasis susceptibility-related noncoding RNA gene, PRINS. *The Journal of biological chemistry* **280**: 24159-24167.
Sossin WS, DesGroseillers L. 2006. Intracellular trafficking of RNA in neurons. *Traffic* **7**: 1581-1589.
Speksnijder JE, Sardet C, Jaffe LF. 1990a. The activation wave of calcium in the ascidian egg and its role in ooplasmic segregation. *The Journal of cell biology* **110**: 1589-1598.
-. 1990b. Periodic calcium waves cross ascidian eggs after fertilization. *Developmental biology* **142**: 246-249.
Srisawat C, Engelke DR. 2002. RNA affinity tags for purification of RNAs and ribonucleoprotein complexes. *Methods* **26**: 156-161.
St Johnston D. 2002. The art and design of genetic screens: Drosophila melanogaster. *Nature reviews* **3**: 176-188.
Steward R. 1989. Relocalization of the dorsal protein from the cytoplasm to the nucleus correlates with its function. *Cell* **59**: 1179-1188.
Strome S, Wood WB. 1983. Generation of asymmetry and segregation of germ-line granules in early C. elegans embryos. *Cell* **35**: 15-25.
Struhl G, Struhl K, Macdonald PM. 1989. The gradient morphogen bicoid is a concentration-dependent transcriptional activator. *Cell* **57**: 1259-1273.
Stuart GW, McMurray JV, Westerfield M. 1988. Replication, integration and stable germ-line transmission of foreign sequences injected into early zebrafish embryos. *Development* **103**: 403-412.
Stuart GW, Vielkind JR, McMurray JV, Westerfield M. 1990. Stable lines of transgenic zebrafish exhibit reproducible patterns of transgene expression. *Development* **109**: 577-584.
Sulston JE, Schierenberg E, White JG, Thomson JN. 1983. The embryonic cell lineage of the nematode Caenorhabditis elegans. *Developmental biology* **100**: 64-119.
Suster ML, Kikuta H, Urasaki A, Asakawa K, Kawakami K. 2009. Transgenesis in zebrafish with the tol2 transposon system. *Methods in molecular biology (Clifton, NJ* **561**: 41-63.
Takahashi S, Yokota C, Takano K, Tanegashima K, Onuma Y, Goto J, Asashima M. 2000. Two novel nodal-related genes initiate early inductive events in Xenopus Nieuwkoop center. *Development* **127**: 5319-5329.
Tao Q, Yokota C, Puck H, Kofron M, Birsoy B, Yan D, Asashima M, Wylie CC, Lin X, Heasman J. 2005. Maternal wnt11 activates the canonical wnt signaling pathway required for axis formation in Xenopus embryos. *Cell* **120**: 857-871.
Tautz D. 1988. Regulation of the Drosophila segmentation gene hunchback by two maternal morphogenetic centres. *Nature* **332**: 281-284.
Thatcher EJ, Paydar I, Anderson KK, Patton JG. 2008. Regulation of zebrafish fin regeneration by microRNAs. *Proceedings of the National Academy of Sciences of the United States of America* **105**: 18384-18389.

Thisse B, Wright CV, Thisse C. 2000. Activin- and Nodal-related factors control antero-posterior patterning of the zebrafish embryo. *Nature* **403**: 425-428.
Tian D, Sun S, Lee JT. 2010. The long noncoding RNA, Jpx, is a molecular switch for X chromosome inactivation. *Cell* **143**: 390-403.
Tian J, Andree B, Jones CM, Sampath K. 2008. The pro-domain of the zebrafish Nodal-related protein Cyclops regulates its signaling activities. *Development* **135**: 2649-2658.
Tran LD, Hino H, Quach H, Lim S, Shindo A, Mimori-Kiyosue Y, Mione M, Ueno N, Winkler C, Hibi M et al. 2012. Dynamic microtubules at the vegetal cortex predict the embryonic axis in zebrafish. *Development* **139**: 3644-3652.
Trinh le A, Hochgreb T, Graham M, Wu D, Ruf-Zamojski F, Jayasena CS, Saxena A, Hawk R, Gonzalez-Serricchio A, Dixson A et al. A versatile gene trap to visualize and interrogate the function of the vertebrate proteome. *Genes & development* **25**: 2306-2320.
Tripathi V, Ellis JD, Shen Z, Song DY, Pan Q, Watt AT, Freier SM, Bennett CF, Sharma A, Bubulya PA et al. 2010. The nuclear-retained noncoding RNA MALAT1 regulates alternative splicing by modulating SR splicing factor phosphorylation. *Molecular cell* **39**: 925-938.
Tsai MC, Manor O, Wan Y, Mosammaparast N, Wang JK, Lan F, Shi Y, Segal E, Chang HY. 2010. Long noncoding RNA as modular scaffold of histone modification complexes. *Science (New York, NY* **329**: 689-693.
Tsou MF, Ku W, Hayashi A, Rose LS. 2003. PAR-dependent and geometry-dependent mechanisms of spindle positioning. *The Journal of cell biology* **160**: 845-855.
Underwood JG, Uzilov AV, Katzman S, Onodera CS, Mainzer JE, Mathews DH, Lowe TM, Salama SR, Haussler D. 2010. FragSeq: transcriptome-wide RNA structure probing using high-throughput sequencing. *Nature methods* **7**: 995-1001.
Urasaki A, Asakawa K, Kawakami K. 2008. Efficient transposition of the Tol2 transposable element from a single-copy donor in zebrafish. *Proceedings of the National Academy of Sciences of the United States of America* **105**: 19827-19832.
van der Weyden L, Adams DJ, Bradley A. 2002. Tools for targeted manipulation of the mouse genome. *Physiological genomics* **11**: 133-164.
Vincent JP, Gerhart JC. 1987. Subcortical rotation in Xenopus eggs: an early step in embryonic axis specification. *Developmental biology* **123**: 526-539.
Vincent JP, Oster GF, Gerhart JC. 1986. Kinematics of gray crescent formation in Xenopus eggs: the displacement of subcortical cytoplasm relative to the egg surface. *Developmental biology* **113**: 484-500.
Wagner DS, Dosch R, Mintzer KA, Wiemelt AP, Mullins MC. 2004. Maternal control of development at the midblastula transition and beyond: mutants from the zebrafish II. *Developmental cell* **6**: 781-790.
Wagner E, Lykke-Andersen J. 2002. mRNA surveillance: the perfect persist. *Journal of cell science* **115**: 3033-3038.
Wallenfang MR, Seydoux G. 2000. Polarization of the anterior-posterior axis of C. elegans is a microtubule-directed process. *Nature* **408**: 89-92.
Wang KC, Yang YW, Liu B, Sanyal A, Corces-Zimmerman R, Chen Y, Lajoie BR, Protacio A, Flynn RA, Gupta RA et al. 2011. A long noncoding RNA maintains active chromatin to coordinate homeotic gene expression. *Nature* **472**: 120-124.

Wang L, Eckmann CR, Kadyk LC, Wickens M, Kimble J. 2002. A regulatory cytoplasmic poly(A) polymerase in Caenorhabditis elegans. *Nature* **419**: 312-316.
Wang S, Krinks M, Lin K, Luyten FP, Moos M, Jr. 1997. Frzb, a secreted protein expressed in the Spemann organizer, binds and inhibits Wnt-8. *Cell* **88**: 757-766.
Weaver C, Farr GH, 3rd, Pan W, Rowning BA, Wang J, Mao J, Wu D, Li L, Larabell CA, Kimelman D. 2003. GBP binds kinesin light chain and translocates during cortical rotation in Xenopus eggs. *Development* **130**: 5425-5436.
Weaver C, Kimelman D. 2004. Move it or lose it: axis specification in Xenopus. *Development* **131**: 3491-3499.
Westerfield M. 2007. *The Zebrafish Book. A Guide for the Laboratory Use of Zebrafish (Danio rerio)* University of Oregon Press.
Wienholds E, Koudijs MJ, van Eeden FJ, Cuppen E, Plasterk RH. 2003. The microRNA-producing enzyme Dicer1 is essential for zebrafish development. *Nature genetics* **35**: 217-218.
Wightman B, Ha I, Ruvkun G. 1993. Posttranscriptional regulation of the heterochronic gene lin-14 by lin-4 mediates temporal pattern formation in C. elegans. *Cell* **75**: 855-862.
Williams PH, Hagemann A, Gonzalez-Gaitan M, Smith JC. 2004. Visualizing long-range movement of the morphogen Xnr2 in the Xenopus embryo. *Curr Biol* **14**: 1916-1923.
Wood AJ, Lo TW, Zeitler B, Pickle CS, Ralston EJ, Lee AH, Amora R, Miller JC, Leung E, Meng X et al. 2011. Targeted genome editing across species using ZFNs and TALENs. *Science (New York, NY* **333**: 307.
Wood WB. 1988. Determination of pattern and fate in early embryos of Caenorhabditis elegans. *Dev Biol (N Y 1985)* **5**: 57-78.
Wreden C, Verrotti AC, Schisa JA, Lieberfarb ME, Strickland S. 1997. Nanos and pumilio establish embryonic polarity in Drosophila by promoting posterior deadenylation of hunchback mRNA. *Development* **124**: 3015-3023.
Wu LH, Lengyel JA. 1998. Role of caudal in hindgut specification and gastrulation suggests homology between Drosophila amnioproctodeal invagination and vertebrate blastopore. *Development* **125**: 2433-2442.
Xu Z, Wei W, Gagneur J, Perocchi F, Clauder-Munster S, Camblong J, Guffanti E, Stutz F, Huber W, Steinmetz LM. 2009. Bidirectional promoters generate pervasive transcription in yeast. *Nature* **457**: 1033-1037.
Yamanaka Y, Mizuno T, Sasai Y, Kishi M, Takeda H, Kim CH, Hibi M, Hirano T. 1998. A novel homeobox gene, dharma, can induce the organizer in a non-cell-autonomous manner. *Genes & development* **12**: 2345-2353.
Yang J, Mei W, Otto A, Xiao L, Tao Q, Geng X, Rupp RA, Ding X. 2002. Repression through a distal TCF-3 binding site restricts Xenopus myf-5 expression in gastrula mesoderm. *Mechanisms of development* **115**: 79-89.
Yeo C, Whitman M. 2001. Nodal signals to Smads through Cripto-dependent and Cripto-independent mechanisms. *Molecular cell* **7**: 949-957.
Yoon C, Kawakami K, Hopkins N. 1997. Zebrafish vasa homologue RNA is localized to the cleavage planes of 2- and 4-cell-stage embryos and is expressed in the primordial germ cells. *Development* **124**: 3157-3165.

Yoshida S, Marikawa Y, Satoh N. 1996. Posterior end mark, a novel maternal gene encoding a localized factor in the ascidian embryo. *Development* **122**: 2005-2012.

Yost C, Torres M, Miller JR, Huang E, Kimelman D, Moon RT. 1996. The axis-inducing activity, stability, and subcellular distribution of beta-catenin is regulated in Xenopus embryos by glycogen synthase kinase 3. *Genes & development* **10**: 1443-1454.

Zalokar M, Sardet C. 1984. Tracing of cell lineage in embryonic development of Phallusia mammillata (Ascidia) by vital staining of mitochondria. *Developmental biology* **102**: 195-205.

Zhang C, Basta T, Jensen ED, Klymkowsky MW. 2003. The beta-catenin/VegT-regulated early zygotic gene Xnr5 is a direct target of SOX3 regulation. *Development* **130**: 5609-5624.

Zhang J, King ML. 1996. Xenopus VegT RNA is localized to the vegetal cortex during oogenesis and encodes a novel T-box transcription factor involved in mesodermal patterning. *Development* **122**: 4119-4129.

Zhang J, Talbot WS, Schier AF. 1998. Positional cloning identifies zebrafish one-eyed pinhead as a permissive EGF-related ligand required during gastrulation. *Cell* **92**: 241-251.

Zhao J, Ohsumi TK, Kung JT, Ogawa Y, Grau DJ, Sarma K, Song JJ, Kingston RE, Borowsky M, Lee JT. 2010. Genome-wide identification of polycomb-associated RNAs by RIP-seq. *Molecular cell* **40**: 939-953.

Zhao J, Sun BK, Erwin JA, Song JJ, Lee JT. 2008. Polycomb proteins targeted by a short repeat RNA to the mouse X chromosome. *Science (New York, NY* **322**: 750-756.

Zu Y, Tong X, Wang Z, Liu D, Pan R, Li Z, Hu Y, Luo Z, Huang P, Wu Q et al. 2013. TALEN-mediated precise genome modification by homologous recombination in zebrafish. *Nat Meth* **10**: 329-331.

List of Publications

Kumari, P.*, Gilligan, P.C.*, **Lim, S.**, Tran, L.D., Winkler, S., Philp, R., and Sampath, K. (2013) An essential role for maternal control of Nodal signaling. **Elife 2:e00683. doi: 10.7554/eLife.00683.**

Lim, S.*, Wang, Y.*, Yu, X.Y., Huang, Y.A., Featherstone, M.S., Sampath K. (2013) A simple strategy for heritable chromosomal deletions in zebrafish via the combinatorial action of targeting nucleases. **Genome Biology 14:R69 doi:10.1186/gb-2013-14-7-r69**

*co-authors

Tran, L.D., Hino, H., Quach, H., **Lim, S.**, Shindo, A., Mimori-Kiyosue, Y., Mione, M., Ueno, N., Winkler, C., Hibi, M., and Sampath, K. (2012) Dynamic microtubules at the vegetal cortex predict the embryonic axis in zebrafish. **Development 139(19): 3644-3652.**

Lim, S., Kumari, P., Gilligan, P., Quach, H.N., Mathavan, S., and Sampath, K. (2012) Dorsal activity of maternal *squint* is mediated by a non-coding function of the RNA. **Development 139(16): 2903-2915.**

Gilligan, P.C., Kumari, P., **Lim, S.**, Cheong, A., Chang, A., and Sampath, K. (2011) Conservation defines functional motifs in the *squint/nodal-related 1* RNA dorsal localization element. **Nucleic Acids Res. 39(8): 3340-9.**

List of posters, awards and invited talks

Poster presenter at **10th International Conference on Zebrafish Development and Genetics**, June 20-24, 2012 Madison, Wisconsin, United States of America
"Dorsal activity of maternal squint is mediated by a non-coding function of the RNA"

Poster presenter at **7th European Zebrafish Meeting**, July 5-9, 2011 Edinburgh, Scotland *"Dorsal activity of maternal squint is mediated by a non-coding function of the RNA"*

Speaker at **Singapore Zebrafish Symposium 2010**, November 8, 2010, Singapore
"Dorsal axis formation by maternal squint is mediated by a non-coding function of the RNA"

Speaker at **43rd Annual Meeting for the Japanese Society of Developmental Biologists**, June 21-23, 2010 Kyoto, Japan
"Dorsal axis formation by maternal squint is mediated by a non-coding function of the RNA"